***Thomas Reimann***, ***Rudolf Liedl*** *(TU Dresden),* ***Steffen Birk*** *(Uni Graz),* ***Sebastian Bauer*** *(Uni Kiel)*

*This document describes work in progress and will be continuously updated and revised. For the latest version of the executable source code and the documentation please contact Thomas.Reimann@tu-dresden.de.*

*The herein described modified CFP package, subsequently named CFPv2, is actually a research version provided without any warranty.*

# OVERVIEW

This document describes changes to MODFLOW-2005 Conduit Flow Process Mode 1 (CFPM1). The first part deals with updates regarding CFPM1 flow subroutines. The specific modifications and enhancements are documented in terms of intention, necessary input file modifications and (annexed) technical information of the source code implementation. Subsequently, the functionality of these enhancements is demonstrated by several test cases (Annex AT).

The second part describes heat and solute transport subroutines that were added based on corresponding modules from the software Carbonate Aquifer Void Evolution (CAVE). This part starts with a short overview about the underlying physics and then describes each added process in terms of intention, input file modifications, and results for test cases. At the end, some known limitations of the implemented transport routines are discussed (Annex BT).

# A) FIRST PART – MODIFICATIONS AND ENHANCEMENTS TO CFPM1 FLOW SUBROUTINES

## A1. FIXED HEAD LIMITED FLOW (FHLQ) BOUNDARY CONDITION

*Package existent in CAVE; modified and transferred to CFPv2 Mode 1*

### Intention

A conduit with fixed head boundary condition can strongly affect in- or outflow of the highly permeable pipe network. For example, water abstraction from a well developed conduit network with sufficiently large diameters, e.g. for water supply reasons, will almost ever result in water inflow through the fixed head boundary (because water inflow via matrix transfer is most likely constrained by the hydraulic conditions of the matrix continuum). The FHLQ boundary condition is intended to limit inflow or outflow at constant head boundaries. If a user defined flow rate (threshold) is exceeded, the boundary condition switches from a fixed head to a constant flow boundary (which results in variable head) [*Bauer et al.*, 2005]

$$FHLQ = \begin{cases} h = H, & Q \leq Q_L \\ Q = Q_L, & \text{else} \end{cases} \qquad \text{eq. A1–1}$$

where $h$ is the head at the conduit node, $H$ fixed head value (FH), $Q$ is the discharge at the boundary (negative values denote outflow), and $Q_L$ is the limiting flow rate (LQ).

### Modification of input files

The FHLQ boundary condition is activated and defined in the CFP input file (refer to *Shoemaker et al.*, 2008, p. 27 ff). The FHLQ functionality is activated by a keyword in **line 2** (previously '#Required comment line'). The keyword is FBC (further boundary conditions). Several keywords can be linked with a space or an underline "_", e.g. FBC_CADS or FBC CADS. In **line 27** (previously 'NO_N N_HEAD') further boundary conditions are defined. Next in line, a keyword defines the boundary condition type BC_TYPE ('x' = no further boundary condition, 'FHLQ' for the FHLQ boundary). After the FHLQ keyword the LQ value needs to be written. With this, line 27 reads now NO_N N_HEAD BC_TYPE LQ (in case BC_TYPE is FHLQ).

*Example input file:*

```
0.      #Required comment line
1.      1
2.      FBC
...
26.     #Node Head
27.     1       -1      x
        2       -1      x
        3       -1      x
        4       -1      x
        5       -1      x
        6       50.0    FHLQ 0.045
```

### Test and application examples

The FHLQ boundary condition functionality is demonstrated in test cases 5, 8, and 9 within section AT of this report.

# A2. WELL BOUNDARY CONDITION

*Newly developed for CFPv2 MODE1*

## Intention

This boundary condition can be used to apply pumping to a conduit node. Previously, this was done by recharge (RCH) combined with direct recharge percentage (CRCH). However, recharge rates for pumping need to be negative and, therefore, no diffuse recharge occurs in cells with intended pumping. Further, the well boundary condition allows noting pumping rates within the budget files separately.

## Modification of input files

The WELL boundary condition is activated and defined in the CFP input file (*Shoemaker et al.*, 2008, p. 27) and the CRCH input file (refer to *Shoemaker et al.*, 2008, p. 30).

The WELL functionality is activated by a keyword in **line 2** of the CFP input file (previously '#Required comment line'). The keyword is FBC (further boundary conditions). Several keywords can be linked with a space or an underline_ e.g. FBC CADS or FBC_CADS. In **line 27** of the CFP input file (previously 'NO_N N_HEAD') further boundary conditions are defined. Next in line, a keyword defines the boundary condition type BC_TYPE ('x' = no further boundary condition, 'WELL' for the WELL boundary).. With this, line 27 reads now NO_N N_HEAD BC_TYPE (in case BC_TYPE is WELL)

*Example CFP input file (well in node 5):*

```
0.      #Required comment line
1.      1
2.      FBC
...
26.     #Node Head
27.     1       -1      x
        2       -1      x
        3       -1      x
        4       -1      x
        5       -1      WELL
        6       50.0    x
```

The CRCH input file allows definition of pumping rates for every stress period. The intended pumping rates QWELL (positive for infiltration, negative for abstraction) are added in line after the fraction percentage of diffuse / direct recharge P_CRCH. The input reads now NODE_NUMBERS P_CRCH QWELL. Please not that QWELL needs a value of 0 in case the well is not active (i.e. during a recovery period).

*Example CRCH input file (pumping from node 5 with 0.25 $m^3s^{-1}$):*

```
0.      #Required comment line
1.        1
2.      1 0.000
        2 0.000
        3 0.000
        4 0.000
        5 0.000 -0.25
        6 0.000
```

## Test and application examples

The WELL boundary condition functionality is demonstrated in test cases 10 and 11 within section AT of this report.

# A3. CONDUIT-ASSOCIATED DRAINABLE STORAGE (CADS)

*Newly developed package for CFPv2 MODE1*

## Intention

Karst aquifers can be conceptualized in several ways. One common way is to represent the karst system by highly permeable conduits embedded in a low permeability matrix continuum (e.g. Király [1997]). Other concepts describe karst systems as pipes draining associated karstic storage whereas the matrix storage is negligible (e.g. Mangin [1994]). Depending on the investigated karst system as well as the considered time scale, all three karst features

- pipes,
- drainable storage (like caves, large fractures, and fissures), and
- matrix continuum,

can be significant. An obvious example is the large-scale pumping test by *Maréchal et al.* [2008], which demonstrates the drawdown reaction of conduit and matrix heads on long-term pumping. Therefore, this experiment can provide arguments for the presence of karst conduits, associated karstic storage (responsible for conduit drawdown), and matrix storage (responsible for matrix drawdown).

To consider drainable storage within CFP Mode 1, the CADS package (conduit-associated drainable storage) was developed. CAD storage is assumed to be in direct hydraulic contact with draining conduits so that

$$h_{conduit} = h_{CADS} \qquad \text{eq. A3–1}$$

with $h_{conduit}$ the head at the conduit node and $h_{CADS}$ the CADS head, which is also related to the conduit node. It is assumed that water released from the CADS due to head variations immediately enters the conduit resulting in additional discharge. The resulting flow rate from / to the CADS storage, $Q_{CADS}$, is considered as

$$Q_{CADS} = \frac{V_t - V_{t-\Delta t}}{\Delta t} \qquad \text{eq. A3–2}$$

where $V_t$ is the volume of the CAD storage at the time $t$ and $\Delta t$ is the time step size. Finally, the volume of the CADS is computed as

$$V_{CADS} = L_{CADS} W_{CADS} (h_{CADS} - z_{bottom});\ h_{CADS} > z_{bottom} \qquad \text{eq. A3–3}$$

where $L_{CADS}$ is the length, which is assumed to be equal to the length of the conduit, $W_{CADS}$ is the width of the CAD storage, and $z_{bottom}$ is the conduit bottom elevation. Figure A3–1 shows the conceptual implementation of CAD storage for a karst catchment.

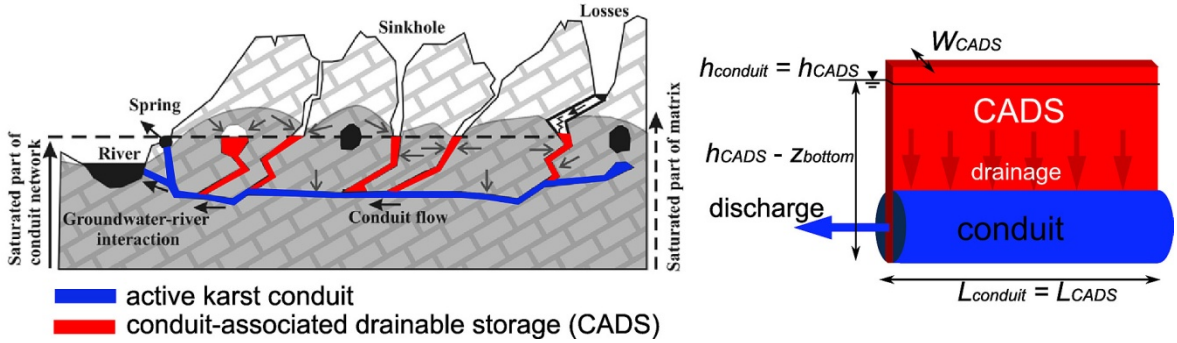


**Figure A3–1:** Conceptual implementation of CAD storage for a karst catchment, left figure modified from *Maréchal et al.* [2008].

## Modification of input files

The CAD storage is activated and defined in the CFP input file (see Shoemaker et al. 2008, pp. 27). The CADS functionality is activated by a keyword in **line 2** (previously '#Required comment line'). The keyword is CADS (conduit-associated drainable storage). Several keywords can be linked with a space or an underline_ e.g. FBC CADS or FBC_CADS. In **line 29** (previously 'NO_N K_EXCHANGE') the width of the CAD storage is defined. Next in line after the exchange coefficient the value of $W_{CADS}$ needs to be written. With this, line 29 reads now NO_N K_EXCHANGE W_CADS.

*Example input file with $W_{CADS}$ = 0.25 m:*

```
0.      #Required comment line
1.      1
2.      CADS
...
28.     #NODE K_EXCHANGE W_CADS
29.     1       0.000050        0.25
        2       0.000100        0.25
        3       0.000100        0.25
        4       0.000100        0.25
        5       0.000100        0.25
        6       0.000050        0.25
```

## Test examples

The CADS functionality is demonstrated in test cases 7 and 9 within section AT of this report.

## Application outlook

Potential application of the CADS functionality within CFPM1 is demonstrated by modeling large scale pumping test data. Measured data for such an experiment are available within literature [Maréchal et al., 2008]. Subsequently, the large scale pumping test scenario is abstracted to a simplified model to present the use of CFPM1 with CADS. A conceptual sketch of the model is shown in Figure A3–2. Parameters used are presented in Table A3–1.

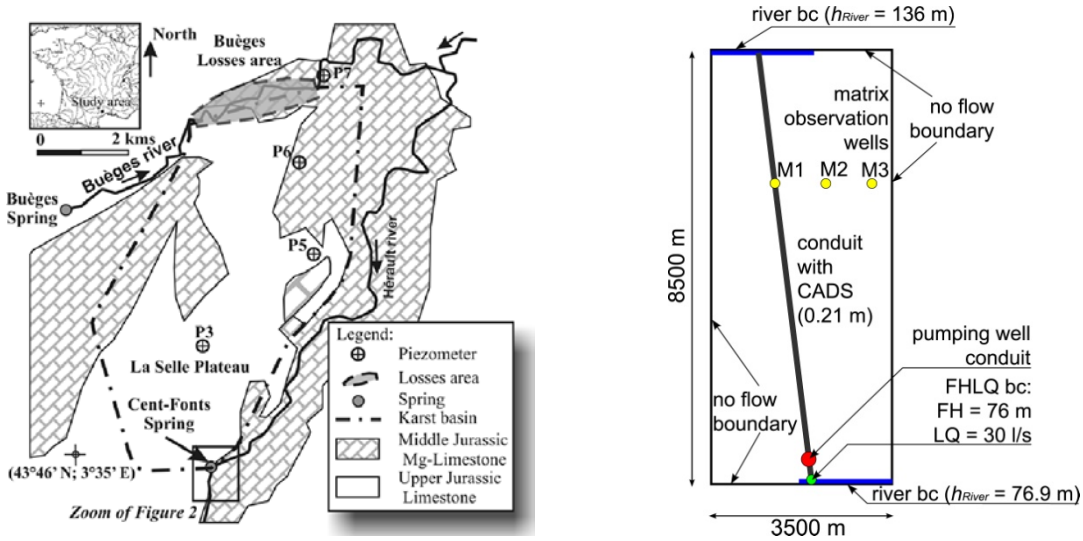


**Figure A3–2:** Left: Map of the catchment where the large scale pumping test was conducted [figure taken from *Maréchal et al.*, 2008]; right: Conceptual representation of the large scale pumping test scenario.

**Table A3–1:** Parameters used for the large scale pumping test model

| Parameter | Data from Maréchal et al. [2008] | Parameter for CFPM1 / CADS |
|---|---|---|
| **Matrix continuum** | | |
| area | 30 $km^2$ | 3.5 km x 8.5 km = 29.75 $km^2$; 35 x 85 cells with $\Delta x$ = $\Delta y$ = 100 m |
| top / bottom | | 250 m / -150 m |
| $T_m$ | 1.6 x $10^{-5}$ $m^2s^{-1}$ | |
| $K_m$ | | 9.0 x $10^{-6}$ $ms^{-1}$ |
| $S_m$ | 0.007 | 0.007 ($S_S$ = 0.00001) |
| **Conduit** | | |
| length | | ~ 9.1 km |
| diameter | | 3.5 m |
| roughness | | 0.01 m |
| $S_c$ (free surface area of de-watering conduit network) | 1900 $m^2$ | $S_C \sim A_{CADS}$; $W_{CADS}$ = 1900 $m^2$ / 9100 m = 0.21 m |
| pipe conductance ($\alpha$) | | 4.5 x $10^{-5}$ $m^2s^{-1}$ |
| time discretization | | P1: 1 day initialization (steady state)<br>P2: 32 days pumping (transient, d$t$ = 1h)<br>P3: 32 days recovery (transient, d$t$ = 1h) |
| diffuse recharge | | P1: 6.3376 x $10^{-9}$ $ms^{-1}$ (200 mm $a^{-1}$)<br>P2: 6.3376 x $10^{-9}$ $ms^{-1}$<br>P3: 6.3376 x $10^{-9}$ $ms^{-1}$ |

Results are presented in Figure A3–3 (computed and measured drawdown at the conduit and in the matrix) and Table A3–2 (computed flows for several compartments of the model).

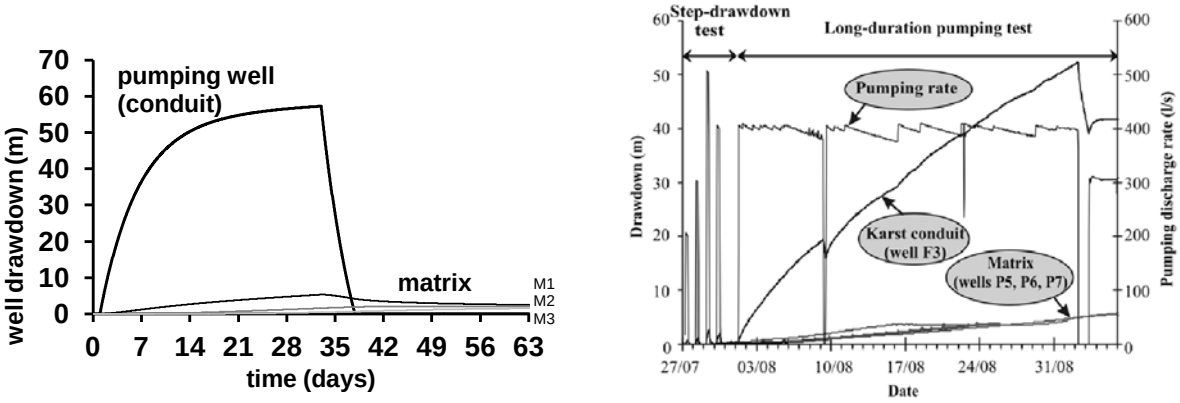


**Figure A3–3:** Left) computed drawdown for matrix and conduit; Right) measured drawdown during the large scale pumping test [figure taken from *Maréchal et al.*, 2008].

**Table A3–2:** Flow data for several model compartments

| Flow compartment | Data from Maréchal et al. [2008] | computed by CFPM1 / CADS |
|---|---|---|
| spring discharge (steady state) | ~0.250 $m^3s^{-1}$ | 0.148 $m^3s^{-1}$ |
| inflow Hérault (river bc, at the karst spring) | ~0.030 $m^3s^{-1}$ | 0.030 $m^3s^{-1}$ (FHLQ bc) |
| Bueges losses (river bc, at the origin of the conduit) | ~0.010 $m^3s^{-1}$ | 0.005 $m^3s^{-1}$ (steady state) up to 0.010 $m^3s^{-1}$ (during pumping) |
| matrix water inflow to conduits | ~0.240 $m^3s^{-1}$ | 0.147 $m^3s^{-1}$ (steady state) up to 0.367 $m^3s^{-1}$ (during pumping) |

Both drawdown and flow terms are reasonable and can be compared with the measured data from *Maréchal et al.* [2008]. Aberrations can occur because the model is very schematic and only little calibrated. Rather, this model application demonstrates the potential applicability of CFPM1 with CADS and the FHLQ boundary condition to represent long term pumping from karst water resources.

# A4. PARTIALLY FILLED PIPE STORAGE (PFPS)

*Newly developed for CFPv2 MODE1 based on existing subroutines to consider pipe storage budget*

## Intention

If pipes are partially filled (i.e. pipe bottom < head < pipe top), CFPM1 corrects the flow computation to consider partially filled pipes [*Shoemaker et al.*, 2008]. The water volume coming from / going to the pipe storage is computed for budget terms.

CFPM1 is modified to consider the partially filled pipe storage (PFPS) in the flow computation, i.e. PFPS is part of the active flow system resulting in additional discharge. Figure A4–1 gives a conceptual sketch of the PFPS implementation.

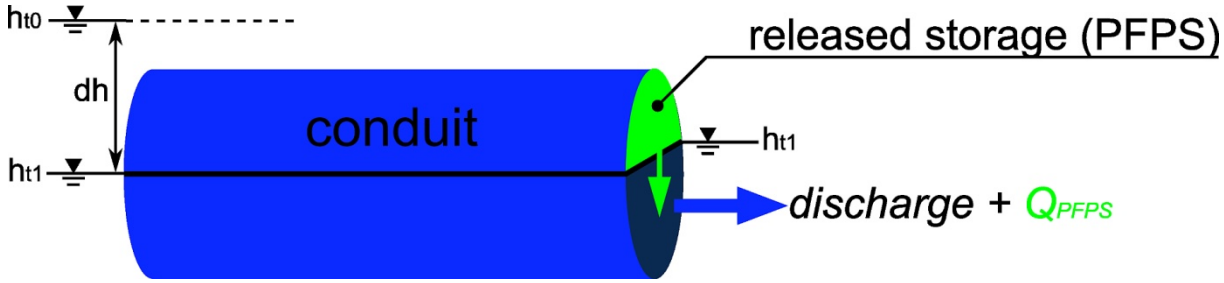


**Figure A4–1:** Conceptual implementation of PFP storage.

Similar to CADS (section A3), PFPS is considered as

$$Q_{PFPS} = \frac{V_{t1} - V_{t0}}{\Delta t} \qquad \text{eq. A4–1}$$

where $V_t$ is the volume at time $t$. Contrary to CADS, the volume is no longer a linear function of head. However, the finite difference of volume resulting from head change can be computed as

$$V_{t1} - V_{t0} = f(h_{t1}) - f(h_{t0}) = \frac{f\left(h_{t1}^{kiter-1}\right) - f(h_{t0})}{h_{t1}^{kiter-1} - h_{t0}} \left(h_{t1}^{kiter} - h_{t0}\right) \qquad \text{eq. A4–2}$$

The functional behavior $V = f(h)$ is described by *Shoemaker et al.* [2008], p. 8. Please note that PFPS doesn't consider dry pipes, i.e. if the head falls below the conduit bottom, PFPS is not active!

It should be noted that CFPM1 is not designed to compute karst hydraulics in partially filled conduits. The free-surface flow processes in partially filled pipes can result in very dynamic hydraulics with considerable effects due to inertia and momentum forces. The steady-state approach implemented in CFPM1 neglects dynamic processes, e.g. water released from PFPS is immediately part of the active flow system resulting in an immediate change of discharge. Therefore, flow computation with PFPS consideration can be unstable for some situations with too much water release from PFPS. For instance, strong head change or large conduit diameters:

→ result in increasing discharge ($Q_{overall}$ + $Q_{PFPS}$),
→ result in increasing heads,
→ result in filled conduits and, therefore, $Q_{PFPS}$ = 0.

## Test and application examples

The PFP storage consideration is demonstrated by test case 12 within section AT of this report.

# A5. CAUCHY BOUNDARY CONDITION

*Newly developed for CFPv2 MODE1*

## Intention

This boundary condition can be used to provide head-dependent flow to a node, similar to the River / GHB package in MODFLOW. Flow at the boundary $Q_{cy}$ is computed as

$$Q_{cy} = c_{cy}(h - h_{cy}) \qquad \text{eq. A5–1}$$

with $c_{cy}$ Cauchy conductance and $h_{cy}$ is Cauchy head. Negative values for $Q_{cy}$ denote inflow into the conduit system. Further, inflow can be limited by a CYLQ condition, similar to the FHLQ boundary described in section A1.

$$CYLQ = \begin{cases} Q = Q_{cy}, & Q \leq Q_L \\ Q = Q_L, & \text{else} \end{cases} \qquad \text{eq. A5–2}$$

The Cauchy boundary condition is fully implemented in CFP including heat and solute transport.

## Modification of input files

The CAUCHY boundary condition is activated and defined in the CFP input file (*Shoemaker et al.*, 2008, p. 27).

The CAUCHY functionality is activated by a keyword in **line 2** of the CFP input file (previously '#Required comment line'). The keyword is FBC (further boundary conditions). Several keywords can be linked with a space or an underline_ e.g. FBC CADS or FBC_CADS. In **line 27** of the CFP input file (previously 'NO_N N_HEAD') further boundary conditions are defined. Here, the head represents the Cauchy head $h_{cy}$. Next in line, a keyword defines the boundary condition type BC_TYPE ('x' = no further boundary condition, 'CAUCHY' for the Cauchy boundary). Next in line the Cauchy conductivity $c_{cy}$ and the Cauchy limited inflow needs to be written. With this, line 27 reads now NO_N HCY BC_TYPE CCY CYLQ (in case BC_TYPE is CAUCHY)

*Example CFP input file (Cauchy boundary in node 6):*

```
0.      #Required comment line
1.      1
2.      FBC
...
26.     #Node Head
27.     1       -1      x
        2       -1      x
        3       -1      x
        4       -1      x
        5       -1      x
        6       50.0    CAUCHY 2E-2 0.045
```

## Test and application examples

The CAUCHY boundary condition functionality is demonstrated in test cases 14 and 15 within the AT section of this report.

# A6. LIMITED HEAD BOUNDARY CONDITION (LH)

*Newly developed for CFPv2 MODE1*

## Intention

This boundary condition can be used to provide a limitation for the node-head, e.g. to represent a flooded sinkhole whereas the limited head is equivalent to the ground surface, Figure A6-1. The limited head (LH) boundary condition reads as

$$h_{LH} = \begin{cases} h\ computed\ (node\ is\ free\ flow), & h \le H_{LH} \\ h = H_{LH}\ (fixed\ head\ boundary), & \text{else} \end{cases} \qquad \text{eq. A6–1}$$

with $h_{LH}$ head at the limited head boundary node, $H_{LH}$ limited head. The LH boundary condition is fully implemented in CFP including heat and solute transport. Please note that LH boundaries cover only outflow situations and, therefore, are equivalent to FHLQ boundaries with LQ = 0 (but they allow to better trace water flow within budgets).

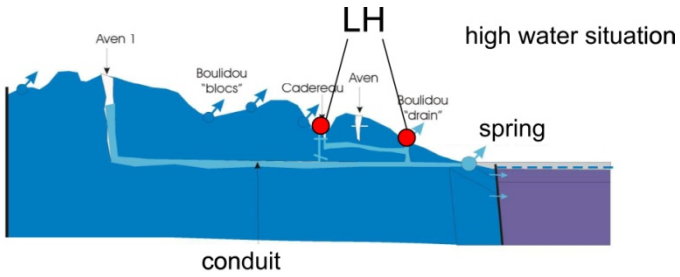


**Figure A6–1:** Conceptual application of the LH boundary (from Maréchal 2006).

## Modification of input files

The LH boundary condition is activated and defined in the CFP input file (*Shoemaker et al.*, 2008, p. 27). The LH functionality is activated by a keyword in **line 2** of the CFP input file (previously '#Required comment line'). The keyword is FBC (further boundary conditions). Several keywords can be linked with a space or an underline_ e.g. FBC CADS or FBC_CADS. In **line 27** of the CFP input file (previously 'NO_N N_HEAD') further boundary conditions are defined. Here, the head represents the limited head $H_{LH}$. Next in line, a keyword defines the boundary condition type BC_TYPE ('x' = no further boundary condition, 'LH' for the limited head boundary). With this, line 27 reads now NO_N HLH BC_TYPE (in case BC_TYPE is LH)

*Example CFP input file (LH boundary in node 3):*

```
0.      #Required comment line
1.      1
2.      FBC
...
26.     #Node Head
27.     1       -1      x
        2       -1      x
        3       60.0    LH
        4       -1      x
        5       -1      x
        6       50.0    x
```

## Test and application examples

The LH b.c. functionality is demonstrated in test cases 16 / 17 within the AT section of this report.

# A7. TIME DEPENDENT BOUNDARY CONDITIONS (TD)

*Newly developed for CFPv2 MODE1*

Karst conduits can react on boundary conditions very fast and sensitive because of their high conductivity. Consequently, transient models can require time dependent (TD) boundary conditions, e.g. pumping rates (Well boundary, see also Figure A3-3 left) or river stages (Cauchy boundary). Originally, time dependent input is considered by dividing the model time in several periods. However, for karst situations this can result in very inefficient input files with a large number of periods. To account for time dependent boundary conditions within one time period, CFPM1 was enhanced to read time dependent data from an external file and to iterate data for the respective model time step. This functionality is considered for the

- fixed head boundary,
- fixed head boundary with limited flow (head FH)
- well boundary (QWELL),
- Cauchy boundary (Cauchy head HCY).

Linear interpolation is done with an easy and straightforward approach as

$$x_t = \frac{t-t_p}{t_n-t_p}\left(x_n - x_p\right) + x_p \qquad \text{eq. A6–1}$$

with $x_t$ interpolated value at time $t$, $t_p$ time of previous data entry, $t_n$ time of next data entry, $x_p$ previous data entry and, $x_n$ next data entry.

## Modification of input files

Time dependent input data need to be saved in an external file (ASCII file). The structure of this file is shown in the following example:

*Example time dependent boundary data file:*

```
1.      3
2.      0       50
3.      1800    55
4.      3600    50
```

Line explanation

1) Number of data sets
2) this line and subsequent lines: time *t* and value *x(t)*. Time needs to be related to model time, beginning with 0. Please make sure that time dependent data enclose the overall model time.

The name of this external file has to be included in the NAM file (file type DATA; in the example below the file EXT1.txt with unit number 70).

*Example NAM file:*

```
CFP     57 SC.cfp
COC     59 SC.coc
DATA    70 EXT1.txt
```

The TD functionality of boundary conditions is activated within CFP input files (*Shoemaker et al.*, 2008, pp. 27) by the key-symbol TD (time dependent). The TD tag is directly added to the boundary notifier. The unit number of the external input file replaces originally time constant data, except the

well boundary, where the unit number is subsequently noted. The following examples demonstrate the activation of TD functionality for all supported boundary conditions:

*Example CFP input file(s); unit number for external data is 70:*

**Fixed head TD boundary in node 6** (*Shoemaker et al.*, 2008, p. 27)

```
...
26.     #Node Head
27.     1       -1      x
        ...
        6       70.0    TD
```

**FHLQ TD boundary in node 6** (see also section A1)

```
...
26.     #Node Head
27.     1       -1      x
        ...
        6       70.0    FHLQTD 1.0
```

**Cauchy TD boundary in node 6** (see also section A2)

```
...
26.     #Node Head
27.     1       -1      x
        ...
        6       70.0    CAUCHYTD 0.005 1.0
```

**Well TD boundary in node 6** (see also section A5)

```
...
26.     #Node Head
27.     1       -1      x
        ...
        5       -1      WELLTD 70
```

## Test and application examples

The TD functionality is demonstrated in test cases 18 within the AT section of this report.

## Application outlook

The large scale pumping test (Maréchal et al. 2008), already introduced in section A3, is used for an application outlook. Hence, measured pumping rates are considered as time dependent data (see also Figure A3-3 right) with a temporal resolution of 3 600 seconds. Results are presented in Figure A7-1. It is obvious that (1) variable pumping rates are correctly considered by the numerical model and (2) that this relative small variability can cause significant variation of well drawdown.

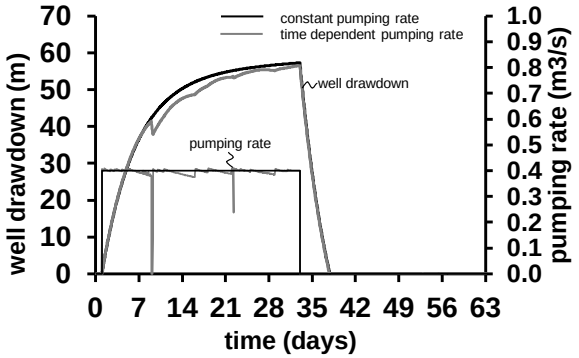


**Figure A7–1:** Application outlook of time dependent boundary conditions (pumping rate from Maréchal 2006; see also Figure A3-3).

# A8. MINOR MODIFICATIONS

Subsequently minor modifications are documented:

Time Series Analysis (TSA) output: This functionality provides an additional output file (TSA.out) that contains for every time step a list with all in- and outflow terms of the conduit. TSA output is activated within the Conduit Output Control (COC) file (Shoemaker et al. 2008, p. 30). Here, NNODES (line 2) need to be assigned as negative number.

*Example COC input file (NNODES is intended as 6)*

```
0.      #Required comment line
1.      #Required comment line
2.      -6
```

# B) SECOND PART – ADDITION OF TRANSPORT SUBROUTINES TO CFPM1

# B1. TRANSPORT MODELING IN CFPM1

This section aims to give an overview about heat and solute transport physics as well as about existing numerical routines to consider these processes. These existing routines provide the framework for the here reported adaptations and modifications. A detailed description of the physics in context with the CAVE hybrid model is given, amongst others, by *Birk* [2002] and *Birk et al.* [2005].

## B1.1 Physical framework

Some of the underlying processes for heat and solute transport are similar. For that reason, the subsequent part is organized in the following way: first, an overview about the boundary layer theory that describes the conduit-matrix interaction is given (section B1.1.1). Subsequently, transport processes for solutes (section B1.1.2; for common measures the index c is used) and heat (section B1.1.3, for common measures the index h is used) are specifically described.

### B1.1.1 Boundary layer theory

The bulk water flowing in the conduit interacts with the rock matrix. Such processes can be described by using the boundary layer theory. Several textbooks provide insights in this, for example *Incropera et al.* [2007]. Hence, a boundary layer of thickness $\varepsilon$ will separate the bulk water from the wall (i.e. the rock matrix). If water with uniform concentration respectively heat enters a conduit, a specific concentration respectively heat distribution will develop throughout the entrance region. Figure B1–1 illustrates boundary layer measures and processes.

Dimensionless numbers are used to describe the processes related with the concentration boundary layer. The ratio between kinematic viscosity of water $\nu_W$ and diffusion is expressed for solute transport as Schmidt number $N_{Sc}$

$$N_{Sc} = \frac{\nu_W}{D_{diff}} \qquad \text{eq. B1–1}$$

with $D_{diff}$ the coefficient of molecular diffusion of the solute in water. Equivalently for heat transport, the ration between kinematic viscosity and thermal diffusivity of water is expressed as Prandtl number $N_{Pr}$

$$N_{Pr} = \frac{\nu_W}{k_W} \qquad \text{eq. B1–2}$$

where $k_w$ is the thermal diffusivity of water, which is defined as:

$$k_w = \frac{\lambda_w}{\rho_w c_w}. \qquad \text{eq. B1–3}$$

whit $\rho_w$ water density, $c_w$ specific heat of water and $\lambda_w$ thermal conductivity of water. The dimensionless length within the concentration boundary layer $x^*$ is

$$x^* = \frac{x/d}{N_{Re} N_{DL}} \qquad \text{eq. B1–4}$$

where $x$ is the spatial coordinate in flow direction, $d$ is the conduit diameter, $N_{Re}$ is the well known Reynolds number, and $N_{DL}$ is the dimensionless number describing the ratio between kinematic viscosity of water and diffusion (Schmidt number $N_{Sc}$ for solute transport; Prandtl number $N_{Pr}$ for heat transport).

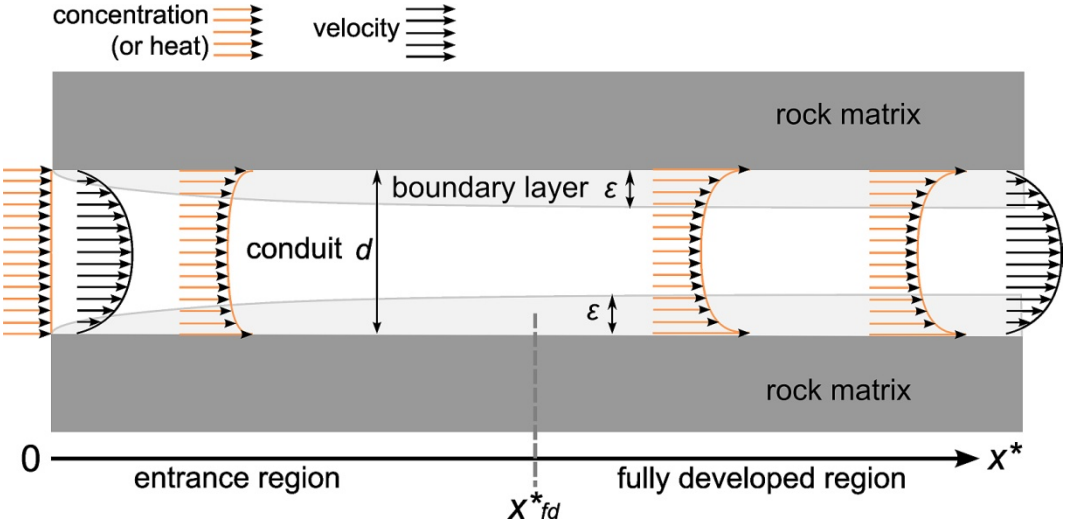


**Figure B1–1**: Conduit with developing boundary layer; $x^*_{fd}$ denotes the dimensionless length where the boundary layer is fully developed.

## B1.1.2 Physical framework for solute transport modeling

Subsequently, a condensed overview about physics describing solute transport in karst conduits is provided, which is mainly based on *Birk* [2002]. It should be noted that solution processes of the karst system (i.e. increased concentrations due to karstification) are neglected here meaning that the following equations are intended for short-scale processes.

Transport of solutes in conduits can be described with the one-dimensional advection-dispersion equation [*Clark*, 1996]

$$\frac{\partial C}{\partial t} = -v\frac{\partial C}{\partial x} + D_{dis}\frac{\partial^2 C}{\partial x^2} + S_C(x,t,C) \qquad \text{eq. B1–5}$$

where $C$ is the solute concentration, $D_{dis}$ is the dispersion coefficient, $t$ is time, $v$ is velocity, and $S_C$ is a source term representing the increase of solute mass due to reactions. As subsequently explained, the source term used here represents diffusive mass flux between the bulk water in the conduit and the matrix wall across the boundary layer.

Dispersion can occur for several reasons (e.g. mixing with immobile water), whereas the whole range of processes can be hardly covered (see also *Birk* [2002], p. 11 for further explanation). Commonly, the dispersion coefficient is determined based on dispersivity $\alpha$, which can be adjusted during model calibration:

$$D_{dis} = \alpha v \qquad \text{eq. B1–6}$$

A more physical approach to consider dispersion is provided by *Taylor* [1953] for laminar flow and by *Taylor* [1954] for turbulent flow. Therewith, laminar flow dispersion is computed as [*Taylor* 1953]

$$D_{dis} = \frac{a^2 v^2}{48 D_{diff}} \qquad \text{eq. B1–7}$$

where *a* is the conduit radius. Laminar dispersion as introduced by equation B1–7 is limited by $D_{Dis,l}$ according to the following relation [*Taylor*, 1953]:

$$\frac{L}{v_0} \gg \frac{a^2}{3{\cdot}8^2 D_{diff}} \qquad \text{eq. B1–8}$$

with *L* the conduit length and $v_0$ the maximum velocity in the middle of the conduit (according to *Taylor* [1954] the medium conduit velocity $v = 0.5 v_0$). Please refer to section B2, equations B2–2 and B2-3, for further details. The relevance of the limiting condition is illustrated by Figure B1–2. Therewith, it is assumable that laminar dispersion is limited with increasing conduit diameter.

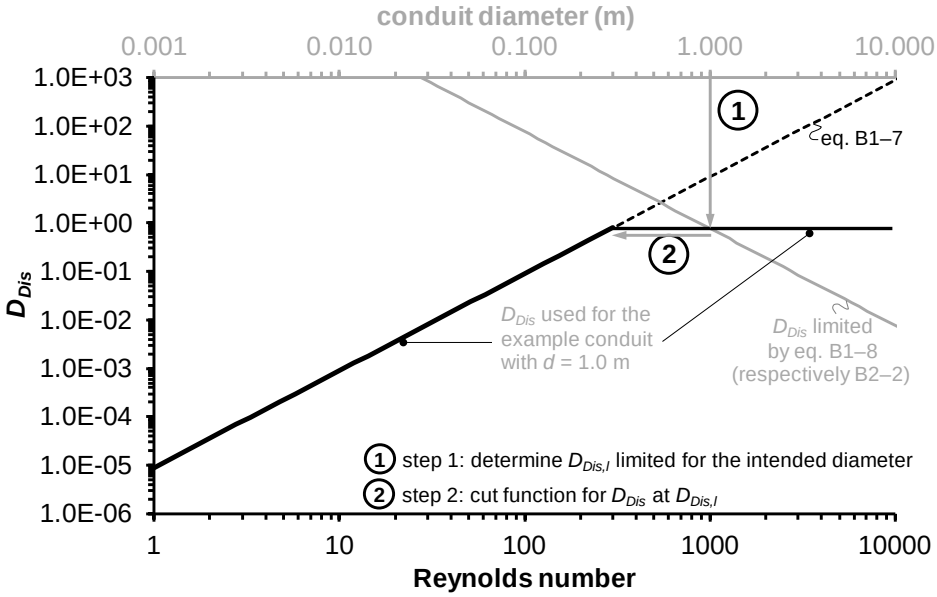


**Figure B1–2**: Laminar dispersion as function of the Reynolds number; the example for the conduit with *d* = 1.0 m demonstrate the limiting of $D_{Dis}$ by eq. B1–8.

Turbulent flow dispersion is computed as [*Taylor* 1954]

$$D_{dis} = 10.1 a v_* \qquad \text{eq. B1–9}$$

where friction velocity $v_*$ is given by the following equation:

$$v_* = \sqrt{\frac{\tau_0}{\rho_w}} = \sqrt{\frac{ag}{2}\frac{\Delta h}{L}} \qquad \text{eq. B1–10}$$

Here $\tau_0$ represents the wall shear stress.

Boundary layer processes, as described in section B1.1.1, are considered for solute transport. The thickness of the boundary layer can be expressed by the dimensionless Sherwood number as:

$$N_{Sh} = \frac{d}{\varepsilon_c} \qquad \text{eq. B1–11}$$

with $\varepsilon_c$ thickness of the concentration boundary layer. Diffusive mass flux $F_m$ across the boundary layer is described as [*Birk*, 2002]:

$$F_m = k(C_{r0} - C) \qquad \text{eq. B1–12}$$

where $k$ is the mass transfer coefficient and $C_{r0}$ is the concentration at the rock matrix surface. The mass transfer coefficient $k$ is expressed as

$$k = \frac{D_{diff}}{\varepsilon} = N_{Sh}\frac{D_{diff}}{d} \qquad \text{eq. B1–13}$$

The boundary layer develops downstream from the entrance region. At $x_c^*{}_{fd}$ it is assumed that the boundary layer is fully developed (see also Figure B1–1). For laminar flow, the entrance region is assumed for $x_c^* < 0.05$ respectively $x_c^*{}_{fd} \sim 0.05$ (see also equation B1–4). Outside of the entrance region, the Sherwood number representing the fully developed boundary region under the assumption of a constant wall concentration (and laminar flow) with

$$N_{Sh} = 3.66 \qquad \text{eq. B1–14}$$

Sherwood numbers at the entrance region can be much larger than for the fully developed region (compare equation B1–11). Several equations are available to compute laminar Sherwood numbers, for example from *Grigull and Tratz* [1965]

$$N_{Sh} = 3.66 + \frac{0.23616}{(x_c^*)^{0.488} exp(57.2 x_c^*)} \qquad \text{eq. B1–15}$$

Alternatively, the Sherwood number in the entrance region can be computed more easily as:

$$N_{Sh} = 1.08(x_c^*)^{-\frac{1}{3}} \qquad \text{eq. B1–16}$$

If $N_{Sh}$ in equation B1–16 falls below the value for the fully developed boundary (equation B1–14), $N_{Sh}$ = 3.66 is used. Figure B1–3 illustrates the behavior of the Sherwood number in the entrance region for laminar flow.

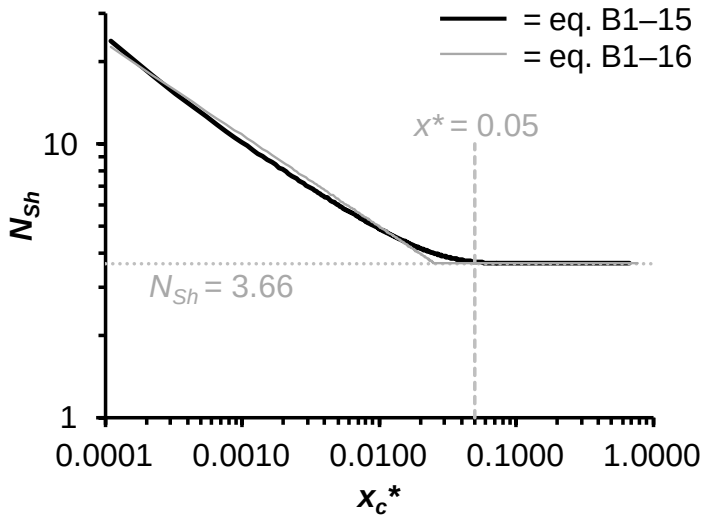


**Figure B1–3**: Sherwood number as function of the dimensionless length of the concentration boundary layer $x_c^*$.

The entrance region for turbulent flow is usually short with $10 < x/d < 60$ and, therefore, it is reasonable to assume an average Sherwood number valid for a fully developed boundary layer [*Incropera* et al., 2007]. Hence, the Sherwood number for turbulent flow is computed as [*Beek and Muttzall*, 1975]

$$N_{Sh} = 0.027 N_{Re}^{4/5} N_{Sc}^{1/3} \qquad \text{eq. B1–17}$$

or more accurately as [*Gnielinski*, 1976]

$$N_{Sh} = \frac{(f/8)(N_{Re}-1000)N_{Sc}}{1+12.7(f/8)^{1/2}\left(N_{Sc}^{2/3}-1\right)} \qquad \text{eq. B1–18}$$

where $f$ is the friction factor.

Finally, the resulting source term for a circular conduit is

$$S_C(x,t,C) = \frac{4}{d} F_m = \frac{4k(x,t)}{d}(C_{r0} - C) \qquad \text{eq. B1–19}$$

The concentration in the rock matrix (affecting conduit transport through the rock-surface concentration $C_{r0}$) can be further affected by diffusion and sorption processes within the rock matrix. For this reason, radial rock matrix diffusion with retardation (due to linear sorption) perpendicular to the x-axis is considered by:

$$R\frac{\partial C_r}{\partial t} = D_{diff,r}\left(\frac{\partial^2 C_r}{\partial r^2} + \frac{1}{r}\frac{\partial C_r}{\partial r}\right) \qquad \text{eq. B1–20}$$

with $R$ retardation factor (linear sorption; $R = 1 + \rho_r n_e^{-1} K_D$ with $\rho_r$ rock density, $n_e$ effective porosity, and $K_D$ linear sorption coefficient), $C_r$ concentration in the rock matrix, $D_{diff,r}$ diffusion coefficient within the rock matrix, and $r$ cylindrical coordinate. The pore diffusion coefficient in the rock matrix is computed as

$$D_{diff,r} = D_{aq} n_e^2 \qquad \text{eq. B1–21}$$

where $D_{aq}$ is the diffusion coefficient in water (here $D_{aq} = D_{diff}$).

The transport equations are solved by an explicit upwind finite-difference scheme [*Birk* 2002, *Birk et al.* 2005], whereas numerical dispersion is assumable. However, numerical dispersion can be determined as [*Birk et al.* 2005]:

$$D_{dis,num} = \frac{vL - v^2 \Delta t}{2} \qquad \text{eq. B1–22}$$

Therewith, the dispersion coefficient $D_{dis,mod}$ used by the numerical routines is corrected [*Birk et al.* 2005]:

$$D_{dis,mod} = D_{dis} - D_{dis,num};\ D_{dis,mod} \geq 0 \qquad \text{eq. B1–23}$$

## B 1.1.3 Physical framework for heat transport modeling

The heat transport functionality of CAVE is reported in detail by *Birk* [2002] pp. 17. Subsequently, a short overview based on *Birk* [2002] is presented. Boundary layer processes, as described in section B1.1.1, are considered for heat transfer between conduits and matrix. Therewith, heat transport is computed with the one-dimensional convection equation accounting for heat transfer across the thermal boundary layer between conduit wall and bulk water:

$$\frac{\partial T}{\partial t} = -v\frac{\partial T}{\partial x} + S_T(x,t,T) \qquad \text{eq. B1–24}$$

with $T$ water temperature in Kelvin and $S_T$ a source term representing heat transfer across the thermal boundary layer.

The dimensionless length within the thermal boundary layer $x_h^*$ is computed according equation B1–4. The thickness of the boundary layer can be expressed by the dimensionless Nusselt number $N_{Nu}$ (equivalent to the Sherwood number $N_{Sh}$ for concentration) as:

$$N_{Nu} = \frac{d}{\varepsilon_h} \qquad \text{eq. B1–25}$$

with $\varepsilon_h$ thickness of the thermal boundary layer. Heat flux $F_h$ across the boundary layer is computed as [*Birk*, 2002]:

$$F_h = h(T_{r0} - T) \qquad \text{eq. B1–26}$$

where $T_{r0}$ is rock temperature at the surface and $h$ is the heat transfer coefficient. This coefficient is computed as

$$h = N_{Nu}\frac{\lambda_w}{d}. \qquad \text{eq. B1–27}$$

As for the concentration boundary layer, the thermal boundary layer develops downstream from the entrance region (compare also Figure B1–1). At $x_h^{*}{}_{fd}$ it is assumed that the thermal boundary layer is fully developed. For laminar flow, the thermal entrance region is assumed for $x_h^* < 0.05$ respectively $x_h^{*}{}_{fd} \sim 0.05$. Outside of the entrance regions, the Nusselt number representing the fully developed boundary region under the assumption of a constant wall temperature (and laminar conditions) is

$$N_{Nu} = 3.66 \qquad \text{eq. B1–28}$$

The Nusselt number for the thermal entrance region can be computed as (compare also Figure B1–3)

$$N_{Nu} = 1.08(x_h^*)^{-\frac{1}{3}} \qquad \text{eq. B1–29}$$

For turbulent flow the Nusselt number is computed as [*Beek and Muttzall*, 1975]

$$N_{Nu} = 0.027N_{Re}^{4/5}N_{Pr}^{1/3} \qquad \text{eq. B1–30}$$

or more accurately as [*Gnielinski*, 1976]

$$N_{Nu} = \frac{(f/8)(N_{Re}-1000)N_{Pr}}{1+12.7(f/8)^{1/2}\left(N_{Pr}^{2/3}-1\right)} \qquad \text{eq. B1–31}$$

Finally, the resulting source term for a circular conduit is

$$S_T(x,t,T) = \frac{4}{d}F_h = \frac{4h(x,t)}{d\,c_w\rho_w}(T_{r0} - T). \qquad \text{eq. B1–32}$$

The rock temperature at the conduit surface $T_{r0}$ is further affected by heat conduction in the rock matrix. Consequently, heat conduction in the rock matrix influences the temperature in the conduit. For this reason, radial heat conduction in the rock perpendicular to the x-axis is considered by

$$\frac{\partial T_r}{\partial t} = k_r \left( \frac{\partial^2 T_r}{\partial r^2} + \frac{1}{r} \frac{\partial T_r}{\partial r} \right) \qquad \text{eq. B1–33}$$

where $T_r$ is rock temperature, $k_r$ is the thermal diffusivity of rock (computed similar to equation B1–3), and $r$ is the cylindrical coordinate. Finally, $T_r$ ($r$ = 0) is $T_{r0}$. The process is illustrated by Figure B1–4.

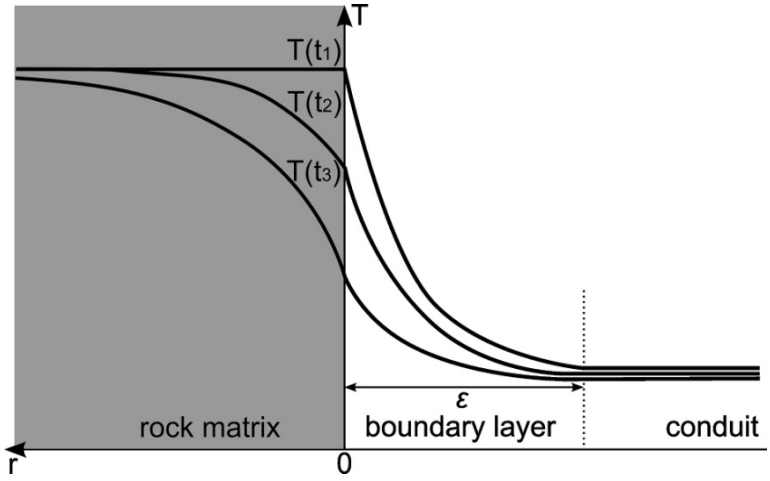


**Figure B1–4**: Temperature distribution in the conduit, across the thermal boundary layer, and in the rock matrix (with consideration of heat conduction in the rock matrix) for three times $t_1 < t_2 < t_3$ (Figure from *Birk* [2002]).

## B1.2. Consideration of transport processes for numerical karst modeling

### Overview

So far, two different ways to consider transport for the MODFLOW / CAVE hybrid models are existent and reported in the literature:

- CAVE contains transport modules that consider transport sequentially after each flow time step, e.g. *Liedl et al.* [2000], *Birk* [2002], *Bauer* [2001], *Birk et al.* [2005].
- UMT3D [*Spiessl*, 2004] compute transport independently based on flow terms, which are transferred with a link file (same way as MT3D does). The underlying flow model is CAVE too.

### Existing routines

CAVE 3.1 originated routines

**CAMT** - carbonate mass transport module: calculates advective mass transport in the conduit system (intended for use with the carbonate dissolution module **CAD2**; CAD2 calculates the rate of carbonate dissolution in the tubes and updates the tube diameter accordingly). These subroutines are used by CAVE 3.1; documentation available in the CAVE user guide (*Birk and Bauer* 2003; unpublished).

**MTM** - mass transport module: calculates advective mass transport in the conduit system (intended for use with the evaporite dissolution module **EDI**; EDI calculates the rate of gypsum dissolution). These subroutines are used by CAVE 3.1; documentation available in the CAVE user guide (*Birk and Bauer* 2003; unpublished).

**HTM** – heat transport module: simulates heat convection in the pipe network and heat conduction in the rock surrounding the pipes.

These subroutines are used by CAVE 3.1; documentation available in the CAVE user guide (*Birk and Bauer* 2003; unpublished).

## CAVE 3.47 originated routines

**CTM** – conduit transport module: calculates advective / dispersive mass transport with gypsum dissolution (further development of MTM and EDI with additional dispersion). This subroutine is used by CAVE 3.47.

**RTM** – reactive transport module: calculates advective / dispersive mass transport with matrix diffusion (linear sorption). In principle, RTM originates from CTM and HTM (for solutes instead heat but without dissolution). This subroutine is used by CAVE 3.47.

## UMT3D-originated routines

The concept and structure of UMT3D is quite similar to the continuum transport model MT3D as UMT3D is an enhanced version that additionally considers conduit transport. For that reason, the conduit flow model needs to be enhanced too in order to generate the necessary flow data for both conduit and matrix as input for the transport model. Further details are given in Figure B1–5.

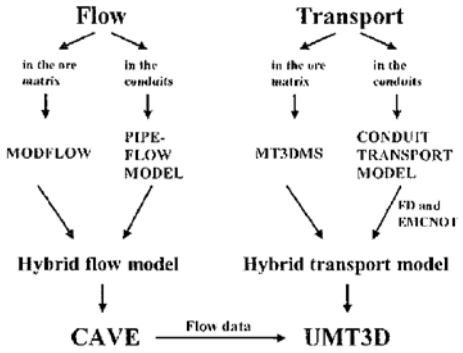


**Figure B1–5**: Model components of CAVE and UMT3D; from *Spiessl et al.* [2002]

*UMT3D: Flow model enhancement (CAVE)*

The flow model (in detail CAVE) was enhanced by a package named CONF. Three additional routines were placed in a source file named CONFLKMT5.f:

- GETHEADERCON: Gathers conduit flow model information relevant for the whole UMT3D simulation; called from CONFLKMT5.INC placed in the main code section
- CON2MTADV: Save conduit flow data to the conduit flow model (CAVE) – MT3D link file for use in the conduit transport module in UMT3D; called from CONFLKMT5.INC placed in the main code section
- CONSSOPTION: Check which conduit sink/source options are used in the flow model (CAVE) for every stress period and save it to the flow model (CAVE) – MT3D link file; this subroutine seems to be obsolete / is not called – functionality seems to be included in CON2MTADV

Further, the CONF package is activated in the main code section of MODFLOW / CAVE (main.f) as IUNIT 39. The include file CONFLKMT5.INC is considered in the main code section. The MODFLOW-MT3D link package was also enhanced to consider conduits – at least one subroutine (CON2MT1) was added. Data written to unformatted files are also stored in formatted files named "check_*"; this feature could be removed once the code is sufficiently tested.

*UMT3D: Transport model enhancement (MT3DMS 4)*

UMT3D is based on MT3DMS v.4, which is enhanced by several subroutines for conduit transport. The subroutines are saved in two source code files named fmi350con1.for and ssm350con1.for. The new subroutines are considered in the main file. Further adaptations are placed within several subroutines to consider conduits.

# B2. STM – ADAPTED PACKAGE FOR CFPM1 SOLUTE TRANSPORT SIMULATION

The STM package originated from the MTM package, which is existent in CAVE 3.47. The STM package considers advective-dispersive solute transport in conduits as well as diffusive mass transfer between the conduit and the rock matrix, i.e. through the boundary layer, together with retarded diffusive transport in the rock matrix. In case the CADS package is active, additional CAD storage is considered by a simple mixing approach. Solute exchange is coupled with $Q_{CADS}$. The mass load is computed with the conduit concentration for flow from the conduit to the CADS, and with the CADS concentration for flow from the CADS to the conduit. The initial concentration for the CADS corresponds to the initial concentration of the rock matrix. The concentration within the CADS $c_{CADS}$ is computed based on the CADS volume as

$$c_{CADS} = \frac{M_{CADS}}{V_{CADS}} \qquad \text{eq. B2–1}$$

with $M_{cads}$ solute mass inside CADS. It is obvious that this very simple approach can result in some inadequate results, e.g. artificial dilution inside CADS if $V_{CADS}$ is large.

## Solute Transport Input Files

Two additional input files, STM and SOC, are necessary to run the solute transport module. Names of these packages and of intended output files need to be included in the MODFLOW NAM file. Similar to the CFP flow model, time dependent boundary conditions can be included (see also section A7).

### Input instructions for the MODFLOW name file - NAM

*Example NAM file:*

```
...
STM   61 SC.stm
SOC   62 SC.soc
DATA  43 C_RESULT.txt
DATA  45 C_NODE.txt
DATA  47 C_BUDGET.txt
...
```

The input structure of the STM and SOC packages are described subsequently. In principle, input files are explained in the CAVE user guide (*Birk and Bauer*, 2003; unpublished); the following text is based on the CAVE user guide (*Birk and Bauer*, 2003; unpublished) and only slightly adapted. Changes in the input files (in comparison to CAVE): STM asks for number of tube sections; CAVE uses this value from the conduit file (= number of segments).

### Input instructions for the SOLUTE TRANSPORT MODULE - STM

FTYPE in the name file: **STM**

Description: Simulates advective / dispersive transport in the pipe network and matrix diffusion in the rock surrounding the pipes.

*Example input file:* The numbers (e.g. '1)') in the first column do not belong to the files. They are only included for reference.

```
1)      #NUMBER OF CELLS PER TUBE
        250
2)      #NUMBER OF NODES IN THE ROCK MATRIX
        30
3)      #CELL INCREMENT OF ROCK MATRIX IN M
        0.0002
4)      #INITIAL CONCENTRATION IN ROCK MATRIX
        0
5)      #DENSITY OF ROCK IN KG/L
        2.7
6)      #EFFECTIVE POROSITY
        0.1
7)      #KD IN L/KG
        0
8)      #DIFFUSION COEFFICIENT (IN WATER) IN M**2/S
        1E-9
9)      #SHERWOOD NUMBER IN LAMINAR FLOW (FLAG)
        -1
10)     #SHERWOOD NUMBER IN TURBULENT FLOW (FLAG)
        1
11)     #DISPERSION (FLAG): DISPERSION COEFFICIENT IS CALCULATED
        # <0  => BASED ON FLOW DATA ACCORDING TO TAYLOR (1953, 1954)
        # >=0 => D_dis= VALUE * VELOCITY, I.E., VALUE=DISPERSIVITY
        -1
        #
        #----------------STRESS PERIOD DATA----------------
12)     #CONCENTRATION OF DIRECT RECHARGE
        1000
13)     #CONCENTRATION OF WELL RECHARGE
        0
14)     #CONCENTRATION OF CAUCHY BC
        0
15)     #CONCENTRATION OF FIXED HEAD / FHLQ
        1000
16)     #CONCENTRATION OF INFLOW FROM FISSURED SYSTEM
        0
17)     #FIXED ONCENTRATION NODES?
        -1
18)     #ENTRY LENGTH DATA SET
        1
        2      5
19)     #STRESS PERIOD DATA VALID UNTIL STRESS PERIOD
        2
```

Lines starting with # are comment lines. You are allowed to include as many comment lines (starting with #) as you like. Additional explanations regarding spatial discretization (lines 1 to 3) are given in Figure B2–1.

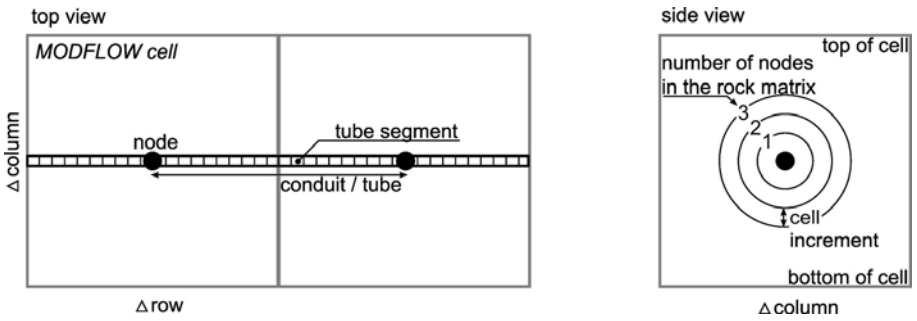


**Figure B2–1**: Some explanation regarding discretization of tubes and the surrounding rock matrix.

**1)** **Subdivision of the tubes** for the calculation of heat transport processes. In the example one flow tube consists of 250 segments.

**2)** **Number of nodes** in the rock matrix, i.e. the spatial discretization of the rock surrounding the pipes.

**3)** **Cell increment for the finite difference grid of the rock matrix**. Multiplying this value by the number of nodes, i.e. '2)', yields approximately the distance from the pipes to the outer boundary for the diffusion calculation. Be sure that this distance is large enough so that the solute transport across the boundary is negligible.

**4)** **Concentration in the rock matrix water**. This value is the initial concentration in the rock matrix water as well as the concentration in the rock matrix water at the outer boundary for the matrix diffusion calculation.

**5)** **Bulk density of the rock** in kg/l (note: l = liter = $m^3$/1000)

**6)** **Effective porosity of the rock matrix**.

**7)** ***$K_D$* value** in l/kg (linear Henry sorption; note: l = liter = $m^3$/1000)

**8)** **Diffusion coefficient in water** in $m^2$/s

**9)** **Flag for Sherwood number computation in laminar conditions**. The Sherwood number is greater in the entrance region where the boundary layer is not fully developed yet. The Sherwood number in the entrance region is a function of distance to the entry point (see also Figure B1–2). Finally, the length of the entrance region is a function of discharge respectively the resulting Reynolds Number and diffusion. The functional behavior for a diffusion coefficient of $D_{Diff}$ = 2E-9 $m^2$/s is shown in Figure B2–2. It is obvious that for large diameter pipes with relatively high laminar Reynolds numbers the entrance region length could extend several meters.

Three different methods for the calculation of the Sherwood number under laminar flow conditions are implemented:

0 Sherwood number equals 3.66, i.e. a fully developed boundary layer according to equation B1–14; suitable for situations with expected short entrance region (compare Figure B2–2)

-1 the Sherwood number will be calculated depending on the distance from the tube entrance according to equation B1–16, i.e. near the tube entrance or possibly all along the tube the Sherwood number is greater than 3.66. The distance of nodes to the entrance point needs to be provided for every stress period in line 17).

>0 an average Sherwood number for a distance from the entry point specified here is calculated. If this value is chosen very large $N_{Sh}$ = 3.66, otherwise it is greater than 3.66; suitable for situations where the expected entrance region length is much longer than the extension of the conduit network (compare Figure B2–2).

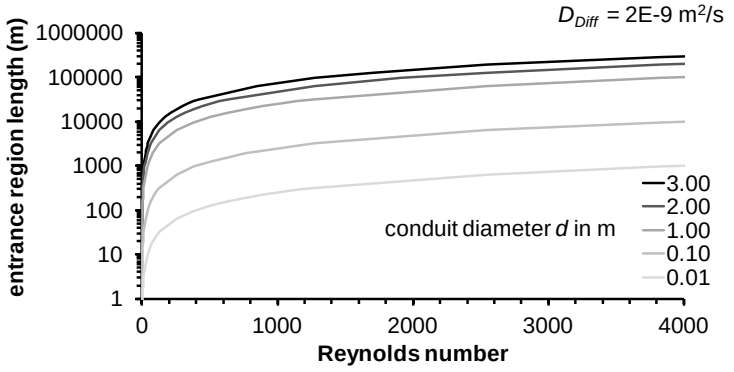


**Figure B2–2**: Entrance region length for the concentration boundary layer as function of Reynolds number

**10) Flag for Sherwood number computation in turbulent conditions**

0 equation B1–18 according to *Gnielinski et al.* [1976] is used (more accurately)

1 equation B1–17 according to *Beek and Muttzall* [1975] is used

**11) Flag for dispersion**

<0 Dispersion is computed with equation B1–7 for laminar conditions and equation B1–9 for turbulent conditions

>= 0 Value for dispersivity $\alpha$ according to equation B1–6

**12) Concentration of recharge**. Here (as well as for 13) to 17)) it is possible to specify a different value for each node by setting the value greater than 1E6 and specifying the values for each node (beginning with node 1) in the following lines (one line for each value).
Concentrations can be considered as time dependent data read from an external file (as well as for 13) to 17)). The TD functionality is activated by the TD key symbol followed by the unit number of external input. For further details refer to section A7. As described above, concentration can be considered as uniform value for all nodes ("bulk") as well as individual value for each node ("array"). Time dependent data can be used in this context (i.e. time dependence for all nodes or time dependent concentrations for specific nodes.) Time dependent input is read only at the beginning, if TD data are read as "bulk". Contrary, if data are read as "array" it is necessary to specify data also for subsequent periods.

**13) Concentration of well recharge** flowing to a node, which represents a well.

**14) Concentration of inflow through Cauchy** boundary cells.

**15) Concentration of inflow through fixed head / FHLQ** boundary.

**16) Concentration of water flowing from the fissured system** into the pipes.

**17) Fixed concentration nodes**. If this parameter is < 0 the concentration at the node is calculated, otherwise the entered value is a fixed concentration.

**18) Entry length data set** to determine the distance between an entry point and the here specified nodes. Line 17) is only active if the flag for the Sherwood number computation in line 9) is set to -1. The following data needs to be provided:

NLINES is the number of lines following

N XSENTRY with N node number and XSENTRY distance to the entry point

Nodes that are not specified here are assumed to have a fully developed boundary layer, i.e. the distance is set to 1E12 m and, therefore, the Sherwood number is set to 3.66.

**19)** Since 12) - 18) can be changed for each stress period, it is necessary to specify how long the values entered above are valid. The values are valid till the stress period number entered here is reached. Then stress period items 12) - 18) are required again. Note that the value of the last entry of this file must be at least equal to the number of stress periods in your simulation!

## Input instructions for the SOLUTE TRANSPORT OUTPUT CONTROL

FTYPE in the name file: SOC

Description: Output control for the Solute Transport Package STM. All output is specified in the SOC input file, i.e. whenever STM is used this package has to be used either.

*Example Input file:* The numbers (e.g. '1)') in the first column do not belong to the files. They are only included for reference.

```
1)      #UNIT NUMBER FOR OUTPUT OF NODE CONCENTRATION AFTER TRANSPORT TIME STEPS
        46
2)      #NUMBER OF NODES FOR OUTPUT (-1 = ALL NODES) / SUBSEQUENT LINES NODE NUMBER
        2
        1
        4
3)      #OUTPUT EACH ... TRANSPORT TIME STEP
        1
4)      #UNIT NUMBER FOR OUTPUT OF STM BUDGET AFTER TRANSPORT TIME STEPS
        47
5)      #OUTPUT EACH ... TRANSPORT TIME STEP
        1
6)      #UNIT NUMBER FOR SOLUTE TRANSPORT OUTPUT AFTER FLOW TIME STEPS
        43
7)      #OUTPUT EACH ... FLOW TIME STEP
        1
8)      #UNIT NUMBER FOR STM NODE MASS BUDGET OUTPUT AFTER FLOW TIME STEPS
        43
9)      #OUTPUT EACH ... FLOW TIME STEP
        1
10)     #UNIT NUMBER FOR OUTPUT OF CADS CONCENTRATION AFTER FLOW TIME STEPS
        49
11)     #OUTPUT EACH ... FLOW TIME STEP
        1
```

Lines starting with # are comment lines. You are allowed to include as many comment lines (starting with #) as you like.

**1)** **Unit number to which the concentrations will be written**. Note that this unit number has to be opened by a statement in the name file. This unit number is the only entry required by SOC. If nothing else is specified for the following items the default values will be used, e.g. if the input file includes only three numbers (one per line) the default values are used for lines 4) - 11).

**2)** **Specification of output nodes**; first line is the maximum number of output nodes, whereas the specific node numbers are listed in the subsequent lines (each node one line). A value of -1 for the maximum number of nodes gives output for all nodes.

**3)** **Frequency of output**. In the given example, node concentrations will be written after each … transport time step (default: 1).

**4)** **Unit number for output of STM budget** data after transport time steps (default: 0, i.e. no output will be written).

**5)** **Frequency of STM budget output**, i.e. output after each ... transport time step (default: 1).

**6)** **Unit number for output of solute transport data** after flow time steps (default: 0, i.e. no output will be written).

**7)** **Frequency of solute transport data output**, i.e. output after each ... flow time step (default: 1).

**8)** **Unit number for output of solute mass budget** after flow time steps (default: 0, i.e. no output will be written).

**9)** **Frequency of solute mass budget output**, i.e. output after each ... flow time step (default: 1).

**10)** **Unit number to which the concentration within the CADS** will be written. Note that this unit number has to be opened by a statement in the name file (default 0).

**11)** **Frequency of CADS concentration output**, i.e. output after each … flow time step (default: 1).

## Further modifications

The STM module was further modified. Some changes are listed subsequently:

- Computation of Taylor dispersion modified / subroutine DISPCALC:
  - Turbulent conditions: $D_{dis*}$ computed according to equations B1–9 / B1–10
  - Laminar conditions: It is checked whether the limiting condition as defined by the right-hand side of equation B1–8 is exceeded by one order of magnitude. For this reason, the following condition is checked

$$10\frac{L}{v} > \frac{a^2}{192 D_{diff}} \qquad \text{eq. B2–2}$$

    → A maximum laminar Taylor dispersion coefficient is calculated in case the limiting condition is exceeded:

$$D_{dis} = 19200\frac{D_{diff}L^2}{a^2} \qquad \text{eq. B2–3}$$

    → Limiting condition not exceeded: $D_{dis}$ computed according to equation B1–7.
- Implementation of budget terms for rates and cumulative flow; an additional mass transport budget is computed including details regarding mass balance errors.
- Mass transfer over a fixed head boundary condition additionally considers dispersive mass flux.
- Implementation of the well boundary condition.
- Implementation of the possibility to produce output for specific nodes.
- Consideration of fixed head concentrations for inflow.

# TEST EXAMPLES

The STM functionality is demonstrated in test case TRANSPORT_02. Please refer to the separate documentation of test cases in section BT.

# B3. HTM – ADAPTED PACKAGE FOR CFPM1 HEAT TRANSPORT SIMULATION

The HTM package is intended to compute heat transport in pipes accounting for convection and heat transfer into / out of the rock matrix as well as conductive heat transport in the rock matrix. The HTM package is based on routines from CAVE, which were slightly adapted respectively modified. In case the CADS package is active, additional CAD storage is considered by a simple mixing approach. Heat exchange is coupled with $Q_{CADS}$. The energy load is computed with the conduit temperature for flow from the conduit to the CADS, and with the CADS temperature for flow from the CADS to the conduit. The initial temperature for the CADS corresponds to the initial temperature of the rock matrix. The temperature within the CADS $T_{CADS}$ is computed based on the CADS volume as

$$T_{CADS} = \frac{H_{CADS}}{c\rho V_{CADS}} \qquad \text{eq. B3–1}$$

with $H_{cads}$ heat inside CADS, $c$ specific heat capacity of water, and $\rho$ water density. It is obvious that this very simple approach can result in some inadequate results, e.g. artificial temperature change inside CADS if $V_{CADS}$ is large.

## Heat Transport Input Files

To run the heat transport module two additional input files, HTM and HOC, are necessary. Names of these packages and of intended output files need to be included in the MODFLOW NAM file.

### Input instructions for the MODFLOW name file - NAM

*Example NAM file:*

```
...
HTM   61 SC.htm
HOC   62 SC.hoc
DATA  43 HEAT_RESULT.txt
DATA  45 HEAT_NODE.txt
...
```

The input structure of the HTM and HOC packages are described subsequently. In principle, input files are explained in the CAVE user guide (*Birk and Bauer*, 2003; unpublished); the following text is based on the CAVE user guide (*Birk and Bauer*, 2003; unpublished) and only slightly adapted. Changes in the input files: HTM asks for number of tube sections; CAVE uses this value from the conduit file (= number of segments).

### Input instructions for the HEAT TRANSPORT MODULE - HTM

FTYPE in the name file: **HTM**

Description: Simulates heat convection in the pipe network and heat conduction in the rock surrounding the pipes.

*Example input file:* The numbers (e.g. '1)') in the first column do not belong to the files. They are only included for reference.

```
1)      #NUMBER OF TUBE SECTIONS
```

```
        100
2)      #NUMBER OF NODES IN THE ROCK MATRIX
        20
3)      #CELL INCREMENT OF ROCK MATRIX IN M
        0.02
4)      #ROCK TEMPERATURE IN °C
        8
5)      #DENSITY OF ROCK IN KG/M^3
        2300
6)      #SPECIFIC HEAT CAPACITY OF ROCK IN J/(KG K)
        810
7)      #THERMAL CONDUCTIVITY OF ROCK IN W/(M K)
        2.15
8)      #SPECIFIC HEAT CAPACITY OF WATER IN J/(KG K)
        4200
9)      #THERMAL CONDUCTIVITY OF WATER IN W/(M K)
        .58
10)     #EQUATION FOR NUSSELT NUMBER IN LAMINAR FLOW (FLAG)
        -1
11)     #EQUATION FOR NUSSELT NUMBER IN TURBULENT FLOW (FLAG)
        1
        #----------------STRESS PERIOD DATA----------------
12)     #TEMPERATURE OF DIRECT RECHARGE IN °C
        6
13)     #TEMPERATUR OF WELL RECHARGE IN °C
        6
14)     #TEMPERATUR OF CAUCHY BC IN °C
        6
15)     #TEMPERATURE OF FIXED HEAD / FHLQ IN °C
        6
16)     #TEMPERATURE OF INFLOW FROM FISSURED SYSTEM
        8
17)     #FIXED TEMPERATURE NODES?
        -1
18)     #ENTRY LENGTH DATA SET
        1
        2       5
19)     #STRESS PERIOD DATA VALID UNTIL STRESS PERIOD
        2
```

Lines starting with # are comment lines. You are allowed to include as many comment lines (starting with #) as you like. Items 1) - 11) contain data for the entire simulation, items 12) - 19) contain the stress period data (i.e. data which can be specified for each stress period). Figure B2–1 in the previous section gives some additional explanation regarding spatial discretization.

**1)** **Subdivision of the tubes** for the calculation of heat transport processes. In the example one flow tube consists of 100 segments.

**2)** **Number of nodes in the rock matrix**, i.e. the spatial discretization of the rock surrounding the pipes; also compare equation B1–34.

**3)** **Cell increment for the finite difference grid of the rock matrix**. Multiplying this value by the number of nodes, i.e. '2)', yields approximately the distance from the pipes to the outer boundary for the conduction calculation. Be sure that this distance is large enough so that the heat flow across the boundary is negligible; also compare equation B1–33.

**4)** **Rock temperature in °C**. This value is the initial rock temperature as well as the rock temperature at the outer boundary for the heat conduction calculation. This value is also the initial temperature in conduits.

**5)** **Bulk density of the rock** $\rho_r$ in kg/m$^3$.

**6)** **Specific heat capacity of the rock** $c_r$ in J/(kg K).

**7)** **Thermal conductivity of rock** $\lambda_r$ in W/(m K).

**8)** **Specific heat capacity of water** $c_w$ in J/(kg K).

**9)** **Thermal conductivity of water** $\lambda_w$ in W/(m K).

**10)** **Flag** for the calculation of the **Nusselt number in laminar** flow. The Nusselt number is greater in the entrance region where the boundary layer is not fully developed yet. The Nusselt number in the entrance region is a function of distance to the entry point. Finally, the length of the entrance region is a function of discharge respectively the resulting Reynolds Number and diffusion. The functional behavior for a diffusion of $D_{Diff}$ = 1.39E-7 m$^2$/s is shown in Figure B3–1. It is obvious that for large diameter pipes with relatively high laminar Reynolds numbers the entrance region length could extend several meters. Three different methods for the calculation of the Nusselt number under laminar flow conditions are implemented:

0 Nusselt number equals 3.66, i.e. a fully developed thermal boundary layer according to equation B1–28; suitable for situations with expected short entrance region (compare Figure B3–1)

-1 the Nusselt number will be calculated depending on the distance from the tube entrance according to equation B1–29, i.e. near the tube entrance or possibly all along the tube the Nusselt number is greater than 3.66. The distance of nodes to the entrance point needs to be provided for every stress period in line 17).

>0 an average Nusselt number for a distance from the entry point specified here is calculated. If this value is chosen very large $N_{Nu}$ = 3.66, otherwise it is greater than 3.66; suitable for situations where the expected entrance region length is much longer than the extension of the conduit network (compare Figure B3–1).

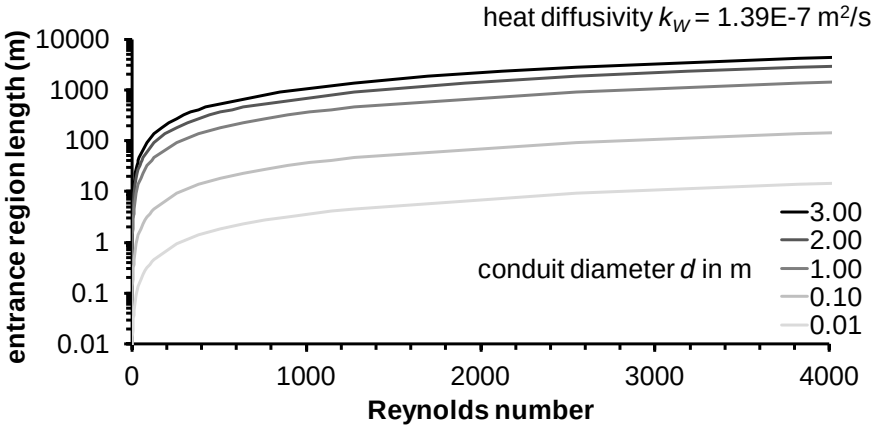


**Figure B3–1**: Entrance region length for the heat boundary layer as function of Reynolds number

**11)** **Flag** for the calculation of the **Nusselt number under turbulent** flow conditions.

0 equation B1–31 according to *Gnielinski et al.* [1976] is used (more accurately)

1 equation B1–30 according to *Beek and Muttzall* [1975] is used

**12)** **Temperature of recharge** (in °C). Here (as well as for 13) to 17)) it is possible to specify a different value for each node by setting the value greater than 1E6 and specifying the values for each node (beginning with node 1) in the following lines (one line for each value).

Temperatures can be considered as time dependent data, read from an external file (as well as for 13) to 17)). The TD functionality is activated by the TD key symbol followed by the unit number of external input. For further details refer to section A7. As described above, temperatures can be considered as uniform value for all nodes ("bulk") as well as individual value for each node ("array"). Time dependent data can be used in this context (i.e. time dependence for

all nodes or time dependent concentrations for specific nodes.) Time dependent input is read only at the beginning, if TD data are read as "bulk". Contrary, if data are read as "array" it is necessary to specify data also for subsequent periods.

**13)** **Temperature of well recharge** (in °C) flowing to a node, which represents a well.

**14)** **Temperature of CAUCHY inflow** (in °C) flowing to a node, which represents a Cauchy bc.

**15)** **Temperature of fixed head /FHLQ inflow** (in °C) flowing to a node.

**16)** **Temperature** (°C) of **water** flowing **from the fissured system** into the pipes.

**17)** **Fixed temperature nodes**. If this parameter is < 0 the temperature at the node is calculated, otherwise the entered value is a fixed temperature.

**18)** Entry length data set to determine the distance between an entry point and the here specified nodes. Line 17) is only active if the flag for the Nusselt number computation in line 10) is set to -1. The following data needs to be provided:

NLINES is the number of lines following

N XHENTRY with N node number and XHENTRY distance to the entry point

Nodes that are not specified here are assumed to have a fully developed boundary layer, i.e. the distance is set to 1E12 m and, therefore, the Nusselt number is set to 3.66.

**19)** Since 12) - 18) can be changed for each stress period, it is necessary to specify how long the values entered above are valid. The values are valid till the stress period number entered here is reached. Then stress period items 12) - 18) are required again. In the examples the stress period data are valid over the entire simulation time consisting of two stress periods. Note that the value of the last entry of this file must be at least equal to the number of stress periods in your simulation!

## Input instructions for the HEAT TRANSPORT OUTPUT CONTROL - HOC

FTYPE in the name file: **HOC**

Description: Output control for the Heat Transport Package HTM. All output is specified in the HOC input file, i.e. whenever HTM is used this package has to be used either.

*Input file:* the numbers (e.g. '1)') in the first column do not belong to the **files**. They are only included for reference.)

```
1)    #UNIT NUMBER FOR OUTPUT OF NODE TEMPERATURE
      45
2)    #NUMBER OF NODES FOR OUTPUT (-1 = ALL NODES) / SUBSEQUENT LINES NODE NUMBER
      2
      1
      4
3)    #OUTPUT EACH ... TRANSPORT TIME STEP
      1
4)    #UNIT NUMBER FOR HEAT TRANSPORT OUTPUT AFTER FLOW TIME STEPS
      43
5)    #OUTPUT EACH ... FLOW TIME STEP
      1
6)    #UNIT NUMBER FOR HEAT BUDGET OUTPUT AFTER FLOW TIME STEPS
      43
7)    #OUTPUT EACH ... FLOW TIME STEP
      1
12)   #UNIT NUMBER FOR OUTPUT OF CADS CONCENTRATION AFTER FLOW TIME STEPS
      49
13)   #OUTPUT EACH ... FLOW TIME STEP
      1
```

Lines starting with # are comment lines. You are allowed to include as many comment lines (starting with #) as you like.

**1)** **Unit number** to which the temperatures will be written. Note that this (and the following) unit number has to be opened by a statement in the **name file**, e.g.

*DATA 45 tnode.txt*

This unit number is the only entry required by HOC. If nothing else is specified for the following items the default values will be used, e.g. if the input file includes only three numbers (one per line) the default values are used for lines 4)-9).

**2)** **Specification of output nodes**; first line is the maximum number of output nodes, whereas the specific node numbers are listed in the subsequent lines (each node one line). A value of -1 for the maximum number of nodes gives output for all nodes.

**3)** **Frequency of output**. In the given example, node temperatures will be written after each … transport time step (default: 1).

**4)** **Unit number** for output of heat transport data after flow time steps (default: 0, i.e. no output will be written).

**5)** **Frequency of output**, i.e. heat transport output data after each ... flow time step (default: 1).

**6)** **Unit number** for output of heat budget after flow time steps (default: 0, i.e. no output will be written).

**7)** **Frequency of output**, i.e. budget output after each ... flow time step (default: 1).

**8)** **Unit number** to which the concentration within the CADS will be written. Note that this unit number has to be opened by a statement in the name file (default 0).

**9)** **Frequency of** CADS concentration **output**, i.e. output after each … flow time step (default: 1).

## Further modifications

The HTM module was further modified. Changes are listed subsequently:

- Internal computation with temperatures in Kelvin
- Implementation of budget terms for rate- and cumulative flow; an additional heat budget for heat transport is computed including details regarding mass balance errors.
- Implementation of the well boundary condition.
- Implementation of the possibility to produce output for specific nodes.
- Consideration of fixed head temperatures for inflow.

## Test examples

The HTM functionality is demonstrated in test cases 0_PHD_BIRK and TRANSPORT_01, _03, _04, and _05. Please refer to the separate documentation of test cases in section BT.

# B4. UMT3D

## Additions and modifications of input files – Flow model (CFPM1)

The additional packages of the flow model to produce the flow-data input files for the transport models were activated in the flow model name file. Namely, the file types (FTYPE) LMT6 for continuum transport and LUT6 for conduit transport need to be specified. Subsequently, an example for the *.nam file extension of the flow model is provided:

*Example NAM file:*

```
...
LMT6    48      SC.lmt
LUT6    49      SC.lut
...
```

## Input instructions for the UMT3D Link file for matrix transport - LMT

FTYPE in the NAM file: **LMT6**

Description: Link file for matrix transport (MT3D).

*Example input file:* The numbers (e.g. '1)') in the first column do not belong to the files. They are only included for reference.)

```
        #
        # INPUT DATA FILE FOR THE LINK-MT3DMS (LMT6) PACKAGE
        #
1)      OUTPUT_FILE_NAME mflow.hff
2)      OUTPUT_FILE_UNIT 88
3)      OUTPUT_FILE_HEADER Standard
4)      OUTPUT_FILE_FORMAT formatted
```

Lines starting with # are comment lines. You are allowed to include as many comment lines (starting with #) as you like.

**1)** Name of the output file with LMT data (flow terms - *.hff)
**2)** Unit number of LMT output data file (*.hff)
**3)** Header for the output file
**4)** Format of the output file

## Input instructions for the UMT3D link file for matrix transport - LUT

FTYPE in the NAM file: **LUT6**

Description: Link file for conduit transport (UMT3D).

*Example input file:* The numbers (e.g. '1)') in the first column do not belong to the files. They are only included for reference.

```
        #
        # INPUT DATA FILE FOR THE LINK-UMT3D (LUT6) PACKAGE
        #
1)      OUTPUT_FILE_NAME cflow.hff
2)      OUTPUT_FILE_UNIT 89
3)      OUTPUT_FILE_HEADER Standard
4)      OUTPUT_FILE_FORMAT formatted
```

Lines starting with # are comment lines. You are allowed to include as many comment lines (starting with #) as you like.

**1)** Name of the output file with LUT data (flow terms - *.hff)
**2)** Unit number of LUT output data file (*.hff)
**3)** Header for the output file
**4)** Format of the output file

## Additions and modifications of input files – Transport model (UMT3D)

The additional packages for conduit flow are activated in the transport model name file. Namely, the file types (FTYPE)

- CONF (input for conduit transport from the flow model, e.g. CFPM1; *.hff file),
- SSC (input for conduit transport),
- OUTC (conduit transport output), and
- CONOBS (conduit transport output observations)

need to be specified. Subsequently, an example for the *.nam file extension of the transport model is given:

*Example NAM file:*

```
…
CONF          12      SC.hff  → input data from the flow model for the transport code
…
SSC           20      SC.ssc  → input data for conduit transport
OUTC          17      SC.out  → conduit transport output
CONOBS        18      SC.cob  → conduit transport output (observations)
…
```

Please note that UMT3D needs all standard MT3D input files. Please refer to *Zheng and Wang* [1999] for more information about the MT3D input files. Subsequently, the UMT3D specific input files with the identifiers SSC, OUTC, and CONOBS are explained.

- BTN: activate SSC package in TRNOP at position 10 (marked bold in the next line) (Line A5)

T T T F T F F F F **T**

- SSM: activate conduits in FNEW at position 7 (marked bold in the next line) (Line D1)

F F T F F F **T**

## Input instructions for the SINK / SOURCE MIXING PACKAGE FOR CONDUITS - SSC

FTYPE in the NAM file: **SSC**

Description: Simulates solute transport in the conduits

*Example Input file:* The numbers (e.g. '1)') in the first column do not belong to the files. They are only included for reference.)

```
1)      T T F
2)      5     4       250
3)      5
4)      1     1.0
5)      0.05
6)      0.0
7)      4
8)      1     1       0.0
```

```
          2     2      0.0
          3     3      0.0
          3     4      0.0
9)        1
10)       4
11)       1     1      1000.0 1
          2     3      1000.0 1
          3     4      1000.0 1
          4     5      1000.0 1
9)        2
10)       4
11)       1     1      0000.0 1
          2     3      0000.0 1
          3     4      0000.0 1
          4     5      0000.0 1
```

**1)** FCONDIR, FCONFIXH, FCONFIX
Flags for conduit sinks/sources (FCONDIR = direct recharge, FCONFIXH = fixed head, and FCONFIX = constant concentration); Input as logical expression (T = true / F = false); Input format: 3L2

**2)** CNCONN,CNCONT,CNCONTS
Maximum number of conduit nodes, tubes, and tube sections; Input format: 3I5

**3)** MXSSCON
Maximum number of conduit point sinks / sources; Input format I10 *(all conduits with fixed head respectively direct recharge)*

**4)** MIXELMCON,PERCELCON
Advection solution option (MIXELMCON) and Courant number for advection calculations (PERCELCON); MIXELMCON = 0 ➞ advection is solved with the explicit FD scheme; MIXELMCON = 1 ➞ advection is solved with the EMCNOT method; Input format: I10, F10.5

Lines 5-6 only if EMCNOT is used (MIXELMCON = 1)

**5)** FRACTIONTRCON
Fraction of minimum residence time which should be used as the transport time step size for the conduit transport model and mt3dms; Input format F10.5

**6)** ALCON
Longitudinal dispersivity; Input format F10.5

**7)** INCOCONT
Flag for initial concentration assignment for conduit tubes (total number of assignments); Input format I5
Line 8 INCOCONT times

**8)** DUMMY, TUBE, CO(1); 2I10, F10.5
Dummy (e.g. consecutive number), tube number and concentration; Input format: 2I10, F10.5

Lines 9 – 11 for every period:

**9)** KKPER
Number of the stress period; Input format I10

**10)** NTMP
Number of conduit point sinks / sources of specified concentrations; Input format I10
Line 11 NTMP times

**11)** DUMMY, NODE, CSS, IQ
Dummy (e.g. consecutive number), node number, sink / source concentration, and type of point sink / source (1 = direct recharge, 2 = fixed head, 3 = fixed concentration); input format: 2I10, F10.0, I10

# EXISTING LIMITATIONS FOR SUBSTANCE- AND HEAT TRANSPORT MODELING

Both the HTM and STM package still have limitations, where some are listed below:

- limited interaction with the matrix-continuum through water transfer $Q_{EX}$ (matrix inflow with fixed temperature respectively fixed concentration; outflow to the matrix is still not further considered). Please note: diffusion respectively heat conduction with the matrix surrounding the conduit is covered by the above mentioned radial symmetric approach (see chapter 6, equations 6–18 and 6–34). Consequently, care is necessary for scenarios with significant water transfer from the conduit to the matrix and subsequent change of this flow direction (e.g. strong recharge pulses in well-coupled conduit-matrix systems).
- Partially filled pipe storage (PFPS) is not considered for transport yet.
- Heat transport in the conduit along the flow direction considers advection and not dispersion / diffusion respectively conduction, see equation B1–24. Hence, HTM should be used with care for settings with very little discharge where conduction can become important.
- CADS consideration for transport is done in a very idealized way by assuming one completely mixed reactor. This can result in some artificial effects like dilution in case $V_{CADS}$ is large.

# LITERATURE (PART A & B)

Bauer, S., R. Liedl, and M. Sauter (2005), Modeling the influence of epikarst evolution on karst aquifer genesis: a time-variant recharge boundary condition for joint karst-epikarst development. Water Resources Research, Vol. 41, w09416, doi:10.1029/2004wr003321.

Bauer, S. (2001), Simulation of the genesis of karst aquifers in carbonate rocks. PhD Thesis, University Tübingen, Germany.

Beek, W. J. and K. M. K. Muttzall (1975), Transport Phenomena. Wiley, London.

Birk, S. (2002), Characterisation of karst systems by simulating aquifer genesis and spring responses: model development and application to gypsum karst. PhD Thesis, University Tübingen, Germany.

Birk, S. and S. Bauer (2003), CAVE user guide, unpublished.

Birk, S. and T. Geyer (2006), Prozessbasierte Charakterisierung der dualen Abfluss- und Transporteigenschaften von Karstgrundwasserleitern. Abschlussbericht DFG-Projekte LI 727/10 und SA 501/17.

Clark, M. M. (1996), Transport modeling for environmental engineers and scientists. Wiley, New York.

Covington, M. D., A. J. Luhmann, F. Gabrovšek, M. O. Saar, and C. M. Wicks (2011), Mechanisms of heat exchange between water and rock in karst conduits, Water Resources Research, 47, W10514, doi: 10.1029/2011WR010683.

Gnielinski, V. (1976), New equations for heat and mass transfer in turbulent pipe and channel flow. International Chemical Engineering 16 (2): 359–368.

Grigull, U. and H. Tratz (1965), Thermischer Einlauf in ausgebildeter laminarer Rohrströmung. Int. J. Heat Mass Transfer 8: 669–678.

Incropera, F. P., D. P. DeWitt, T. L. Bergman, and A. S. Lavine (2007), Fundamentals of heat and mass transfer. 6th ed. John Wiley & Sons, Hoboken, USA.

Király, L. (1997), Modelling karst aquifers by the combined discrete channel and continuum approach, 6th Conference on limestone hydrology and fissured aquifers. Université de Franche-Comté, Sciences et Technique de l'Environment, La Chaux-de-Fonds, pp 1-26.

Liedl, R. and M. Sauter (2000), Charakterisierung von Karstgrundwasserleitern durch Simulation der Aquifergenese und des Wärmetransports. Grundwasser1: 9–16.

Liu, G., P. Wang, C. Zheng (2001), An explicit and mass-conservative scheme without time-step limit for modeling advection-dominated contaminant transport, 2001 MODFLOW international conference, Golden / Colorado, USA.

Maréchal, J. C., Ladouche, B., and N. Dörfliger (2006), Role of karst system in the genesis of flash flood events at the Nimes city, EGU General Assembly, 3rd April 2006.

Maréchal, J. C., Ladouche, B., Dörfliger, N., and P. Lachassagne (2008), Interpretation of pumping tests in a mixed flow karst system, Water Resources Research, 44, W05401, doi: 10.1029/2007WR006288.

Mangin, A. (1994), Karst hydrogeology, in: Stanford, J, Gibert, J., and D. Danielopol (eds), Groundwater ecology. Academic Press, pp. 43-67.

Ogata, A., and Banks, R.B. (1961), A solution of the differential equation of longitudinal dispersion in porous media: U.S. Geological Survey Professional Paper 411-A.

Shoemaker, W.B., E.L. Kuniansky, S. Birk, S. Bauer, and E.D. Swain (2008), Documentation of a Conduit Flow Process (CFP) for MODFLOW-2005. U.S. Geological Survey Techniques and Methodes, Book 6, Chapter A24, 50p, 2008.

Spiessl, S., M. Sauter, C. Zheng, and G. Liu (2002), Comparison of two numerical methods for advection in a pipe network coupled to a continuum transport model. Proceedings of ModelCare 2002, Prague, Czech Republic, June 2002, IAHS Publ. no. 277.

Spiessl, S. (2004), Development and evaluation of a reactive hybrid transport model (RUMT3D), PhD Thesis, University Göttingen, Germany.

Taylor, G. (1953), Dispersion of soluble matter in solvent flowing slowly through a tube. Proceedings of the Royal Society of London, Series A 219: 186–203.

Taylor, G. (1954), The dispersion of matter in turbulent flow through a pipe. Proceedings of the Royal Society of London, Series A 223: 446–468.

Zheng, C. and P. P. Wang (1999), MT3DMS: A modular three-dimensional multispecies transport model for simulation of advection, dispersion, and chemical reactions of contaminants in groundwater systems; documentation and user's guide. Prepared for U.S. Army Corps of Engineers.

# ANNEX

# AT. PART A TESTING: ADDITIONS TO CFPM1 FLOW ROUTINES – TEST CASES

## Case overview

| Case | Intention / specific feature | Tested functionality | Page |
|---|---|---|---|
| **1** | provide initial situation | budget terms | 37 |
| **2** | consider point recharge | budget terms | 39 |
| **3** | pumping from conduit system (negative discharge) | adapted budget terms | 40 |
| **4** | enhanced pumping from conduit system with inflow via constant head | adapted budget terms | 41 |
| **5** | constrained inflow via FHLQ bc | FHLQ bc and adapted budget terms | 42 |
| **6** | transient pumping – initial situation (conduit constant head) | actual state of CFPM1 (as available), cumulative budgets | 43 |
| **7** | transient pumping – CAD storage | Conduit associated drainable storage (CADS), cumulative budgets, correct consideration of CADS volume | 45 |
| **8** | transient pumping – FHLQ bc | FHLQ, cumulative budgets | 47 |
| **9** | transient pumping – CADS and FHLQ | CADS and FHLQ, cumulative budgets | 49 |
| **10** | pumping from conduit system (WELL) | adapted budget terms and WELL bc | 51 |
| **11** | transient pumping with WELL | transient implementation of WELL bc | 52 |
| **12** | transient pumping resulting in partially filled pipes | Partially filled pipe storage (PFPS), PFPS consideration in budget files | 53 |
| **14** | in- and outflow with Cauchy boundary | Cauchy boundary condition, limited inflow with CYLQ, steady state | 55 |
| **15** | pumping with Cauchy boundary | Cauchy boundary, limited inflow with CYLQ, transient conditions i.e. switch between different states | 56 |
| **16** | limited head with LH b.c. (steady state) | LH for steady state conditions | 57 |
| **17** | transient pumping with LH b.c. | LH for transient conditions, inflow through LH | 58 |
| **18** | time dependent boundary data TD | TD for fixed head, FHLQ, well, and Cauchy boundary condition | 59 |

## Case 1 - Basic situation (reference)

A catchment with the following parameters is considered as basic situation (compare Figure AT–1):

- length and width = 1100 m,
- thickness = 150 m (top = 150 m, bottom = 0 m; 1 layer with $\Delta z$ = 150 m),
- 11 x 11 cells with $\Delta x = \Delta y$ = 100 m,
- $K$ = 1E-5 $ms^{-1}$,
- steady state flow.

A central conduit dewaters the matrix towards south. The following parameters are considered for the conduit:

- length = 500 m,

- 6 nodes / 5 tubes à 100 m length,
- diameter = 0.5 m,
- height (node center) = 30 m,
- roughness = 0.01 m,
- pipe conductance (exchange coefficient) = 0.001 $m^2s^{-1}$ (end pipes 0.0005 $m^2s^{-1}$).

The following boundary conditions are applied:

- fixed head at node 6 of the conduit with $h$ = 50 m,
- no flow at all other lateral model boundaries,
- diffuse recharge in all matrix cells with a rate of 8.2645E-8 $ms^{-1}$ (resulting in 0.1 $m^3s^{-1}$ recharge flux for the whole catchment).

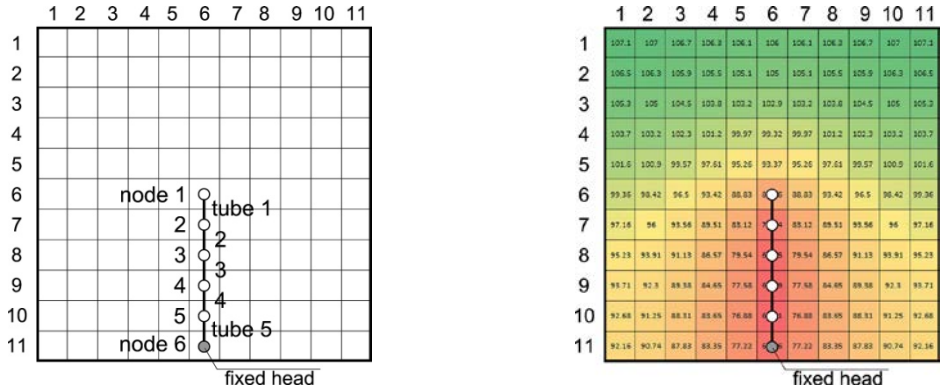


**Figure AT–1:** Basic situation with denotation (left) and resulting matrix heads (in m) for case 1 (right)

Table AT–1 presents the resulting water balance. The matrix obtains 0.1 $m^3s^{-1}$ water from diffuse recharge. This water is completely drained by the conduit system resulting in a spring discharge of 0.1 $m^3s^{-1}$.

**Table AT–1:** Water balance for the conduit system and the matrix flow system (flow terms in $m^3s^{-1}$)

| **CONDUIT FLOW SYSTEM** | | ***NOTES*** |
|---|---|---|
| | ***IN*** | |
| MATRIX EXCHANGE | 0.1000 | *= from MODFLOW* |
| TOTAL IN | 0.1000 | |
| | ***OUT*** | |
| CONSTANT HEAD | 0.1000 | *= spring discharge* |
| TOTAL OUT | 0.1000 | |
| PERCENT ERROR | 0.00 | |
| **MATRIX FLOW SYSTEM** | | |
| | ***IN*** | |
| RECHARGE | 0.1000 | *= diffuse recharge* |
| TOTAL IN | 0.1000 | |
| | ***OUT*** | |
| PIPES | 0.1000 | *= conduit system* |
| TOTAL OUT | 0.1000 | |
| PERCENT DISCREPANCY | 0.00 | |

# Case 2 - Additional point recharge in the conduit system

This scenario demonstrates the consideration of 0.1 $m^3s^{-1}$ point recharge. All other parameters are kept constant respectively are slightly adapted as listed below:

- point recharge is considered by:
  - o increased diffuse recharge (RCH) in the cell with the intended point recharge equal to 1.0083E-5 $ms^{-1}$ ( = 8.2644E-8 $ms^{-1}$ + 0.1 $m^3s^{-1}$ / 10000 $m^2$),
  - o fraction of diffuse recharge partitioned directly into the conduit (P_CRCH with CRCH package) is set to 0.9918.

Figure AT–2 illustrates the scenario. The resulting water balance is presented in Table AT–2.

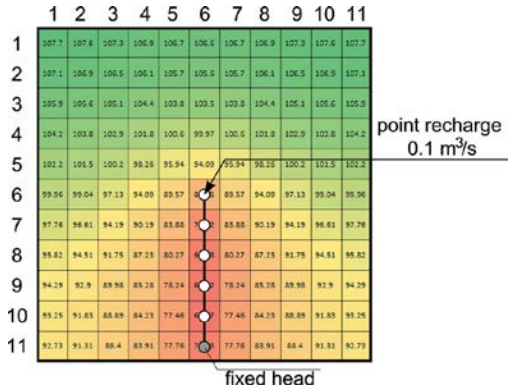


**Figure AT–2:** Case 2 situation and resulting matrix heads

**Table AT–2:** Water balance for the conduit system and the matrix flow system (all flow terms in $m^3s^{-1}$)

| CONDUIT FLOW SYSTEM | | NOTES |
|---|---|---|
| ***IN*** | | |
| PIPE RECHARGE | 0.1000 | *= point recharge* |
| MATRIX EXCHANGE | 0.1000 | *= from MODFLOW* |
| TOTAL IN | 0.2000 | |
| ***OUT*** | | |
| CONSTANT HEAD | 0.2000 | *= spring discharge* |
| TOTAL OUT | 0.2000 | |
| PERCENT ERROR | 0.00 | |
| **MATRIX FLOW SYSTEM** | | |
| ***IN*** | | |
| RECHARGE | 0.1000 | *= diffuse recharge* |
| TOTAL IN | 0.1000 | |
| ***OUT*** | | |
| PIPES | 0.1000 | *= to conduit system* |
| TOTAL OUT | 0.1000 | |
| PERCENT DISCREPANCY | 0.00 | |

The additional input via direct recharge is correctly considered by the budget terms.

# Case 3 - Point recharge and additional water abstraction from conduits

This scenario extends case 2 by additional water abstraction from the conduit system to represent pumping. This scenario demonstrates the (new) ability of CFPM1 to consider water abstraction (= negative recharge) from the conduit system within the budget terms. The model is adapted as listed below:

- water abstraction is considered by:
  - point recharge from conduit node 5 with intended abstraction is -5.0E-6 $ms^{-1}$ (0.05 $m^3s^{-1}$; applied as diffuse recharge through RCH),
  - fraction of diffuse recharge partitioned directly into the conduit (P_CRCH with CRCH package) of this cell (conduit node 5) is set to 1.00.

Figure AT–3 illustrates the scenario. The resulting water balance is presented in Table AT–3.

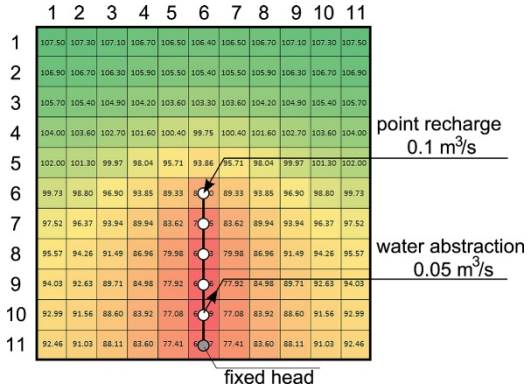


**Figure AT–3:** Case 3 situation and resulting matrix heads

**Table AT–3:** Water balance for the conduit system and the matrix flow system (all flow terms in $m^3s^{-1}$)

| CONDUIT FLOW SYSTEM | | NOTES |
|---|---|---|
| ***IN*** | | |
| PIPE RECHARGE | 0.1000 | *= point recharge* |
| MATRIX EXCHANGE | 0.0992 | *= from MODFLOW* |
| TOTAL IN | 0.1992 | |
| ***OUT*** | | |
| CONSTANT HEAD | 0.1492 | *= spring discharge* |
| PIPE RECHARGE | 0.0500 | *= pumping* |
| TOTAL OUT | 0.1992 | |
| PERCENT ERROR | 0.00 | |
| **MATRIX FLOW SYSTEM** | | |
| ***IN*** | | |
| RECHARGE | 0.0992 | *= diffuse recharge* |
| TOTAL IN | 0.0992 | |
| ***OUT*** | | |
| PIPES | 0.0992 | *= to conduit system* |
| TOTAL OUT | 0.0992 | |
| PERCENT DISCREPANCY | 0.00 | |

The results demonstrate that diffuse recharge is not considered in the water abstraction cell because the intended pumping rate is realized by setting a negative recharge flux. Consequently, overall recharge flux is slightly reduced compared to cases 1 and 2. Water abstraction from the conduit system is considered correctly by the budget terms as pipe recharge (see Table AT-3).

# Case 4 - Point recharge and enhanced additional water abstraction from conduits

This case extends case 3 with enhanced water abstraction from the conduit system, whereas the pumping rate (0.25 $m^3s^{-1}$) exceeds diffuse and direct recharge (both ~0.19 $m^3s^{-1}$; see case 3). Subsequently, water enters the catchment via the conduit fixed head. The model is adapted as listed below:

- water abstraction is considered with:
  - point recharge from conduit node 5 with intended pumping is -2.5E-5 $ms^{-1}$ (0.25 $m^3s^{-1}$; applied as diffuse recharge through RCH),
  - percentage of direct recharge of this cell (conduit node 5) is set to 1.00.

Figure AT–4 illustrates the scenario. The resulting water balance is presented in Table AT–4.

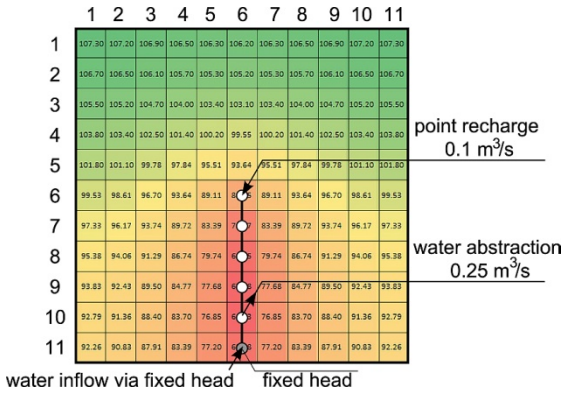


**Figure AT–4:** Case 4 situation and resulting matrix heads

**Table AT–4:** Water balance for the conduit system and the matrix flow system (all flow terms in $m^3s^{-1}$)

| CONDUIT FLOW SYSTEM | | NOTES |
|---|---|---|
| ***IN*** | | |
| CONSTANT HEAD | 0.0508 | *= inflow via node constant head* |
| PIPE RECHARGE | 0.1000 | *= point recharge* |
| MATRIX EXCHANGE | 0.0992 | *= from MODFLOW* |
| TOTAL IN | 0.2500 | |
| ***OUT*** | | |
| PIPE RECHARGE | 0.2500 | *= water abstraction / pumping* |
| TOTAL OUT | 0.2500 | |
| PERCENT ERROR | 0.00 | |
| **MATRIX FLOW SYSTEM** | | |
| ***IN*** | | |
| RECHARGE | 0.0992 | *= diffuse recharge* |
| TOTAL IN | 0.0992 | |
| ***OUT*** | | |
| PIPES | 0.0992 | *= to conduit system* |
| TOTAL OUT | 0.0992 | |
| PERCENT DISCREPANCY | 0.00 | |

The results demonstrate that the resulting inflow via the conduit fixed head is correctly considered by the budget terms.

# Case 5 - Conduit inflow limited by FHLQ boundary condition

This scenario extends case 4 by a flow constraint at the conduit fixed head. By using the implemented FHLQ boundary condition (Fixed Head Limited flow (Q)) water inflow is limited to 0.045 $m^3s^{-1}$. Additionally, a fixed head boundary condition was implemented in the upper left corner of the matrix continuum in order to allow the water budget to balance out (Figure AT-5). Without this fixed head in the continuum, the model run does not converge because this scenario cannot be resolved hydraulically (point- and diffuse recharge + FHLQ inflow ~0.245 $m^3s^{-1}$ whereas the pumping rate is 0.25 $m^3s^{-1}$). The model is adapted as listed below:

- Fixed head in the upper left corner of the matrix with *h* = 107.3 m (compare case 4).
- FHLQ boundary at conduit outlet (node 6); FH with *h* = 50 m and LQ = 0.045 $m^3s^{-1}$.

Figure AT–5 illustrates the scenario. The resulting water balance is presented in Table AT–5.

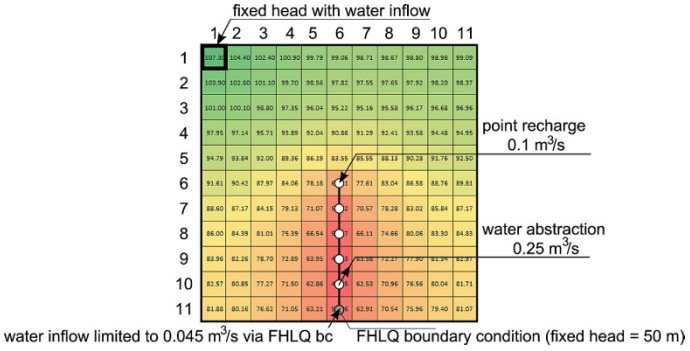


**Figure AT–5:** Case 5 situation and resulting matrix heads

**Table AT–5:** Water balance for the conduit system and the matrix flow system (in $m^3s^{-1}$)

| CONDUIT FLOW SYSTEM | | *Notes* |
|---|---|---|
| ***IN*** | | |
| PIPE RECHARGE | 0.1000 | *= point recharge* |
| MATRIX EXCHANGE | 0.1050 | *= from MODFLOW* |
| FHLQ BC (LQ CASE) | 0.0450 | *= inflow from FHLQ* |
| TOTAL IN | 0.2500 | |
| ***OUT*** | | |
| PIPE RECHARGE | 0.2500 | *= water abstraction / pumping* |
| TOTAL OUT | 0.2500 | |
| PERCENT ERROR | 0.00 | |
| **MATRIX FLOW SYSTEM** | | |
| ***IN*** | | |
| CONSTANT HEAD | 0.0066 | *= constant head cell upper left corner* |
| RECHARGE | 0.0983 | *= diffuse recharge* |
| TOTAL IN | 0.1050 | |
| ***OUT*** | | |
| PIPES | 0.1050 | *= to the conduit system* |
| TOTAL OUT | 0.1050 | |
| PERCENT DISCREPANCY | 0.00 | |

The results demonstrate that the resulting inflow via the FHLQ boundary condition is considered correctly by the budget terms. The FHLQ boundary condition works as intended; due to the inflow constraints, conduit heads drop down to ~33 m (fixed head is 50 m). In comparison to the previous cases, diffuse recharge is further decreased due to the matrix fixed head cell. The water budget is balanced out by inflow via the matrix fixed head (deficit resulting from FHLQ and reduced diffuse recharge).

# Case 6 - Transient water abstraction

This scenario tests the correctness of budget terms for transient situations (i.e. the cumulative budget terms). The basic setup is similar to case 4. Additional changes are:

- Implementation of three time periods:
  - period 1 (initialize) = steady state with 86 400 seconds,
  - period 2 (pumping) = 86 400 seconds with 144 time steps (each 10 minutes),
  - period 3 (recovery) = 172 800 seconds with 288 time steps (each 10 minutes).
- Specific storage = 1E-5 $m^{-1}$, specific yield = 0.01.

The budget terms for a pumping rate of 0.25 $m^3s^{-1}$ (compare period 2 with case 4) are listed in Table AT–6.

**Table AT–6:** Water balance for the conduit system and the matrix flow system (all flow terms in $m^3s^{-1}$); cumulative values (in $m^3$) in square brackets

| CONDUIT FLOW SYSTEM | | | | | | | NOTES |
|---|---|---|---|---|---|---|---|
| ***IN*** | ***END OF P1*** | | ***END OF P2*** | | ***END OF P3*** | | |
| CONSTANT HEAD | 0.0000 | [0.00] | 0.0489 | [4187.73] | 0.0000 | [4187.73] | *= inflow constant head* |
| PIPE RECHARGE | 0.1000 | [8640.28] | 0.1000 | [17280.55] | 0.1000 | [34561.10] | *= point recharge* |
| MATRIX EXCHANGE | 0.1000 | [8640.07] | 0.1011 | [17412.06] | 0.0998 | [34623.11] | *= from MODFLOW* |
| TOTAL IN | 0.2000 | [17280.35] | 0.2500 | [38880.35] | 0.1998 | [73371.95] | |
| ***OUT*** | | | | | | | |
| CONSTANT HEAD | 0.2000 | [17280.35] | 0.0000 | [17280.35] | 0.1998 | [51771.95] | *= spring discharge* |
| PIPE RECHARGE | 0.0000 | [0.00] | 0.2500 | [21600.00] | 0.0000 | [21600.00] | *= water abstraction* |
| TOTAL OUT | 0.2000 | [17280.35] | 0.2500 | [38880.35] | 0.1998 | [73371.95] | |
| PERCENT ERROR | 0.00 | | 0.00 | | 0.00 | | |
| **MATRIX FLOW SYSTEM** | | | | | | | |
| ***IN*** | | | | | | | |
| STORAGE | 0.0000 | [0.00] | 0.0019 | [203.33] | 0.0001 | [269.07] | *= from matrix storage* |
| RECHARGE | 0.1000 | [8640.07] | 0.0992 | [17208.73] | 0.1000 | [34488.87] | *= diffuse recharge* |
| TOTAL IN | 0.1000 | [8640.07] | 0.1011 | [17412.07] | 0.1002 | [34757.94] | |
| ***OUT*** | | | | | | | |
| STORAGE | 0.0000 | [0.00] | 0.0000 | [0.00] | 0.0003 | [134.83] | *= to matrix storage* |
| PIPES | 0.1000 | [8640.07] | 0.1011 | [17412.07] | 0.0998 | [34623.11] | *= to conduit system* |
| TOTAL OUT | 0.1000 | [8640.07] | 0.1011 | [17412.07] | 0.1002 | [34757.94] | |
| PERCENT DISCREPANCY | 0.00 | | 0.00 | | 0.00 | | |

Subsequently, the pumping rate was increased stepwise from 0.25 $m^3s^{-1}$ up to 2 $m^3s^{-1}$. Therewith, the influence of the pumping rate on conduit heads and spring flow was investigated. Figure AT–6 shows the resulting heads at the pumping well and the spring flow.

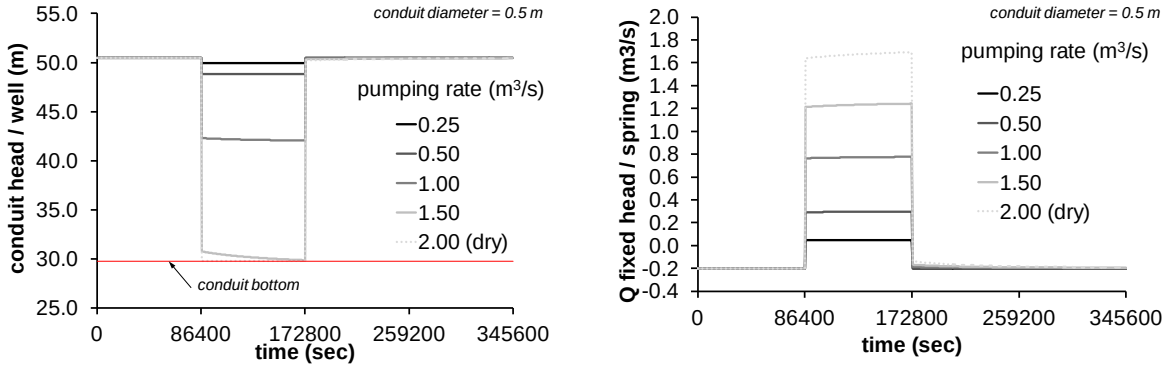


**Figure AT–6:** Conduit head at the pumping well and inflow via conduit constant head boundary for different pumping rates; **conduit diameter = 0.5 m**

For the considered catchment, water can only be provided by matrix storage respectively inflow through the conduit constant head boundary. It is obvious that, for the used parameters, the conduit flow capacity limits water inflow through the conduit constant head – subsequently the conduit head in the pumping well drops. This effect can potentially increase water transfer with the matrix – however this is defined / limited by matrix parameters and the transfer coefficient. With a pumping rate of 2.0 $m^3s^{-1}$ the conduit finally falls dry resulting in an erroneous water balance (because discharge is set to 0 in dry pipes).

For another setup, the conduit diameter was increased to 2.5 m. Figure AT–7 shows the resulting heads at the pumping well and the spring flow.

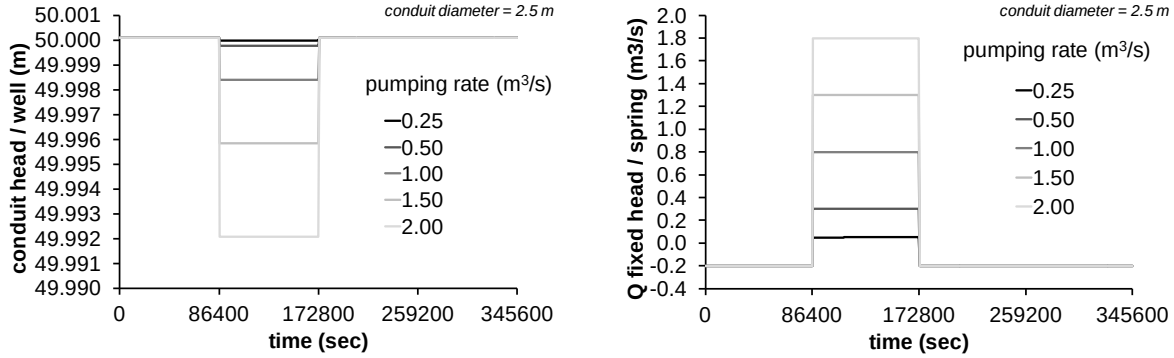


**Figure AT–7:** Conduit head at the pumping well and inflow via conduit constant head boundary for different pumping rates; **conduit diameter = 2.5 m**

It is obvious that, with a sufficiently large conduit, unhampered water inflow via the conduit constant head boundary occurs. Conduit heads are basically not affected by pumping. Therefore, the hydraulic conditions in the matrix are not affected by water abstraction from the conduit system meaning that this model setup (large conduit with constant head boundary condition) cannot produce water level drawdown within the matrix.

# Case 7 - Transient water abstraction with CAD storage

This scenario additionally considers CAD storage, which can provide water for transient situations with active flow constraints (compare case 6 where the 0.5 diameter conduit hampers water inflow from the fixed head boundary and water transfer / matrix hydraulics limits water inflow from the continuum). Originally, CFPM1 did not consider transient hydraulics for the discrete conduit system resulting in an immediate drawdown if flow constraints are active. For the following test case, CAD storage is considered with a storage width $W_{CADS}$ = 0.5 m.

As in case 6, the pumping rate was increased stepwise from 0.25 $m^3s^{-1}$ up to 2 $m^3s^{-1}$. Results are presented for a conduit with 0.5 m diameter; model runs for a conduit with 2.5 m diameter (as also investigated in test case 6) do not result in a flow constraint and, therefore, conduit heads remain more or less constant resulting in insignificant CAD storage (compare Figure AT–7). The budget terms for a pumping rate of 0.25 $m^3s^{-1}$ are listed in Table AT–7.

**Table AT–7:** Water balance for the conduit system and the matrix flow system (all flow terms in $m^3s^{-1}$); cumulative values in square brackets (in $m^3$)

| CONDUIT FLOW SYSTEM | | | | | | | NOTES |
|---|---|---|---|---|---|---|---|
| ***IN*** | ***END OF P1*** | | ***END OF P2*** | | ***END OF P3*** | | |
| CONSTANT HEAD | 0.0000 | [0.00] | 0.0489 | [4095.69] | 0.0000 | [4095.69] | *= inflow constant head* |
| PIPE RECHARGE | 0.1000 | [8640.28] | 0.1000 | [17280.55] | 0.1000 | [34561.10] | *= point recharge* |
| MATRIX EXCHANGE | 0.1000 | [8640.07] | 0.1011 | [17410.24] | 0.0998 | [34624.05] | *= from MODFLOW* |
| CAD STORAGE | 0.0000 | [0.00] | 0.0001 | [113.19] | 0.0000 | [113.19] | *= from CAD storage* |
| TOTAL IN | 0.2000 | [17280.35] | 0.2500 | [38899.68] | 0.1998 | [73394.04] | |
| ***OUT*** | | | | | | | |
| CONSTANT HEAD | 0.2000 | [17280.35] | 0.0000 | [17299.68] | 0.1998 | [51681.14] | *= spring discharge* |
| PIPE RECHARGE | 0.0000 | [0.00] | 0.2500 | [21600.00] | 0.0000 | [21600.00] | *= water abstraction* |
| CAD STORAGE | 0.0000 | [0.00] | 0.0000 | [0.00] | 0.0001 | [112.90] | *= to CAD storage* |
| TOTAL OUT | 0.2000 | [17280.35] | 0.2500 | [38899.68] | 0.1998 | [73394.04] | |
| PERCENT ERROR | 0.00 | | 0.00 | | 0.00 | | |
| **MATRIX FLOW SYSTEM** | | | | | | | |
| ***IN*** | | | | | | | |
| STORAGE | 0.0000 | [0.00] | 0.0019 | [201.51] | 0.0002 | [269.11] | *= from matrix storage* |
| RECHARGE | 0.1000 | [8640.07] | 0.0992 | [17208.73] | 0.1000 | [34488.87] | *= diffuse recharge* |
| TOTAL IN | 0.1000 | [8640.07] | 0.1011 | [17410.24] | 0.1002 | [34757.98] | |
| ***OUT*** | | | | | | | |
| STORAGE | 0.0000 | [0.00] | 0.0000 | [0.00] | 0.0003 | [133.93] | *= to matrix storage* |
| PIPES | 0.1000 | [8640.07] | 0.1011 | [17410.24] | 0.0998 | [34624.05] | *= to conduit system* |
| TOTAL OUT | 0.1000 | [8640.07] | 0.1011 | [17410.24] | 0.1002 | [34757.98] | |
| PERCENT DISCREPANCY | 0.00 | | 0.00 | | 0.00 | | |

Figure AT–8 shows the resulting heads at the pumping well and the spring flow. It is obvious that with increasing drawdown in the conduit (induced here by an increased pumping rate) the CAD storage gets more significant. Water coming from the CAD storage results in a damping of the head drawdown (Figure AT–8 left) and a damping of spring inflow (Figure AT–8 right).

Subsequently, the scenario was further adapted to represent long term pumping (i.e. to result in a steady state situation). Therewith, the correct volumetric representation of CAD storage can be proofed. This was done by comparing the CAD storage calculated based on conduit heads with the budget terms (based on cumulative flow terms). Necessary modifications to the case 7 scenario were:

- time discretization:
  - o period 1 (initialize) = steady state with 1 day
  - o period 2 (pumping) = transient with 365 days with 365 time steps
  - o period 3 (recovery) = transient with 365 days with 365 time steps
- pumping rate 1.3 $m^3s^{-1}$

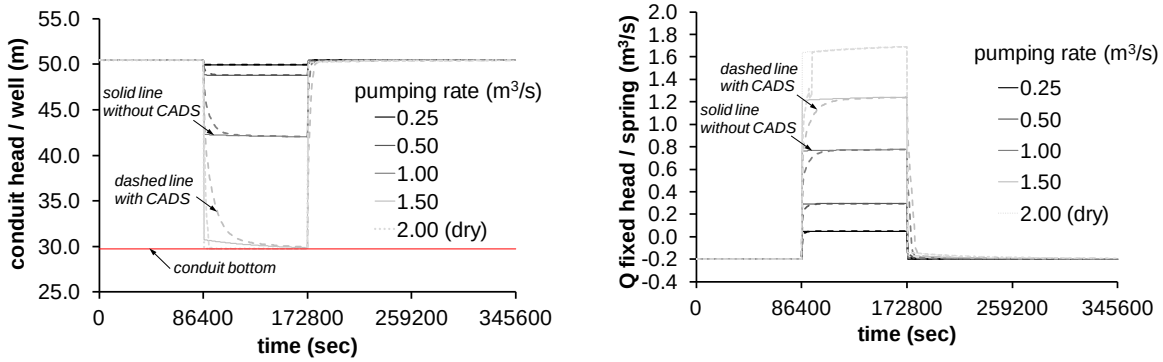


**Figure AT–8:** Conduit head at the pumping well and inflow via conduit constant head boundary condition for different pumping rates with additional use of CAD storage.

Figure AT–9 shows the resulting drawdown in the conduit node during long-term pumping. Table AT–8 presents the CAD storage computation based on conduit heads in comparison to the CFPM1 budget files.

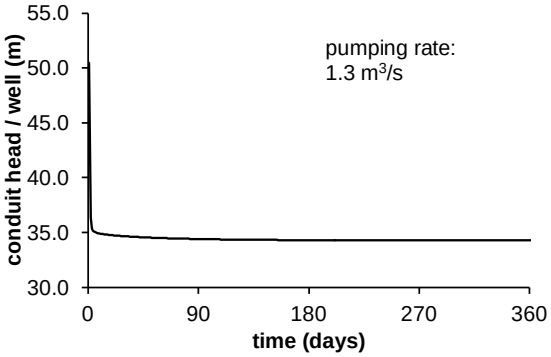


**Figure AT–9:** Conduit head at the pumping well for the long term pumping scenario

**Table AT–8:** CAD storage change based on node heads / computed by CFPM1 budgets

| node | conduit length (m) | period 1 (initialize) | | period 2 (pumping) | | period 3 (recovery) | |
|---|---|---|---|---|---|---|---|
| | | head (m) | $V_{CADS}$ ($m^3$) | head (m) | $V_{CADS}$ ($m^3$) | head (m) | $V_{CADS}$ ($m^3$) |
| **1** | 50 | 51.578 | 545.689 | 35.425 | 141.886 | 51.577 | 545.679 |
| **2** | 100 | 51.405 | 1082.769 | 35.249 | 274.970 | 51.405 | 1082.750 |
| **3** | 100 | 51.162 | 1070.593 | 34.999 | 262.426 | 51.162 | 1070.576 |
| **4** | 100 | 50.849 | 1054.950 | 34.676 | 246.298 | 50.849 | 1054.938 |
| **5** | 100 | 50.464 | 1035.721 | 34.278 | 226.418 | 50.464 | 1035.713 |
| **6** | 50 | 50.000 | 506.250 | 50.000 | 506.250 | 50.000 | 506.250 |
| **all nodes** | | | 5295.971 | | 1658.247 | | 5295.906 |
| d*V* | | | 0.000 | | 3637.724 | | -3637.659 |
| budget file | | | 0.000 | | 3637.724 | | -3637.659 |

# Case 8 - Transient water abstraction with FHLQ boundary condition

In this case inflow over the conduit constant head boundary is limited by the FHLQ boundary condition. As in case 5, a constant head boundary was implemented in the upper left corner of the matrix continuum in order to allow the water budget to balance out. Used parameters for the boundary conditions are similar to case 5 (FHLQ with $h$ = 50 m and LQ = 0.045 $m^3s^{-1}$; matrix constant head with $h$ = 107.3 m). Model runs were performed for two conduit systems: 0.5 m diameter and 2.5 m diameter (see case 6).

The budget terms for the 0.5 m diameter conduit and a pumping rate of 0.25 $m^3s^{-1}$ (compare period 2 with case 5) are listed in Table AT–9. Budgets demonstrate the correct implementation of the FHLQ boundary condition for transient situations.

**Table AT–9:** Water balance for the conduit system and the matrix flow system (all flow terms in $m^3s^{-1}$); cumulative values in square brackets ($m^3$)

| CONDUIT FLOW SYSTEM | | | | | | | NOTES |
|---|---|---|---|---|---|---|---|
| ***IN*** | ***END OF P1*** | | ***END OF P2*** | | ***END OF P3*** | | |
| CONSTANT HEAD | 0.0000 | [0.00] | 0.0000 | [0.00] | 0.0000 | [0.00] | *= inflow constant head* |
| PIPE RECHARGE | 0.1000 | [8640.28] | 0.1000 | [17280.55] | 0.1000 | [34561.10] | *= point recharge* |
| MATRIX EXCHANGE | 0.9977 | [8620.27] | 0.1050 | [17691.99] | 0.0993 | [34754.41] | *= from MODFLOW* |
| FHLQ BC (LQ CASE) | 0.0000 | [0.00] | 0.0450 | [3888.00] | 0.0000 | [3888.00] | *= inflow FHLQ* |
| TOTAL IN | 0.1998 | [17260.55] | 0.2500 | [38860.55] | 0.1994 | [73203.51] | |
| ***OUT*** | | | | | | | |
| CONSTANT HEAD | 0.1998 | [17260.55] | 0.0000 | [17260.55] | 0.1994 | [51603.51] | *= spring discharge* |
| PIPE RECHARGE | 0.0000 | [0.00] | 0.2500 | [21600.00] | 0.0000 | [21600.00] | *= water abstraction* |
| TOTAL OUT | 0.1998 | [17260.55] | 0.2500 | [38860.55] | 0.1994 | [73203.51] | |
| PERCENT ERROR | 0.00 | | 0.00 | | 0.00 | | |
| **MATRIX FLOW SYSTEM** | | | | | | | |
| ***IN*** | | | | | | | |
| STORAGE | 0.0000 | [0.00] | 0.0061 | [522.85] | 0.0004 | [694.27] | *= from matrix storage* |
| CONSTANT HEAD | 0.0006 | [51.60] | 0.0006 | [103.21] | 0.0006 | [206.45] | *= matrix constant head* |
| RECHARGE | 0.0992 | [8568.66] | 0.0983 | [17065.92] | 0.0992 | [34203.25] | *= diffuse recharge* |
| TOTAL IN | 0.0997 | [8620.27] | 0.1050 | [17691.98] | 0.1002 | [35103.97] | |
| ***OUT*** | | | | | | | |
| STORAGE | 0.0000 | [0.00] | > 0.0000 | [> 0.00] | 0.0008 | [349.57] | *= to matrix storage* |
| CONSTANT HEAD | 0.0000 | [0.00] | 0.0000 | [0.00] | 0.0000 | [0.00] | *= matrix constant head* |
| PIPES | 0.0997 | [8620.27] | 0.1050 | [17691.99] | 0.0993 | [34754.41] | *= to conduit system* |
| TOTAL OUT | 0.0997 | [8620.27] | 0.1050 | [17692.00] | 0.1002 | [35103.98] | |
| PERCENT DISCREPANCY | 0.00 | | 0.00 | | 0.00 | | |

Figure AT–10 (left) presents the spring discharge in case the FHLQ boundary condition is used. Results are nearly identical for both conduits (0.5 m and 2.5 m diameter). Figure AT–10 (right) presents the corresponding conduit heads at the pumping node. It is obvious that the drawdown behavior is quite similar because the conduit diameter is not longer limiting hydraulics in case the FHLQ boundary constraint is active. Hence, these results demonstrate that the system reaction (catchment) is less dependent on conduit hydraulics (i.e. constraint by the conduit flow capacity) if the FHLQ boundary condition is active. Rather, the matrix continuum, which provides water transfer, is limiting. Therewith, the FHLQ boundary condition can reproduce realistic natural conditions where water inflow through the spring (in case of water abstraction / pumping) is limited.

Subsequently, the pumping rate was increased from 0.25 $m^3s^{-1}$ to 0.5 $m^3s^{-1}$. Due to the limited inflow through the FHLQ boundary condition, the water removed by pumping needs to be replaced through water transfer from the matrix (provided through the matrix constant head boundary). However, due

to the hydraulic properties of the matrix and relatively small water transfer coefficient, water replenishment is not sufficient resulting in dry conduits (associated with an erroneous water balance).

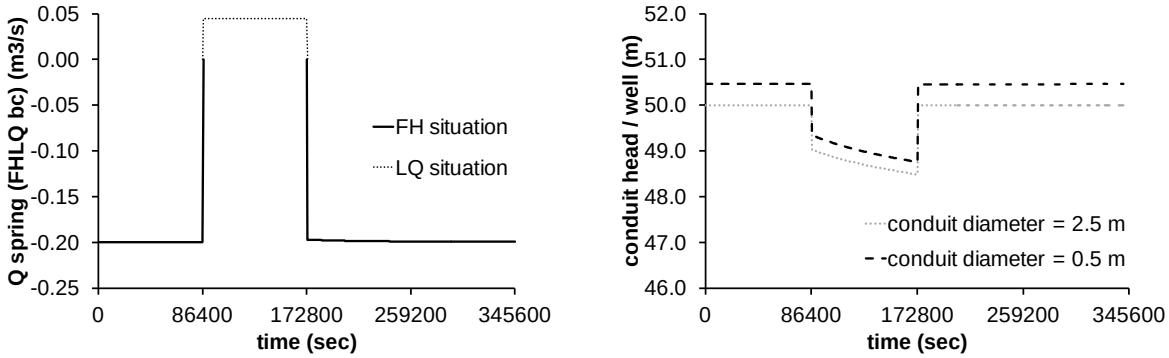


**Figure AT–10:** Inflow via conduit FHLQ boundary condition and conduit head at the pumping well for different conduit diameters (d = 0.5 and d = 2.5) with fixed head and FHLQ boundary.

# Case 9 - Transient water abstraction with FHLQ boundary and CADS

This scenario aims to simulate the CAD storage in systems constrained by an FHLQ boundary condition. The initial situation is a combination of case 7 (CADS) and case 8 (FHLQ). The basic model setup considers the subsequently listed parameters. Parameter variations are listed in brackets.

- conduit diameter: $d$ = 0.5 m (2.5 m)
- pumping rate = 0.25 $m^3s^{-1}$ (0.3 $m^3s^{-1}$, 0.32 $m^3s^{-1}$, 0.5 $m^3s^{-1}$)
- CADS width $W_{CADS}$ = 0.25 m (0.5 m, 1.0 m, 1.5 m)
- FHLQ with FH = 50 m, LQ = 0.045 $m^3s^{-1}$

The budget terms for the basic model ($d$ = 0.5 m, pumping rate = 0.25 $m^3s^{-1}$, $W_{CADS}$ = 0.25 m) are listed in Table AT–10.

**Table AT–10:** Water balance for the conduit system and the matrix flow system (all flow terms in $m^3s^{-1}$); cumulative values in square brackets ($m^3$)

| CONDUIT FLOW SYSTEM | | | | | | | NOTES |
|---|---|---|---|---|---|---|---|
| ***IN*** | ***END OF P1*** | | ***END OF P2*** | | ***END OF P3*** | | |
| CONSTANT HEAD | 0.0000 | [0.00] | 0.0000 | [93.62] | 0.0000 | [93.62] | *= inflow constant head* |
| PIPE RECHARGE | 0.1000 | [8640.28] | 0.1000 | [17280.55] | 0.1000 | [34561.10] | *= point recharge* |
| MATRIX EXCHANGE | 0.9977 | [8620.27] | 0.1043 | [17564.29] | 0.0994 | [34669.88] | *= from MODFLOW* |
| CAD STORAGE | 0.0000 | [0.00] | 0.0007 | [170.72] | 0.0000 | [170.72] | *= from CADS storage* |
| FHLQ BC (LQ CASE) | 0.0000 | [0.00] | 0.0450 | [3753.00] | 0.0000 | [3753.00] | *= inflow FHLQ* |
| TOTAL IN | 0.1998 | [17260.55] | 0.2500 | [38862.18] | 0.1994 | [73248.33] | |
| ***OUT*** | | | | | | | |
| CONSTANT HEAD | 0.1998 | [17260.55] | 0.0000 | [17262.18] | 0.1994 | [51477.89] | *= spring discharge* |
| PIPE RECHARGE | 0.0000 | [0.00] | 0.2500 | [21600.00] | 0.0000 | [21600.00] | *= water abstraction* |
| CAD STORAGE | 0.0000 | [0.00] | 0.0000 | [0.00] | < 0.0001 | [170.44] | *= to CADS storage* |
| TOTAL OUT | 0.1998 | [17260.55] | 0.2500 | [38862.18] | 0.1994 | [73248.33] | |
| PERCENT ERROR | 0.00 | | 0.00 | | 0.00 | | |
| **MATRIX FLOW SYSTEM** | | | | | | | |
| ***IN*** | | | | | | | |
| STORAGE | 0.0000 | [0.00] | 0.0053 | [395.16] | 0.0003 | [532.06] | *= from matrix storage* |
| CONSTANT HEAD | 0.0006 | [51.60] | 0.0006 | [103.21] | 0.0006 | [206.44] | *= matrix constant head* |
| RECHARGE | 0.0992 | [8568.66] | 0.0983 | [17065.92] | 0.0992 | [34203.25] | *= diffuse recharge* |
| TOTAL IN | 0.0997 | [8620.27] | 0.1043 | [17564.29] | 0.1001 | [34941.75] | |
| ***OUT*** | | | | | | | |
| STORAGE | 0.0000 | [0.00] | > 0.0000 | [> 0.00] | 0.0006 | [271.87] | *= to matrix storage* |
| CONSTANT HEAD | 0.0000 | [0.00] | 0.0000 | [0.00] | 0.0000 | [0.00] | *= matrix constant head* |
| PIPES | 0.0997 | [8620.27] | 0.1043 | [17564.29] | 0.0994 | [34669.88] | *= to conduit system* |
| TOTAL OUT | 0.0997 | [8620.27] | 0.1043 | [17564.29] | 0.1001 | [34941.75] | |
| PERCENT DISCREPANCY | 0.00 | | 0.00 | | 0.00 | | |

The computed budget terms are reasonable and, therefore, indicate the correct implementation of the FHLQ and CADS features in CFPM1.

Subsequently, pumping rate and CADS width were varied in order to investigate their significance. The influence of the pumping rate on the drawdown of the conduit pumping well is shown in Figure AT–11 for conduits with a diameter of 0.5 m (Figure AT–11 left) and 2.5 m (Figure AT–11 right). Both results are similar. This demonstrates that the drawdown behavior in case of an active hydraulic constraint (FHLQ boundary) is not necessarily dependent on conduit hydraulics (here varied by the diameter).

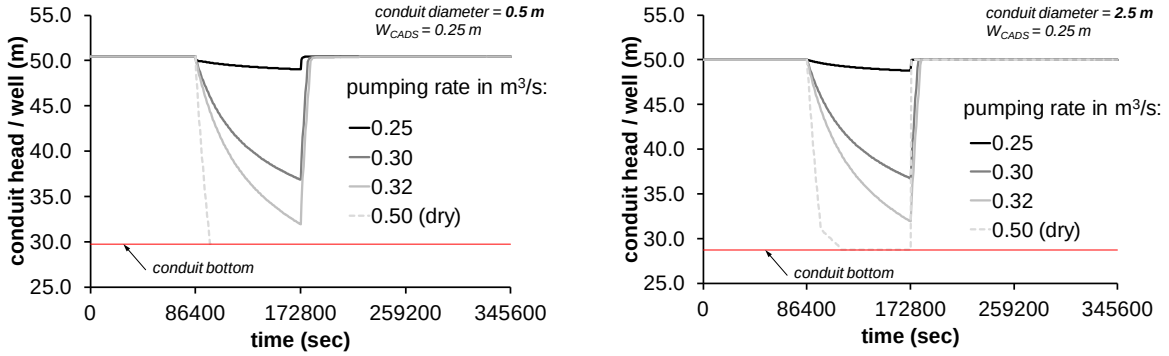


**Figure AT–11:** Conduit head at the pumping well for different pumping rates for a conduit with $d$ = 0.5 m (left) and a conduit with $d$ = 2.5 m (right), each with $W_{CADS}$ = 0.25 m

Resulting conduit heads for variable CADS widths are presented in Figure AT–12 for both investigated conduit diameters ($d$ = 0.5 m and $d$ = 2.5 m). Again, resulting drawdowns are similar. For both conduits an increasing CAD storage volume results in reduced drawdown during pumping and enlarged recovery times if pumping is stopped.

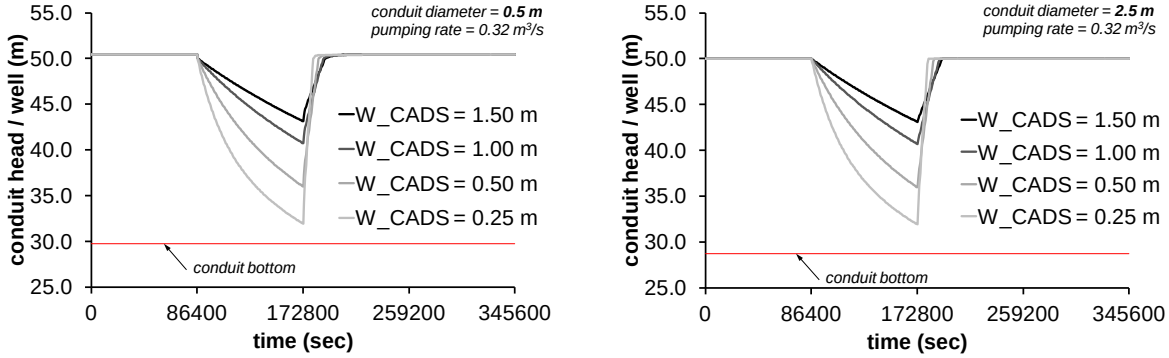


**Figure AT–12:** Conduit head at the pumping well for different CAD storage widths for a conduit with $d$ = 0.5 m (left) and a conduit with $d$ = 2.5 m (right)

# Case 10 - Point recharge and additional water abstraction from the conduit system realized with WELL boundary condition (steady state)

This case is similar to case 3. Water abstraction, i.e. the pumping well, is simulated with the newly implemented WELL boundary condition. Hence, this case demonstrates the new functionality of CFPM1 to consider water abstraction from the conduit system by using the WELL boundary. The model is adapted as listed below:

- water abstraction is considered with (refer to Figure 1 for node denotation):
  - WELL boundary at node 5 with QWELL = -0.05 $m^3s^{-1}$ (run A)
  - WELL boundary at node 1 with QWELL = 0.1 $m^3s^{-1}$ (run B)
  - WELL boundary at node 1 (0.1 $m^3s^{-1}$) and node 5 (-0.05 $m^3s^{-1}$) (run C)

**Table AT–11:** Water balance for the conduit system and the matrix flow system (all flow terms in $m^3s^{-1}$)

| | case 3 | run A | run B | run C | |
|---|---|---|---|---|---|
| **CONDUIT FLOW SYSTEM** | | | | | **NOTES** |
| ***IN*** | | | | | |
| PIPE RECHARGE | 0.1000 | 0.1000 | 0.0000 | 0.0000 | *= point recharge* |
| WELL BC | 0.0000 | 0.0000 | 0.1000 | 0.1000 | *= well infiltration* |
| MATRIX EXCHANGE | 0.0992 | 0.1000 | 0.0992 | 0.1000 | *= from MODFLOW* |
| TOTAL IN | 0.1992 | 0.2000 | 0.1992 | 0.2000 | |
| **OUT** | | | | | |
| CONSTANT HEAD | 0.1492 | 0.1500 | 0.1492 | 0.1500 | *= spring discharge* |
| PIPE RECHARGE | 0.0500 | 0.0000 | 0.0500 | 0.0000 | *= pumping (via RCH / CRCH)* |
| WELL BC | 0.0000 | 0.0500 | 0.0000 | 0.0500 | *= well pumping* |
| TOTAL OUT | 0.1992 | 0.2000 | 0.1992 | 0.2000 | |
| PERCENT ERROR | 0.00 | 0.00 | 0.00 | 0.00 | |
| **MATRIX FLOW SYSTEM** | | | | | |
| ***IN*** | | | | | |
| RECHARGE | 0.0992 | 0.1000 | 0.0992 | 0.1000 | *= diffuse recharge* |
| TOTAL IN | 0.0992 | 0.1000 | 0.0992 | 0.1000 | |
| ***OUT*** | | | | | |
| PIPES | 0.0992 | 0.1000 | 0.0992 | 0.1000 | *= to conduit system* |
| TOTAL OUT | 0.0992 | 0.1000 | 0.0992 | 0.1000 | |
| PERCENT DISCREPANCY | 0.00 | 0.00 | 0.00 | 0.00 | |

The results demonstrate the correct implementation of the WELL boundary condition. Infiltration as well as abstraction was considered correctly. If water abstraction (pumping) is considered by the WELL boundary condition, diffuse recharge is no longer affected resulting in the intended value of 0.1 $m^3s^{-1}$ for the whole catchment.

# Case 11 – Transient pumping with the WELL boundary condition

This scenario is comparable with case 6 (transient water abstraction), however pumping and water infiltration is realized with the WELL boundary. The conduit diameter is 0.5 m and the pumping rate in period 2 at node 5 is -0.25 $m^3s^{-1}$. Water is infiltrated at node 1 with 0.1 $m^3s^{-1}$ for all periods.

**Table AT–12:** Water balance for the conduit system and the matrix flow system (all flow terms in $m^3s^{-1}$); cumulative values in square brackets

| CONDUIT FLOW SYSTEM | | | | | | | NOTES |
|---|---|---|---|---|---|---|---|
| ***IN*** | ***END OF P1*** | | ***END OF P2*** | | ***END OF P3*** | | |
| CONSTANT HEAD | 0.0000 | [0.00] | 0.0486 | [4170.77] | 0.0000 | [4170.77] | *= inflow constant head* |
| PIPE RECHARGE | 0.0000 | [0.00] | 0.0000 | [0.00] | 0.0000 | [0.00] | *= direct recharge* |
| WELL BC | 0.1000 | [8640.00] | 0.1000 | [17280.00] | 0.1000 | [34560.00] | *= infiltration via WELL* |
| MATRIX EXCHANGE | 0.1000 | [8640.04] | 0.1014 | [17429.27] | 0.0999 | [34659.57] | *= from MODFLOW* |
| TOTAL IN | 0.2000 | [17280.04] | 0.2500 | [38880.04] | 0.1998 | [73390.34] | |
| ***OUT*** | | | | | | | |
| CONSTANT HEAD | 0.2000 | [17280.04] | 0.0000 | [17280.04] | 0.1998 | [51790.34] | *= spring discharge* |
| PIPE RECHARGE | 0.0000 | [0.00] | 0.0000 | [0.00] | 0.0000 | [0.00] | *= direct recharge* |
| WELL BC | 0.0000 | [0.00] | 0.2500 | [21600.00] | 0.0000 | [21600.00] | *= pumping well* |
| TOTAL OUT | 0.2000 | [17280.04] | 0.2500 | [38880.04] | 0.1998 | [73390.34] | |
| PERCENT ERROR | 0.00 | | 0.00 | | 0.00 | | |
| **MATRIX FLOW SYSTEM** | | | | | | | |
| ***IN*** | | | | | | | |
| STORAGE | 0.0000 | [0.00] | 0.0014 | [149.20] | 0.0001 | [198.37] | *= from matrix storage* |
| RECHARGE | 0.1000 | [8640.04] | 0.1000 | [17280.08] | 0.1000 | [34560.16] | *= diffuse recharge* |
| TOTAL IN | 0.1000 | [8640.04] | 0.1014 | [17429.27] | 0.1001 | [34758.52] | |
| ***OUT*** | | | | | | | |
| STORAGE | 0.0000 | [0.00] | 0.0000 | [0.00] | 0.0002 | [98.96] | *= to matrix storage* |
| PIPES | 0.1000 | [8640.04] | 0.1014 | [17429.27] | 0.0998 | [34659.57] | *= to conduit system* |
| TOTAL OUT | 0.1000 | [8640.04] | 0.1014 | [17429.27] | 0.1001 | [34758.52] | |
| PERCENT DISCREPANCY | 0.00 | | 0.00 | | 0.00 | | |

The budget demonstrates the correct implementation of the WELL boundary for transient model runs.

## Case 12 – Consideration of partially filled pipe storage (PFPS)

This scenario is similar to case 11 (transient water abstraction with the WELL boundary). However, the pumping rate at node 5 is increased to result in partially filled conduits and, therefore, water release from partially filled pipe storage (PFPS). To do so, the pumping rate at node 5 in period 2 is set to 1.5 $m^3s^{-1}$ (case 11: 0.25 $m^3s^{-1}$). Contrary to previous cases, point recharge at node 1 is set to 0. The conduit diameter is 0.5 m. Additionally, the diameter of tube 1 is varied as listed subsequently, to demonstrate the PFPS functionality (compare also Figure AT–1):

- Basic scenario 1: *d* (tube 1) = 0.5 m
- Scenario 2: *d* (tube 1) = 4.0 m
- Scenario 3: *d* (tube 1) = 5.0 m

Resulting heads are presented in Figure AT–13. It is obvious that especially for scenarios 2 and 3 some parts of the conduit system are dewatered.

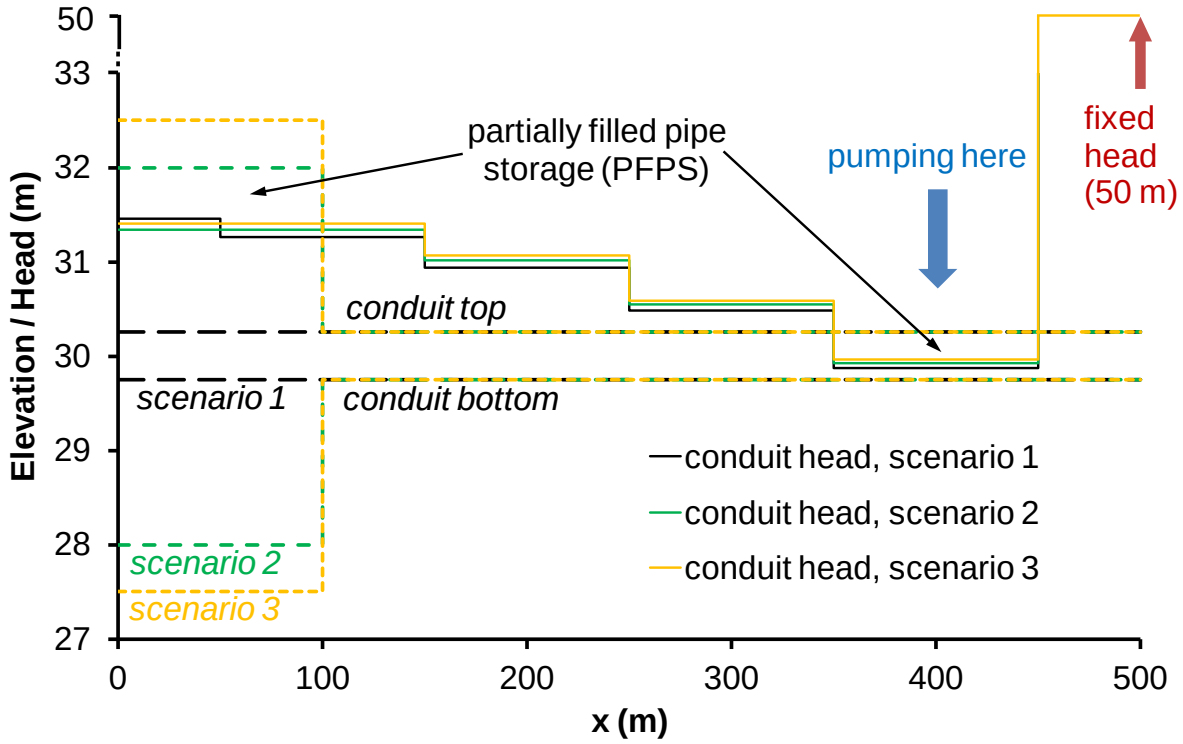


**Figure AT–13:** Resulting heads along the conduit for three different scenarios. For each scenario the first conduit from x = 0 (node 1) to x = 100 m (node 2) is varied: 1) *d* = 0.5 m, 2) *d* = 4.0 m, 3) *d* = 5.0 m; pumping at x = 400 m (node 5); fixed head (node 6) at x = 500 m; see also Figure AT–1.

Water budgets, as shown in Table AT–13, are used to check the correct implementation of the PFPS functionality. They demonstrate the functioning of the PFP storage module. Water released from PFPS is included in the active hydraulic system, resulting in discharge (i.e. additional spring discharge for the here investigated situation), which can be concluded from the perfectly matched water balance as presented in Table AT–13.

**Table AT–13:** Water balance of the conduit system and the matrix flow system for scenario 2 (*d* tube 1 = 4.0 m; flow terms in $m^3s^{-1}$); cumulative values in square brackets ($m^3$)

| CONDUIT FLOW SYSTEM | | | | | | | NOTES |
|---|---|---|---|---|---|---|---|
| ***IN*** | ***END OF P1*** | | ***END OF P2*** | | ***END OF P3*** | | |
| CONSTANT HEAD | 0.0000 | [0.00] | 1.2403 | [106265.39] | 0.0000 | [106310.20] | *= inflow constant head* |
| PIPE RECHARGE | 0.0000 | [0.00] | 0.0000 | [0.00] | 0.0000 | [0.00] | |
| WELL BC | 0.1000 | [8640.00] | 0.1000 | [17280.00] | 0.1000 | [34560.00] | *= point recharge* |
| MATRIX EXCHANGE | 0.1000 | [8640.04] | 0.1575 | [23186.38] | 0.0953 | [38448.43] | *= from MODFLOW* |
| PFP STORAGE | 0.0000 | [0.00] | 0.0022 | [148.26] | 0.0000 | [148.26] | *= pipe storage* |
| TOTAL IN | 0.2000 | [17280.04] | 1.5000 | [146880.04] | 0.1953 | [179466.90] | |
| ***OUT*** | | | | | | | |
| CONSTANT HEAD | 0.2000 | [17280.04] | 0.0000 | [17280.04] | 0.1953 | [49718.63] | *= spring discharge* |
| PIPE RECHARGE | 0.0000 | [0.00] | 0.0000 | [0.00] | 0.0000 | [0.00] | *= water abstraction* |
| WELL BC | 0.0000 | [0.00] | 1.5000 | [129600.00] | 0.0000 | [129600.00] | |
| PFP STORAGE | 0.0000 | [0.00] | 0.0000 | [0.00] | 0.0000 | [148.26] | *= pipe storage* |
| TOTAL OUT | 0.2000 | [17280.04] | 1.5000 | [146880.04] | 0.1953 | [179466.90] | |
| PERCENT ERROR | 0.00 | | 0.00 | | 0.00 | | |
| **MATRIX FLOW SYSTEM** | | | | | | | |
| ***IN*** | | | | | | | |
| STORAGE | 0.0000 | [0.00] | 0.0575 | [5906.31] | 0.0046 | [7841.73] | *= from matrix storage* |
| RECHARGE | 0.1000 | [8640.04] | 0.1000 | [17280.08] | 0.1000 | [34560.16] | *= diffuse recharge* |
| TOTAL IN | 0.1000 | [8640.04] | 0.1575 | [23186.39] | 0.1046 | [42401.88] | |
| ***OUT*** | | | | | | | |
| STORAGE | 0.0000 | [0.00] | 0.0000 | [0.00] | 0.0093 | [3953.45] | *= to matrix storage* |
| PIPES | 0.1000 | [8640.04] | 0.1575 | [23186.38] | 0.0953 | [38448.43] | *= to conduit system* |
| TOTAL OUT | 0.1000 | [8640.04] | 0.1575 | [23186.39] | 0.1046 | [42401.88] | |
| PERCENT DISCREPANCY | 0.00 | | 0.00 | | 0.00 | | |

Overall, these conclusions are valid for scenarios 1 and 2. The increased conduit diameter in scenario 3 results in some numerical instability: water released from PFPS increases discharge and, subsequently, increases heads. Hence, a changeover from partially filled conduits back to fully filled conduits occurs. The resulting numerical oscillations prevent convergence for this time step resulting in a slightly erroneous water balance. Typically for the scenarios investigated here, the model converges in subsequent time steps such that overall results are only little affected. An overview about all three scenarios is given in Table AT–14.

**Table AT–14:** Results for all three scenarios of case 12

| | **Scenario 1** | **Scenario 2** | **Scenario 3** |
|---|---|---|---|
| Discrepancy cumulative water balance conduit system | 0.0000 | 0.0000 | -10.9912 $m^3$ |
| Percentage error cumulative water balance conduit system | 0.00 | 0.00 | 0.00 |
| Discrepancy cumulative water balance entire system | -0.0004 $m^3$ | 0.0001 $m^3$ | 0.0001 $m^3$ |
| Percentage error cumulative water balance entire system | 0.00 | 0.00 | 0.00 |
| PFPS at the end of period 2 – CFPM1 budget | 16.1654 $m^3$ | 148.2623 $m^3$ | 321.7948 $m^3$ |
| PFPS at the end of period 2 – computed with conduit heads | 16.1656 $m^3$ | 148.2626 $m^3$ | 332.9702 $m^3$ |
| Convergence | converged always | converged always | conduit system didn't converge in period 2 time step 1 |

# Case 14 – In- and outflow with Cauchy boundary

This scenario demonstrates the functioning of the Cauchy boundary condition. Therefore, the basic setup was modified as shown in Figure AT-14.

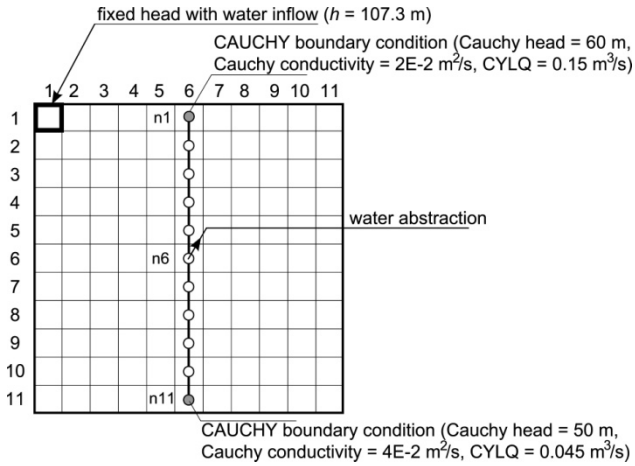


**Figure AT–14:** Case 14 / 15 situation.

Three situations are considered: (1) Comparison with fixed head boundary (at nodes 1 and 11), (2) unrestricted Cauchy flow, and (3) water abstraction at node 6 with $Q$ = 0.3 $m^3s^{-1}$ resulting in limited inflow (CYLQ).

Results for all scenarios are presented in Table AT-15. With adequate parameters (large CCY, similar HCY), the Cauchy and fixed head boundary condition give equal results (scenario 1). Unrestricted Cauchy flow is computed according equation to A5-1 (scenario 2). In case inflow is limited by a CYLQ condition, CFPM1 computes smaller conduit heads because additional conduit drawdown is necessary to compensate limited inflow (node 1). The unrestricted boundary (node 11) results in flow according to equation A5-1 (scenario 3).

**Table AT–15:** Results for all three scenarios of case 14

| | Scenario 1 FH | Scenario 1 Cauchy | Scenario 2 | Scenario 3 |
|---|---|---|---|---|
| Node head in m (n1 / n11) | 60.000 / 50.000 | 60.000 / 50.000 | 56.680 / 54.533 | 51.086 / 49.188 |
| CFPM1 $Q_{fix}$ in $m^3s^{-1}$ (n1 / n11) | -0.221 / 0.335 | 0.000 / 0.000 | 0.000 / 0.000 | 0.000 / 0.000 |
| CFPM1 $Q_{cy}$ in $m^3s^{-1}$ (n1 / n11) | 0.000 / 0.000 | -0.221 / 0.335 | -0.066 / 0.181 | -0.150* / 0.032 |
| EQ A5-1 $Q_{cy}$ in $m^3s^{-1}$ (n1 / n11) | - | - | -0.066 / 0.181 | -0.178 / 0.032 |
| Percentage error cumulative water balance conduit system | 0.00 | 0.00 | 0.00 | 0.00 |

** = CYLQ*

## Case 15 – Variable water abstraction with Cauchy boundary condition

This case is similar to case 14 (Figure AT-14). The transient model considers four periods

- period 1, steady state, 86 400 seconds, no water abstraction
- period 2, transient, 86 400 seconds, no water abstraction
- period 3, transient, 86 400 seconds, water abstraction with $Q$ = 0.3 $m^3s^{-1}$ (results in CYLQ)
- period 4, transient, 172 800 seconds, no water abstraction

Results, presented in Figure AT-15, are comparable with steady state results (compare with Table AT-15; periods 2 and 4 are similar to case 14 / scenario 2, and period 3 is similar to case 14 / scenario 3).

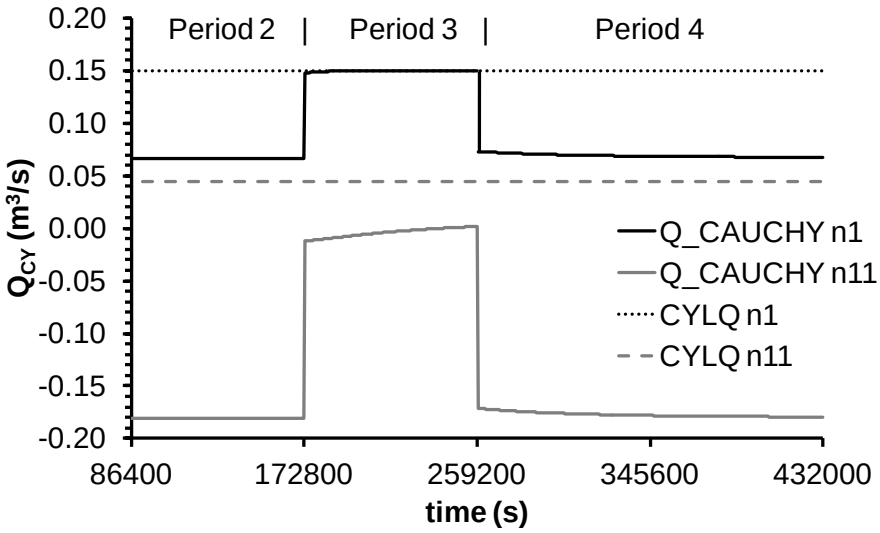


**Figure AT–15:** Results for case 15.

Hence, the Cauchy boundary condition correctly considers transient conditions as well as the change-over from unrestricted flow to limited inflow (CYLQ).

## Case 16 – Limited head with LH boundary condition

This scenario demonstrates the functioning of the LH boundary condition according to equation A6-1 under steady state conditions. Therefore, the basic setup (case 1) was modified as listed:

- node 1: 0.1 $m^3s^{-1}$ inflow by well boundary,
- node 3: LH boundary with limiting head as 51.0 m.

Results are presented in Figure AT-16 and Table AT-16. Hence, the LH boundary works as intended and results are similar to the FHLQ boundary (with LQ = 0). The advantage of the LH boundary is the display of separate flow budget terms together with a potentially more stable numerical implementation.

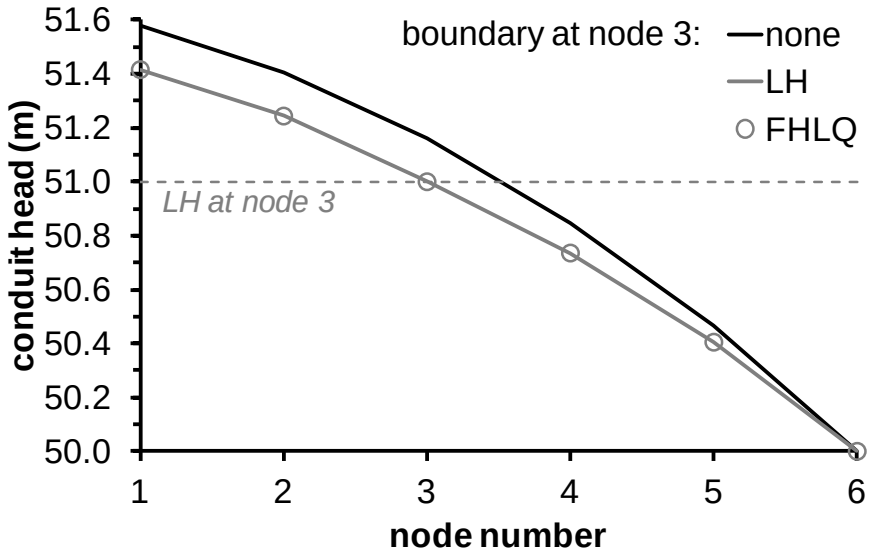


**Figure AT–16:** Conduit heads for case 16.

**Table AT–16:** Conduit budget for case 16, all budget terms in $m^3s^{-1}$

| boundary at node 3 | **none** | **LH** | **FHLQ** |
|---|---|---|---|
| IN – matrix exchange | 0.1000 | 0.1000 | 0.1000 |
| IN – well bc | 0.1000 | 0.1000 | 0.1000 |
| OUT – constant head | 0.2000 | 0.1874 | 0.2000 |
| OUT – limited head (LH) | 0.0000 | 0.0126 | 0.0000 |
| percentage error | 0.00 | 0.00 | 0.00 |

# Case 17 – Limited head with LH boundary condition for transient pumping

This scenario demonstrates the functioning of the LH boundary condition under transient conditions, which is practically more useful because the LH boundary and the FHLQ boundary are only active under certain conditions. Therefore, the case 16 setup was modified as listed below:

- 3 periods
  - period 1: 86 400 seconds steady state; node 1: 0.1 $m^3s^{-1}$ inflow
  - period 2: 86 400 seconds transient; node 1: 0.3 $m^3s^{-1}$ inflow
  - period 3: 172 800 seconds transient; node 1: 0.1 $m^3s^{-1}$ inflow
- node 3: limited head boundary with LH = 55 m
- node 6: fixed head boundary with FH = 50 m
- CADS mit $W_{cads}$ = 1.0 m

Hence, the inflow increase in period 2, in interaction with active CAD storage, results in gradually increasing conduit heads. Figure AT-17 shows conduit heads and outflow at node 3 and, therewith, demonstrates the proper functioning of the LH boundary condition. Results are similar to the FHLQ boundary (with LQ = 0). Cumulative budgets are comparable without a significant percentage error. As already mentioned, the advantage of the LH boundary is the display of separate flow budget terms together with a potentially more stable numerical implementation.

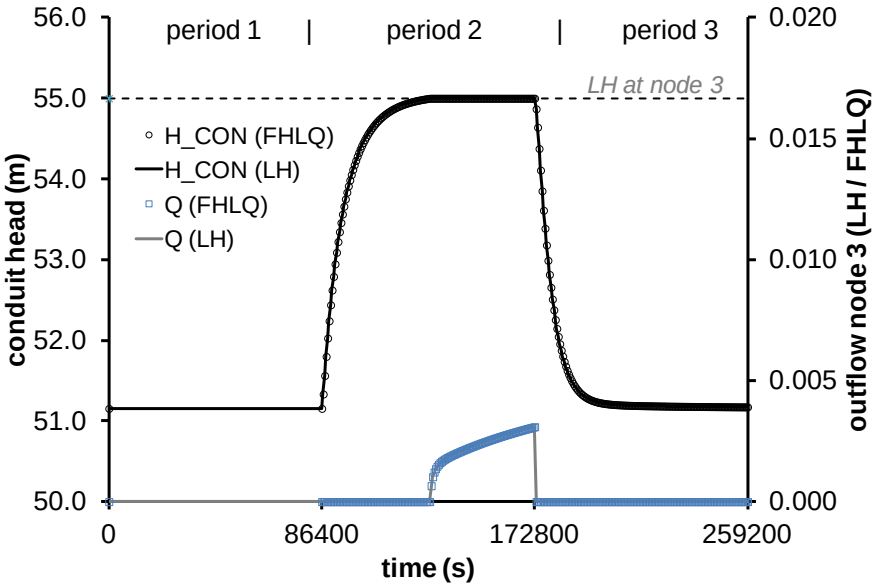


**Figure AT–17:** Conduit heads and outflow at node 3 for case 17.

# Case 18 – Time dependent boundary data TD

The ability to process time dependent boundary data is validated for each applicable boundary condition (fixed head, FHLQ, Cauchy, and well). A first scenario replicates case 11 (transient pumping with well boundary condition) respectively case 6 (transient pumping). Time dependent data were set such that flow is identical to case 6 / 11. For a second scenario, time dependent data were slightly varied. Specific data for both scenarios are subsequently provided.

Fixed head boundary:

- TD data for the fixed head in node 6
- scenario 1: fixed head constant 50 m
- scenario 2: fixed head constant 50 m, additional increase to 52 m from $t$ = 86 400 s to 100 000 s and decrease to 50 m from $t$ = 100 000 s to 172 800 s.

FHLQ boundary:

- TD data for the FHLQ boundary in node 6; LQ is set to 1.0 $m^3s^{-1}$
- scenario 1: fixed head constant 50 m
- scenario 2: fixed head constant 50 m, additional increase to 52 m from $t$ = 86 400 s to 100 000 s and decrease to 50 m from $t$ = 100 000 s to 172 800 s
- for an additional model run LQ was set to 0.05 $m^3s^{-1}$ to result in a temporary LQ situation

Cauchy boundary:

- TD data for the Cauchy boundary in node 6; CCY = 1E10 $ms^{-1}$ and CYLQ = 1.0 $m^3s^{-1}$
- scenario 1: HCY constant 50 m
- scenario 2: HCY constant 50 m, additional increase to 52 m from $t$ = 86 400 s to 100 000 s and decrease from 52 m to 50 m from $t$ = 100 000 s to 172 800 s.

Well boundary:

- TD data for the pumping well in node 5
- scenario 1: $Q_{well}$ is 0 in period 1 and 3 and -0.2 $m^3s^{-1}$ in period 2 (see also case 6)
- scenario 2: $Q_{well}$ is 0 in period 1 and 3; in period 2 pumping starts with $Q_{well}$ = -0.25 $m^3s^{-1}$ increase to -0.30 $m^3s^{-1}$ from $t$ = 86 400 s to 100 000 s and decrease to 0.25 $m^3s^{-1}$ from $t$ = 100 000 s to 172 800 s.

The resulting cumulative budget terms for the conduit system are presented in Table AT-17. All budget terms are similar to case 11 and, therefore, proof that time dependent input files are correctly considered.

**Table AT–17:** Cumulative budget for the conduit system at the end of period 3 for scenario 1 of case 18; all budget terms in $m^3$

| | case 11 | fixed head TD | FHLQ TD | Cauchy TD | Well TD |
|---|---|---|---|---|---|
| IN – constant head | 4 171 | 4 171 | 4 171 | 0 | 4 171 |
| IN – matrix exchange | 34 660 | 34 660 | 34 660 | 34 660 | 34 660 |
| IN – cauchy bc | 0 | 0 | 0 | 4 171 | 0 |
| IN – well bc | 34 560 | 34 560 | 34 560 | 34 560 | 34 560 |
| OUT – constant head | 51 790 | 51 790 | 51 790 | 0 | 51 790 |
| OUT – well bc | 21 600 | 21 600 | 21 600 | 21 600 | 21 600 |
| OUT - Cauchy bc | 0 | 0 | 0 | 51 792 | 0 |
| percentage error | 0.00 | 0.00 | 0.00 | 0.00 | 0.00 |

For the second scenario, a slight variation of time dependent input values is intended, which can be observed in terms of the conduit head at node 6 (for the fixed head, FHLQ, and Cauchy boundary) respectively the pumping rate at node 5 (well boundary). Results, shown in Figure AT-18, demonstrate the correct functioning of the TD boundary condition.

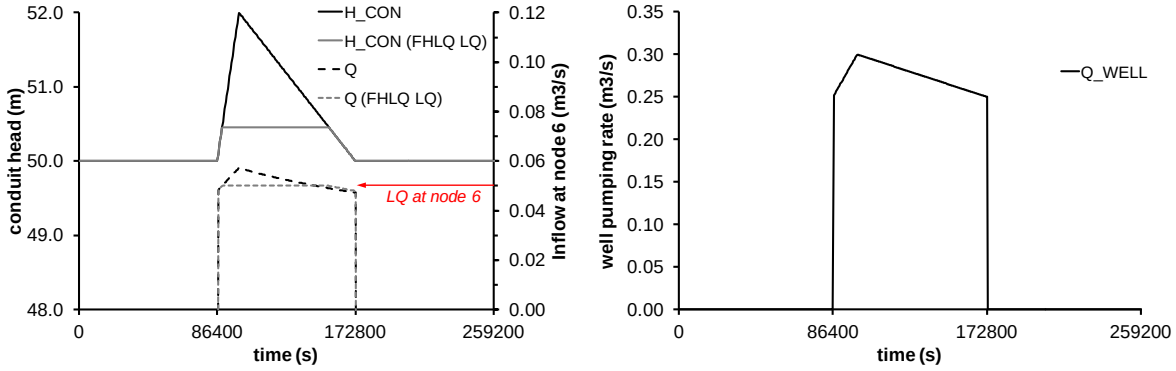


**Figure AT–18:** Left) conduit heads and inflow at node 6 for case 18 / scenario 2. Results denoted by H_CON and Q are similar for the fixed head, Cauchy, and FHLQ (FH case) boundaries; right) pumping rate at node 5 for case 18 / scenario 2.

# BT. PART B TESTING: CFPM1 TRANSPORT – TEST CASES

The intention of the following test cases is to demonstrate the correct technical functioning of heat transport (HTM) and solute transport (STM) subroutines implemented in CFPM1. Test Case 0 considers benchmarks and examples published previously by Birk [2002]. Test cases 1 - … demonstrate and proof the HTM/STM functionality for a schematic and idealized karst catchment (similar to test cases used to investigate flow model modification – section 5 of this report).

## Case overview

| Case | Intention / specific feature | Tested functionality | Page |
|---|---|---|---|
| **0 PhD Birk** | proof implementation of HTM in CFPM1 | heat transport computation | 62 |
| **1** | proof heat transport equations for pipe flow (isolated conduit) addition / reduction of heat (+2°C / -2°C) | heat transport computation with convection only; convection with thermal boundary layer, convection with themal boundary layer and rock conduction, mass balance computation / budgets | 66 |
| **2** | proof solute transport equations for pipe flow (isolated conduit); mass injection with direct recharge | STM, LUT / UMT3D; advection only, advection and dispersion; advection, dispersion, and matrix diffusion | 70 |
| **3** | proof implementation of well boundary condition for HTM / STM transport packages | HTM / STM transport with recharge well (inflow) | 77 |
| **4** | proof implementation of fixed head / FHLQ boundary conditions for HTM / STM transport packages | HTM / STM transport with fixed head / FHLQ boundary | 78 |
| **5** | proof implementation of transport consideration for the CADS package | HTM / STM transport for different infiltration and exfiltration scenarios | 81 |
| **6** | proof implementation of Cauchy boundary condition for HTM / STM transport packages | HTM / STM transport with Cauchy flow (unrestricted and restricted by CYLQ) | 85 |
| **7** | proof implementation of time dependent boundary conditions (TD) for HTM / STM transport packages | HTM / STM with time dependent concentration / heat | 88 |

# Case 0: PhD Birk – Heat transport in meshed and isolated conduits

Two different settings are considered, a conduit network with relatively short pipes to compute heat transport in conduits (short conduits to minimize rock matrix conduction), and a long (hydraulically) isolated conduit to compute heat transport in conduits with rock matrix interaction (long conduit to enhance effects of heat exchange through the thermal boundary layer and rock matrix conduction). A detailed description of both tests (meshed and isolated conduits) is given by *Birk* [2002].

## Conduit network (heat transfer in conduit flow – short conduits)

*Basic situation*

The basic situation is presented in Figure BT–1. Further data are listed below in Table BT–1.

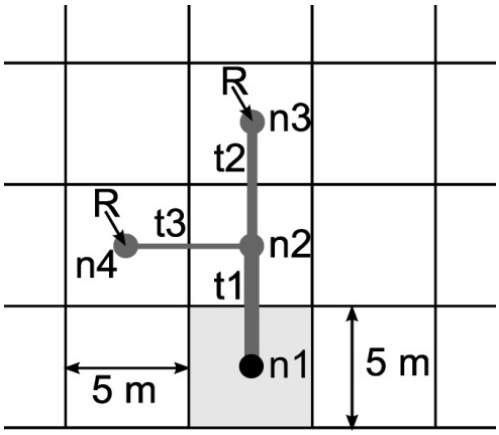


**Figure BT–1:** Basic situation for the conduit network

**Table BT–1:** Input data for conduit network scenario

| | |
|---|---|
| **Conduits** | |
| pipe diameter $d$ | tube 1: $d$ = 0.1 m, tube 2: $d$ = 0.05 m, tube 3: $d$ = 0.025 m |
| roughness | 0.01 x $d$ |
| water transfer coefficient $\alpha$ | node 1: 0.0001 $m^2s^{-1}$; node 2-4: 0 |
| **Heat transport parameter** | |
| initial temperature in matrix and conduit | 8 °C |
| temperature of matrix inflow | 8 °C (applies in node 1) |
| temperature of direct recharge | 6 °C |
| rock density $\rho_r$ | 2320 kg $m^{-3}$ |
| specific heat of rock $c_r$ | 1088 J $kg^{-1}K^{-1}$ |
| thermal conductivity of rock $\lambda_r$ | 1.297 W $m^{-1}K^{-1}$ |
| specific heat of water $c_W$ | 4198 J $kg^{-1}K^{-1}$ |
| thermal conductivity of water $\lambda_W$ | 0.582 W $m^{-1}K^{-1}$ |
| **Boundary conditions** | |
| fixed head | in both conduit (node 1) and matrix (grey cell), see figure 1. Head difference between both fixed head cells is 1 m (50 m in the conduit node, 51 m in the matrix cell). |
| recharge | 0.3142 $ls^{-1}$ for turbulent situations and 0.03927 $ls^{-1}$ for laminar situations |

*Results*

Results, based on figures from *Birk* [2002], are presented in Figures 10–2 to 10–6. Data computed by CFPM1-HTM are added to these figures as discrete symbols.

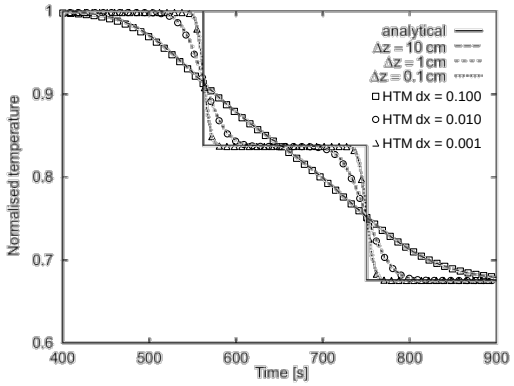


**Figure BT–2:** (Figure 3.19 from *Birk* [2002]) Laminar flow with fully developed thermal boundary layer; $N_{Nu}$ = 3.66 according to equation B1–28; dashed / dotted lines are CAVE results; symbols are CFPM1-HTM results, please note: $\Delta x$ in m.

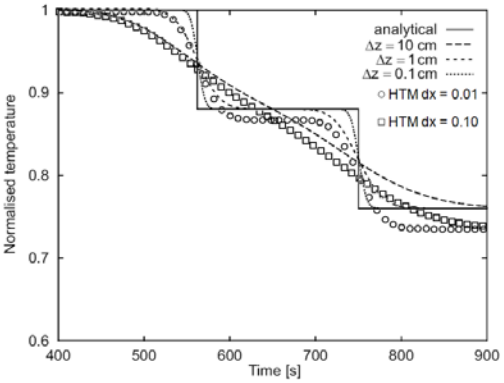


**Figure BT–3:** (Figure 3.20 from *Birk* [2002]) Laminar flow with developing boundary layer; $N_{Nu}$ according to equation B1–29 with a distance from the entrance according to Figure BT–1 (node 1: 10 m, node 2: 5 m, node 3 / 4: 0 m); dashed / dotted lines are CAVE results; symbols are CFPM1-HTM results, please note: $\Delta x$ in m; for clarity of presentation, results for $\Delta x$ = 0.001 m are omitted.

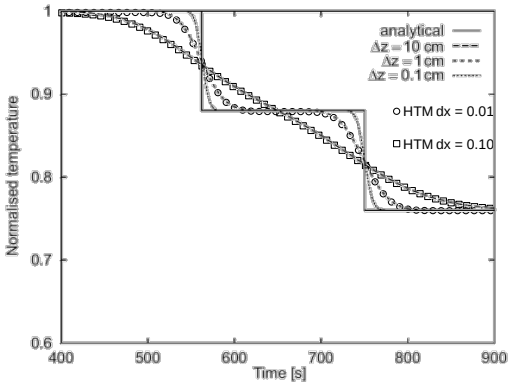


**Figure BT–4:** (Figure 3.20 from *Birk* [2002]) Laminar flow with developing boundary layer; $N_{Nu}$ according to equation B1–29 with a uniform distance from the entrance of 5 m; dashed / dotted lines are CAVE results; symbols are CFPM1-HTM results, please note: $\Delta x$ in m; for clarity of presentation, results for $\Delta x$ = 0.001 m are omitted.

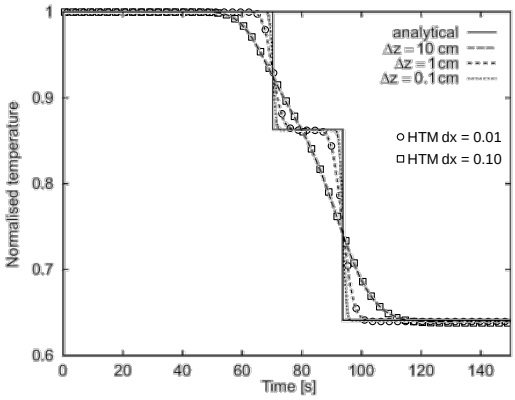


**Figure BT–5:** (Figure 3.18 from *Birk* [2002]) Turbulent flow with $N_{Nu}$ according to equation B1–31 [*Gnielinski* 1976]; dashed / dotted lines are CAVE results; symbols are CFPM1-HTM results, please note: $\Delta x$ in m; for clarity of presentation, results for $\Delta x$ = 0.001 m are omitted.

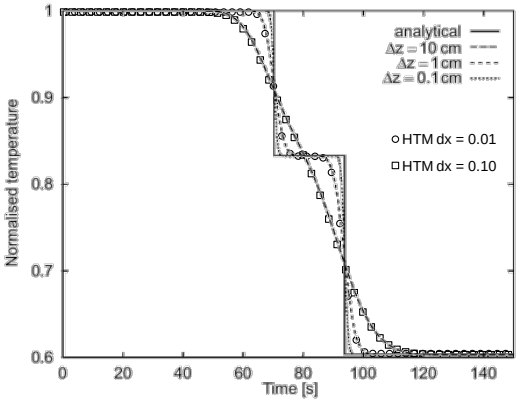


**Figure BT–6:** (Figure 3.17 from *Birk* [2002]) Turbulent flow with $N_{Nu}$ according to equation B1–30 [*Beek and Muttzall,* 1975]; dashed / dotted lines are CAVE results; symbols are CFPM1-HTM results, please note: $\Delta x$ in m; for clarity of presentation, results for $\Delta x$ = 0.001 m are omitted.

Overall, CFPM1-HTM results match those from CAVE and, therefore, proof the correct implementation of the HTM subroutines in CFPM1. The apparent differences in Figure BT–3 are caused by the new implemented option to define the distance of each node to the entry point; CAVE considers the entry point at the beginning of each tube. CFPM1 accounts for the larger distance between the entry points (nodes 3 and 4) and node 1. Consequently, the thermal boundary layer is further developed with smaller values for $N_{Nu}$ and results from CFPM1 move slightly towards the scenario with fully developed boundary layer (compare Figures BT–2 and BT–3).

## Isolated conduit (coupled heat transfer in conduit flow and rock – long conduit)

*Basic situation*

The basic situation is shown in Figure BT–7. Further data (if different to the previous situation) are listed below in Table BT–2:

**Table BT–2:** Input data for isolated conduit scenario

| **Conduits** | |
|---|---|
| pipe diameter *d* | t1…t5: *d* = 0.1 m |
| water transfer coefficient $\alpha$ | n1-6: 0 |
| **Boundary conditions** | |
| fixed head | in the conduit (node 1), see Figure BT–7 |
| recharge | 7.854 $ls^{-1}$ resulting in a turbulent flow velocity of 1 $ms^{-1}$ |

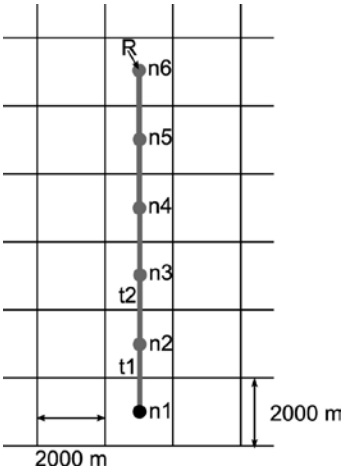


**Figure BT–7:** Basic situation for the isolated conduit

*Results*

Figure BT–8 compares the results from CFPM1-HTM with CAVE for different spatial discretizations $\Delta r$ of the radial rock matrix surrounding the conduit. Results from CFPM1-HTM fit CAVE results very well demonstrating the correct implementation of heat conduction within the radial rock matrix.

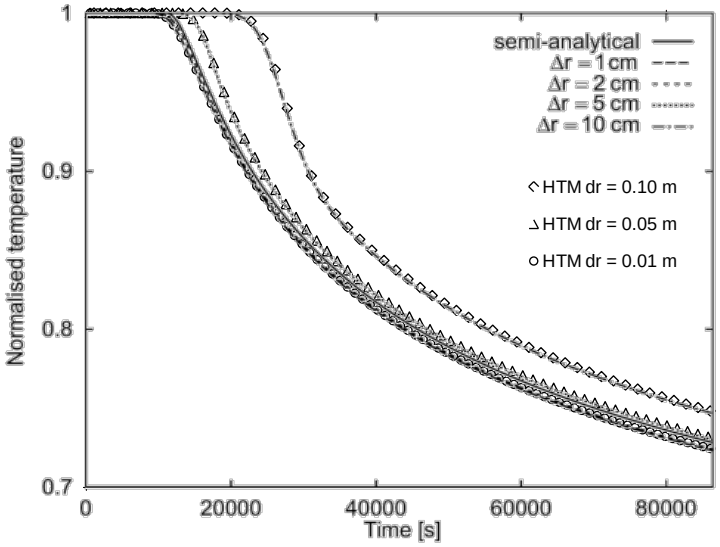


**Figure BT–8:** (Figure 3.21 from *Birk* [2002]) Temperatures at the conduit outlet (node 1; see Figure BT–7) for different discretizations $\Delta r$ of the radial rock matrix; lines are CAVE results, symbols are CFPM1-HTM results.

*[Note: Covington et al. [2011] provide an analytical solution for planar situations with some evidence for what situations the planar solution is valid for cylindrical scenarios. Hence, the semi-analytical solution in Figure BT–8 can be improved.]*

# Case 1 – Heat transport in an isolated conduit

A catchment with the following parameters is considered as basic situation (compare Fig. BT–9):

- length and width = 1100 m, subdivided in 11 x 11 cells with $\Delta x = \Delta y = 100$ m,
- thickness = 150 m (top = 150 m, bottom = 0 m; 1 layer with $\Delta z = 150$ m),
- matrix conductivity $K$ = 1E-5 $ms^{-1}$.

A central conduit with the following parameters is placed within the matrix:

- length = 500 m, diameter = 0.5 m, roughness = 0.01 m, height (node center) = 30 m,
- 6 nodes / 5 tubes á 100 m length, each tube is initially subdivided in 200 section ($\Delta x$ = 0.5 m),
- pipe conductance (transfer coefficient) = 0 (not connected to the matrix).

Parameters for heat transport are:

- initial temperature in rock matrix and conduit: 10 °C,
- bulk rock density: 2300 kg $m^{-3}$, specific heat capacity of rock: 810 J $kg^{-1}K^{-1}$, thermal conductivity of rock: 2.15 W $m^{-1}K^{-1}$,
- specific heat capacity of water: 4200 J $kg^{-1}K^{-1}$, thermal conductivity of water: 0.58 W $m^{-1}K^{-1}$.

The model considers two time periods:

- period 1: 3600 seconds with 60 time steps à 60 seconds, steady state,
- period 2: 7200 seconds with 120 time steps à 60 seconds, transient.

The following boundary conditions are applied to the flow model (uniform for periods 1 and 2):

- fixed head in the conduit with $h$ = 50 m, fixed head in the lower left matrix cell to allow dewatering of diffuse recharge,
- direct recharge in the conduit with $Q_{DIR}$ = 0.1 $m^3s^{-1}$,
- diffuse recharge (continuum cells) with a rate of 8.2645E-8 m/s (resulting in 0.1 $m^3s^{-1}$ recharge flux for the whole catchment).

The following boundary conditions are applied for the transport model:

- system input via direct recharge ($Q_{DIR}$) with the following temperature:
    - period 1: $T$ = 10°C,
    - period 2: $T$ = 8°C (heat removal) / 12°C (heat injection).

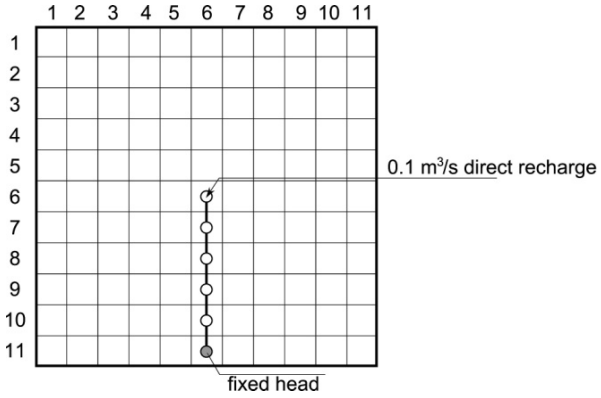


**Figure BT–9:** Basic situation for transport case 1, only the central conduit is considered for transport computation (see also Figure AT–1).

Heat $H$ can be computed with the following equation:

$$H = c\rho VT \qquad \text{eq. BT–1}$$

with $c$ specific heat capacity, $\rho$ density, $V$ volume, and $T$ temperature in Kelvin. Subsequently, heat and heat flux are computed for the water filled conduits with the following data:

- specific heat capacity of water $c_W$ = 4200 J kg$^{-1}$ K$^{-1}$,
- density of water $\rho_W$ = 1000 kg m$^{-3}$,
- volume of conduits $V_C = \pi/4\ d_C^2\ L_C$ = 98.17 m$^3$ ($d_C$ = 0.5 m, $L_C$ = 500 m),
- initial temperature $T_{ini}$ = 283.15 K (= 10°C).

## Results – Convection only

To consider convection only (without heat transfer across the thermal boundary layer), the thermal conductivity of both rock and water are set to very small values of 1 x 10$^{-12}$ Wm$^{-1}$K$^{-1}$ each. The resulting initial heat in the conduit system, calculated with equation 10–1, is $H_{ini}$ = 116 747 MJ. The initial heat computed by HTM is 116 717 MJ (-30 MJ). The computed heat (= cumulative heat flux) for the heat removal scenario ($\Delta T$ = -2°C) and for the heat injection scenario ($\Delta T$ = +2°C) are presented in Table BT–3. The values computed with the heat transport equation (equation 10–1) slightly differ from CFPM1-HTM. This is probably caused by the water density, which is computed by HTM as function of temperature and, therefore, is slightly reduced compared to the value used for the analytic calculation.

The computed temperatures at the outlet node are shown in Figure BT–10. The comparison with analytical values ($T_{out}$ = $T_{in}$; time shift according to flow velocity) demonstrate that the HTM module can correctly compute heat transport in an isolated conduit. The aberrations of outlet temperatures from the theoretical values (slightly damped break through) are caused by minor numerical dispersion.

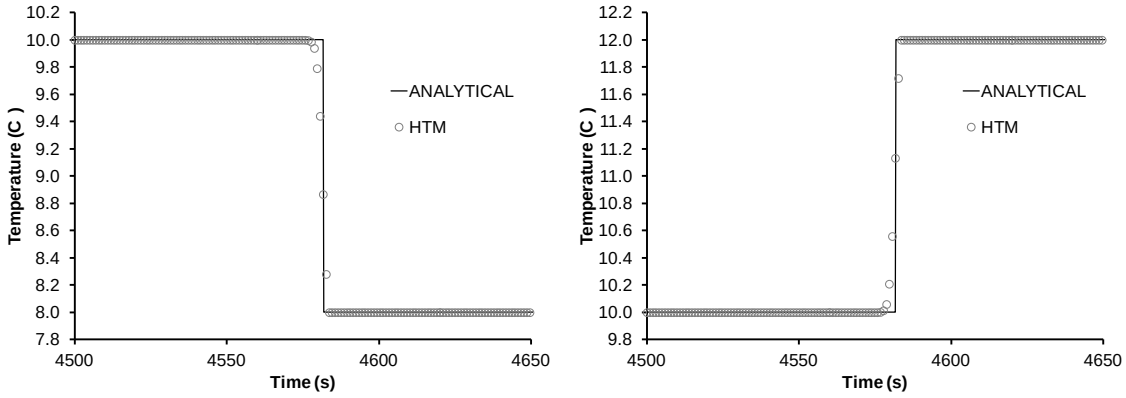


**Figure BT–10:** Results for heat transport with CFPM1 / HTM (convection only); left heat removal scenario, right heat injection scenario

## Results – Convection and heat exchange via the thermal boundary layer

In this scenario, heat exchange with the rock matrix via the thermal boundary layer (TBL) is considered but the rock matrix temperature is kept constant. Therefore, the spatial discretization of the rock matrix is enlarged to $\Delta r$ = 1000 m resulting in constant rock temperatures. The outlet temperature can be computed with the following analytical solution [*Birk*, 2002]:

$$T_{out} = T_{r0} - (T_{r0} - T_{in})\exp\left(-\overline{N_{Nu}} k_w \frac{\pi L}{Q}\right) \qquad \text{eq. BT–2}$$

with $T_{out}$ outlet temperature. The Nusselt number is computed according to equation B1–30 as 971. Therewith, the outlet temperatures are (with $k_w$ = 1.39 x 10$^{-7}$ m$^2$s$^{-1}$ and $T_{r0}$ initial temperature, compare Figure B1–4):

- $T_{out}$ = 9.76 °C (heat removal),
- $T_{out}$ = 10.24 °C (heat injection).

Results, shown in Figure BT–11, match the analytical values demonstrating the correct implementation of the HTM module. Comparison with Figure BT–10 highlights the influence of heat exchange with the rock matrix. The computed heat balance (cumulative heat flux) for the heat removal ($\Delta T$ = -2°C) and the heat injection scenario ($\Delta T$ = +2°C) are presented in Table BT–3 (end of the section).

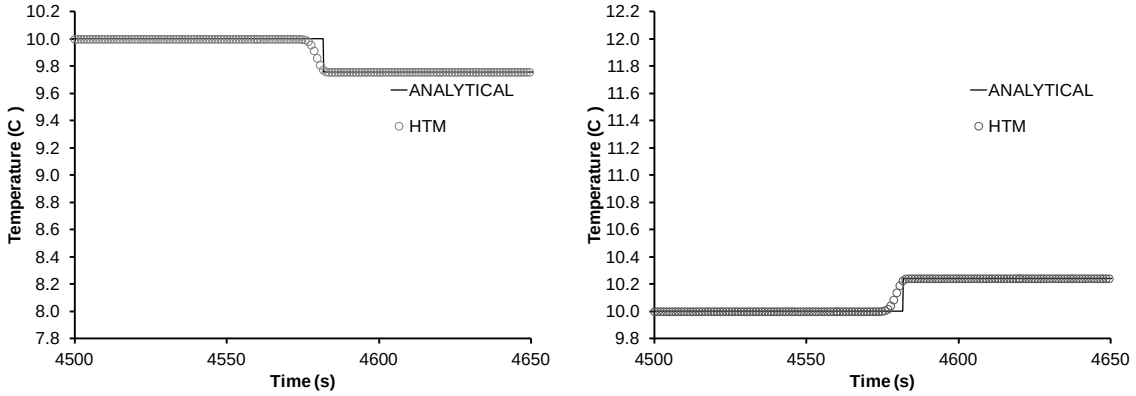


**Figure BT–11:** Results for heat transport with CFPM1 / HTM (convection and heat transfer with rock matrix); left heat removal scenario, right heat injection scenario; scaling similar to Figure BT–10 to allow direct comparison.

## Results – Convection, heat exchange via the thermal boundary layer, and heat conduction in rock

In this scenario, in addition to heat exchange with the rock matrix, heat conduction in the rock matrix is considered. Consequently, the rock temperature is no longer a constant. The spatial discretization of the rock matrix is set to $\Delta r$ = 0.02 m (see test cases from *Birk* [2002] for the isolated conduit, reported in the previous section) with 200 nodes in the rock matrix.

Results are shown in Figure BT–12. Comparison with the analytical calculated values (with constant rock temperature – without heat conduction in rock) highlights the influence of heat conduction inside the rock matrix. The computed heat flux respectively heat for the heat removal ($\Delta T$ = -2°C) and the heat injection scenario ($\Delta T$ = +2°C) are presented in Table BT–3.

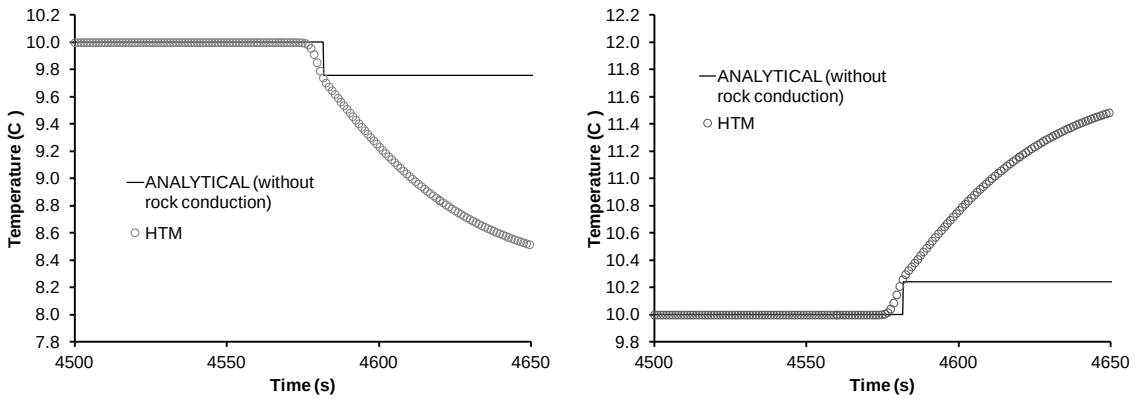


**Figure BT–12:** Results for heat transport with CFPM1 / HTM (convection, heat transfer with rock matrix and heat conduction in the rock matrix); left: heat removal scenario; right: heat injection scenario; scaling similar to Figure BT–11 to allow direct comparison.

**Table BT–3:** Cumulative heat balance (in MJ) for transport case 1

| | ***eq. BT–1*** | ***HTM conv*** | ***HTM conv+TBL*** | ***HTM conv+TBL+RCond*** |
|---|---|---|---|---|
| **Period 1** – both heat removal and heat injection scenario ($T$ = 10°C, $Q_{DIR}$ = 0.1 $m^3s^{-1}$; 3600 s) | | | | |
| IN $Q_{DIR}$ | 428123 | 427 994 | 427 994 | 427 994 |
| IN STORAGE | 0 | 0 | 0 | 0 |
| IN ROCK EXCHANGE | 0 | 0 | 0 | 0 |
| OUT STORAGE | 0 | 0 | 0 | 0 |
| OUT FIXED HEAD | 428123 | 427 994 | 427 994 | 427 994 |
| IN-OUT | 0 | 0.0000 | 0.0000 | 0.0000 |
| ERROR % | 0 | 0.0000 | 0.0000 | 0.0000 |
| **Period 2 – heat removal scenario** ($T$ = 8°C, $Q_{DIR}$ = 0.1 $m^3s^{-1}$, 7200 s) | | | | |
| IN $Q_{DIR}$ | 1 278 321 | 1 277 936 | 1 277 936 | 1 277 936 |
| IN STORAGE | 825 | 824 | 343 | 811 |
| IN ROCK EXCHANGE | 0 | 0 | 5 070 | 319 |
| OUT STORAGE | 0 | 0 | 0 | 0 |
| OUT FIXED HEAD | 1 279 146 | 1 278 760 | 1 283 350 | 1 279 066 |
| OUT ROCK EXCHANGE | 0 | 0 | 0 | 0 |
| IN-OUT | 0 | 0.8244 | 0.0997 | 0.7933 |
| ERROR % | 0 | 0.0001 | 0.0000 | 0.0001 |
| **Period 2 – heat injection injection scenario** ($T$ = 12°C, $Q_{DIR}$ = 0.1 $m^3s^{-1}$, 7200 s) | | | | |
| IN $Q_{DIR}$ | 1 290 417 | 1 290 029 | 1 290 029 | 1 290 029 |
| IN STORAGE | 0 | 0 | 0 | 0 |
| IN ROCK EXCHANGE | 0 | 0 | 0 | 0 |
| OUT STORAGE | 825 | 824 | 343 | 811 |
| OUT FIXED HEAD | 1 289 592 | 1 289 205 | 1 284 616 | 1 288 899 |
| OUT ROCK EXCHANGE | 0 | 0 | 5 070 | 319 |
| IN-OUT | 0 | -0.8244 | -0.0997 | -0.7933 |
| ERROR % | 0 | -0.0001 | -0.0000 | -0.0001 |

These results are plausible demonstrating the functioning of heat budget calculation.

# Case 2 – Solute transport in an isolated conduit

Case 2 is similar to case 1 but with mass transport (instead of heat). Case 2 is intended to demonstrate mass transport computation with CFPM1:

- implemented as STM module,
- implemented as LUT module to provide input for UMT3D,

and to compare the abilities of both packages (STM and UMT3D), whereas UMT3D can compute mass transfer with two methods:

- (1) explicit FD and
- (2) EMCNOT [*Liu et al.* 2001].

The input concentration via direct recharge ($Q_{DIR}$) was set to:

- period 1: $C = 0$,
- period 2: $C = 1000$ mol m$^{-3}$.

## Results – Advection only

Model results are presented in Figure BT–15 and Table BT–4. Both CFPM1-STM and UMT with the explicite FD compute reliable concentrations. Results from the EMCNOT solver in UMT vary with the used TRCON parameter whereas an overall tendency to numerical dispersion is obvious (Figure BT–13 right).

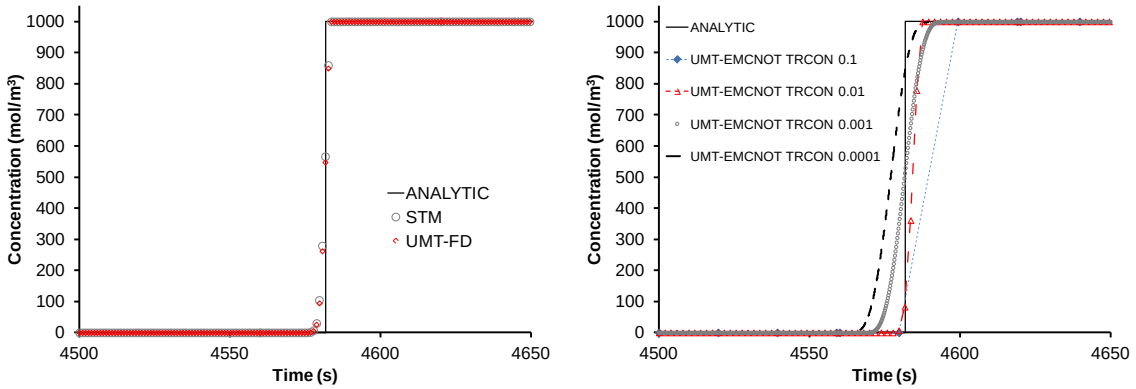


**Figure BT–13:** Model results; solute transport for the advection only scenario

**Table BT–4:** Cumulative mass balance (in mol) for solute flow – scenario: advection only

| | **Volumetric** | **STM** | **UMT FDex** | **UMT EMCNOT** *(TRCON 0.001)* |
|---|---|---|---|---|
| **Period 1** ($C = 0$, $Q_{DIR} = 0.1$ m$^3$s$^{-1}$; 3600 s) | | | | |
| IN $Q_{DIR}$ | 0 | 0 | 0 | 0 |
| IN STORAGE | 0 | 0 | 0 | 0 |
| OUT STORAGE | 0 | 0 | 0 | 0 |
| OUT FIXED HEAD | 0 | 0 | 0 | 0 |
| IN-OUT | 0.0000 | 0.0000 | 0.0000 | 0.0000 |
| ERROR % | 0.0000 | 0.0000 | 0.0000 | 0.0000 |
| **Period 2** ($C = 1000$ mol m$^{-3}$ , $Q_{DIR} = 0.1$ m$^3$s$^{-1}$, 7200 s) | | | | |
| IN $Q_{DIR}$ | 720 000 | 720 000 | 720 060 | 720 023 |
| IN STORAGE | 0 | 0 | 0 | 0 |
| OUT STORAGE | 98 175 | 98 175 | 98 174 | 98174 |
| OUT FIXED HEAD | 621 825 | 621 923 | 621 970 | 621 910 |
| IN-OUT | 0.0000 | -98 | -84 | -61 |
| ERROR % | 0.0000 | -0.0136 | -0.0014 | -0.0010 |

## Results – Advection and dispersion

To consider dispersion, the dispersivity $\alpha$ was set to 5 m. UMT3D was run with the EMCNOT solver and TRCON = 0.001 as this value seemed most adequate in the previous scenario (see Figure BT–13 / Table BT–4); the FD solver in UMT3D does not consider dispersion (see chapter B4). Model results are presented in Figure BT–14. Results demonstrate that CFPM1-STM calculations are more close to the analytical solution. The cumulative mass balance exhibits some aberrations for UMT3-EMCNOT. Computer run time is very dependent on spatial discretization. For large cells, STM is faster than UMT3D-EMCNOT, but for small cells, UMT3D-EMCNOT is faster (see Table BT–5).

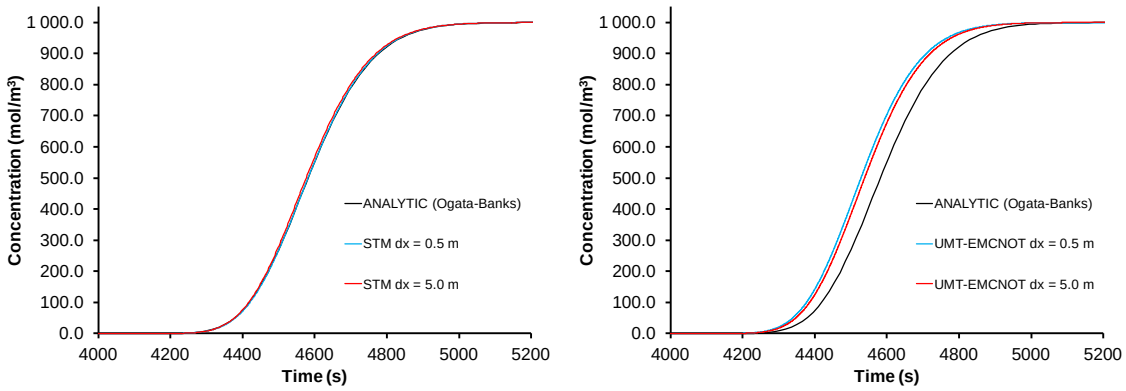


**Figure BT–14:** Model results; solute transport for the advection-dispersion scenario

**Table BT–5:** Cumulative mass balance (in mol) for solute flow – scenario: advection and dispersion

| | **Volumetric** | **STM** *(dx = 0.5 m)* | **UMT EMCNOT** *(dx = 0.5 m)* |
|---|---|---|---|
| **Period 1** ($C$ = 0, $Q_{DIR}$ = 0.1 $m^3s^{-1}$; 3600 s) | | | |
| IN $Q_{DIR}$ | 0 | 0 | 0 |
| IN STORAGE | 0 | 0 | 0 |
| OUT STORAGE | 0 | 0 | 0 |
| OUT FIXED HEAD | 0 | 0 | 0 |
| IN-OUT | 0.0000 | 0.0000 | 0.0000 |
| ERROR % | 0.0000 | 0.0000 | 0.0000 |
| **Period 2** ($C$ = 1000 mol $m^{-3}$ , $Q_{DIR}$ = 0.1 $m^3s^{-1}$, 7200 s) | | | |
| IN $Q_{DIR}$ | 720 000 | 720 000 | 720 415 |
| IN STORAGE | 0 | 0 | 0 |
| OUT STORAGE | 98 175 | 98 175 | 105 580 |
| OUT FIXED HEAD | 621 825 | 621 830 | 625 046 |
| IN-OUT | 0.0000 | -5<br>*(-323 for Δx = 5.0 m)* | -10 211<br>*(-110293 for Δx = 5.0 m)* |
| ERROR % | 0.0000 | -0.0006<br>*(-0.0449 for Δx = 5.0 m)* | 0.1759<br>*(1.7785 for Δx = 5.0 m)* |
| **Computer Run time** (T7500@2.2GHz, 3GB, WinXP) | | | |
| | | ~ 400 sec (Δx = 0.5 m)<br>~ 1 sec (Δx = 5.0 m) | ~ 145 sec (Δx = 0.5 m)<br>~ 37 sec (Δx = 5.0 m) |

## Results – Advection and Taylor dispersion

To proof the correct implementation of Taylor dispersion, three model runs were performed and results are compared with equations B1–7 respectively B1–9 (respecting the diffusion coefficient); the resulting break-through curves were compared with the previously used analytical solution [*Ogata and Banks,* 1961]. Table BT–6 gives an overview about the performed model runs.

**Table BT–6:** Some data for the model runs with Taylor dispersion

| | laminar (unlimited) | laminar (limited*) | turbulent |
|---|---|---|---|
| discharge | 0.001 $m^3s^{-1}$ | 0.001 $m^3s^{-1}$ | 0.1 $m^3s^{-1}$ |
| diffusion coefficient | 1E-8 $m^2s^{-1}$ | 1E-12 $m^2s^{-1}$ | 1E-12 $m^2s^{-1}$ |
| conduit length | 100 m | 100 m | 100 m |
| head difference | 0.00001 m | 0.00001 m | 0.12904 m |
| $D_{dis}$ (eq. B1–3 / eq 6–5) | 3.377 m | 3.072 E-03 m | 0.1004 m |
| $D_{dis}$ (CFPM1) | 3.377 m | 3.072 E-03 m | 0.1004 m |
| $D_{dis,num}$ (CFPM1) | 1.273 E-03 m | 9.002 E-04 m | 0.0562 m |
| $D_{dis,mod}$ (CFPM1) | 3.376 m | 2.172 E-03 m | 0.0443 m |
| break through curve | Figure BT–15 | Figure BT–16 | Figure BT–17 |

*limited due to the small diffusion coefficient; compare equations B1–8 respectively B2–2 / B2–3

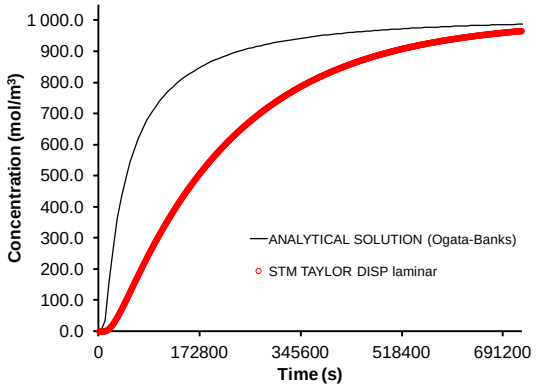


**Figure BT–15:** Model results; solute transport for the advection-dispersion scenario with Taylor dispersion for laminar conditions (dispersion coefficient unlimited according to equation B1–7)

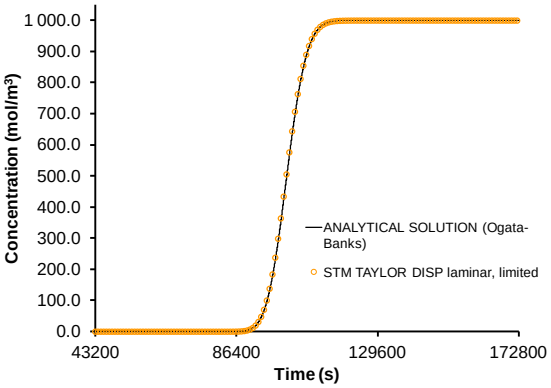


**Figure BT–16:** Model results; solute transport for the advection-dispersion scenario with Taylor dispersion for laminar conditions (dispersion coefficient limited according to equations B1-8 respectively B2–2 / B2–3)

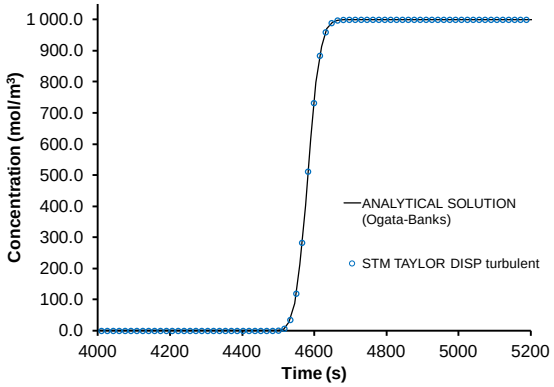


**Figure BT–17:** Model results; solute transport for the advection-dispersion scenario with Taylor dispersion for turbulent conditions (dispersion coefficient according to equation B1–9)

**Table BT–7:** Cumulative mass balance (in mol) for solute flow – scenario: advection-dispersion after Taylor

| | **Taylor laminar** | **Taylor laminar limited** | **Taylor turbulent** |
|---|---|---|---|
| **Period 1** ($C$ = 0, 3600 s) | | | |
| $Q_{Dir}$ | 0.001 $m^3s^{-1}$ | 0.001 $m^3s^{-1}$ | 0.1 $m^3s^{-1}$ |
| IN $Q_{DIR}$ | 0 | 0 | 0 |
| IN STORAGE | 0 | 0 | 0 |
| OUT STORAGE | 0 | 0 | 0 |
| OUT FIXED HEAD | 0 | 0 | 0 |
| IN-OUT | 0.0000 | 0.0000 | 0.0000 |
| ERROR % | 0.0000 | 0.0000 | 0.0000 |
| **Period 2** ($C$ = 1000 mol $m^{-3}$) | | | |
| $Q_{Dir}$ | 0.001 $m^3s^{-1}$ | 0.001 $m^3s^{-1}$ | 0.1 $m^3s^{-1}$ |
| *Duration* | 720 000 | 720 000 | 7 200 |
| IN $Q_{DIR}$ | 720 000 | 720 000 | 720 000 |
| IN STORAGE | 0 | 0 | 0 |
| OUT STORAGE | 95 632 | 98 175 | 98 175 |
| OUT FIXED HEAD | 624 366 | 621 854 | 621 880 |
| OUT ROCK DIFF | 2 | 0 | 0 |
| IN-OUT | 0 | -29 | -55 |
| ERROR % | 0.0000 | -0.0040 | -0.0076 |
| **Computer Run time** (T7500@2.2GHz, 3GB, WinXP) | | | |
| | very long (several hours) | ~ 50 sec ($\Delta x$ = 0.5 m) | ~ 35 sec ($\Delta x$ = 0.5 m) |

Results demonstrate that CFPM1-STM correctly computes Taylor dispersion. It is obvious that in most situations turbulent or limited laminar Taylor dispersion will occur. The conditions for unlimited laminar Taylor dispersion (see eq. B1–8) will rarely appear in natural karst conduits and if so, diffusion / dispersion will be dominant (instead of advection). However, CFPM1 STM is not intended for such diffusion / dispersion-dominated systems and, therefore, results can differ from analytical solutions as shown in Figure BT–15.

## Results – Advection and solute exchange via the concentration boundary layer

In this scenario, solute exchange with the rock matrix via the concentration boundary layer (CBL) is considered but the concentration of the rock matrix is kept constant. Therefore, the spatial discretiza-

tion of the rock matrix is enlarged to $\Delta r$ = 1000 m resulting in constant rock concentrations. The outlet concentration can be computed with the following analytical solution [*Birk*, 2002]:

$$C_{out} = C_{r0} - (C_{r0} - C_{in})\exp\left(-\overline{N_{Sh}} D_{Diff} \frac{\pi L}{Q}\right) \qquad \text{eq. BT–3}$$

with $C_{out}$ outlet concentration and $C_{in}$ inlet concentration. The Sherwood number is calculated according to equation B1–17 as 8598. Therewith, the outlet concentration is $C_{out}$ = 973.35 mol m$^{-3}$ (with $D_{Diff}$ = 2 x 10$^{-10}$ m$^2$s$^{-1}$ and $C_{r0}$ initial concentration = 0, compare Figure B1–4).

Results, shown in Figure BT–18, match the analytical values demonstrating the correct implementation of the HTM module. The computed mass balances are presented in Table BT–8 (next section).

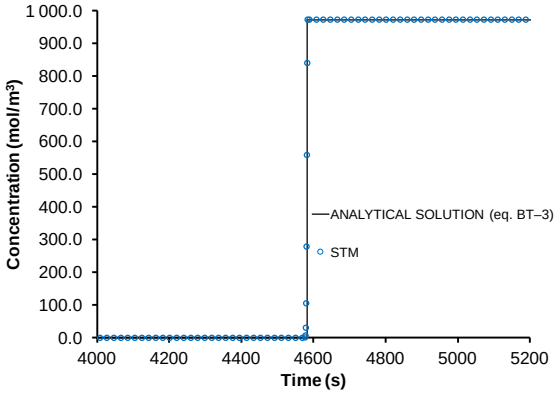


**Figure BT–18:** Results for solute transport with CFPM1 / STM (advection and solute exchange with the concentration boundary layer).

## Results – Advection, CBL and matrix diffusion

In this scenario the concentration in the rock matrix (affected by solute exchange via the CBL) is further altered by rock matrix diffusion (RMDIFF). Based on the transport model with $\Delta x$ = 0.5 m two model runs were performed with the following parameters (taken from the DFG final report – karst characterization; *Birk and Geyer* [2006]).

- RMDIFF:
    - radial rock matrix: 30 nodes with $\Delta r$ = 0.0002 m,
    - diffusion coefficient $D_{Diff}$ = 2 x 10$^{-10}$ m$^2$s$^{-1}$,
    - bulk rock density $\rho_r$ = 2700 kg m$^{-3}$,
    - effective porosity $n_e$ = 0.03.
- RMDIFF + sorption:
    - additionally $K_D$ = 6.1 l kg$^{-1}$.

Results are shown in Figure BT–19. It is obvious that concentrations at the wall surface are very sensitive to rock matrix diffusion (with the setting used here $C_{r0}$ increase from initially 0 to ~ $C_{in}$). Consequently, concentrations in the conduit increase too compared to the scenario without RMDIFF (concentration at the rock matrix wall there was constant with $C_{r0}$ ~ 0). Cumulative mass balances, presented in Table BT–8, underline the significance of rock matrix diffusion, which results in decreased mass flow from the conduit to the matrix due to the considerably decreased concentration gradient between matrix wall and conduit (compare also equation B1–12). This process is delayed if sorption is active ($K_D$ > 0; see Figure BT–19, Table BT–8).

The numerical dispersion, evidently shown in Figure BT–19 right, depends on the spatial discretization as well as the sorption coefficient ($K_D$) whereas this numerical effect occurs (at least for the scenario considered here) with sparse spatial discretization and very small $K_D$ values (in the conducted model run for $\Delta x$ > ~ 0.25 m and $K_D$ < ~ 0.01 l kg$^{-1}$). Consequently, discretization and transport parameters should be carefully checked.

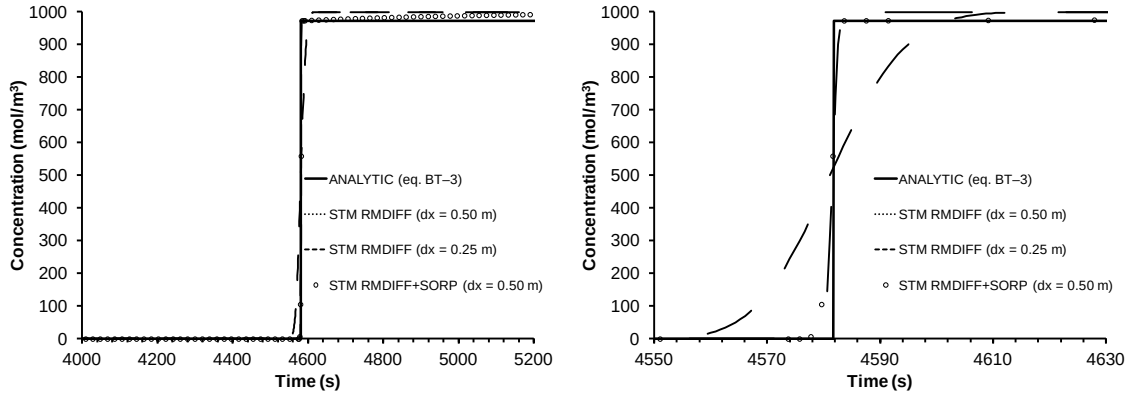


**Figure BT–19:** Model results; solute transport for the advection-CBL-matrix diffusion scenario (left side with scaling comparable to previous figures, right side with refined scaling)

**Table BT–8:** Cumulative Mass Balance (in mol) for the advection-CBL-matrix diffusion scenario

| | **Volumetric** | **STM CBL** | **STM CBL+RMDIFF** ($\Delta x$ = 0.50 m) | **STM CBL+RMDIFF+SORP** ($\Delta x$ = 0.50 m) |
|---|---|---|---|---|
| **Period 1** ($C$ = 0, $Q_{DIR}$ = 0.1 m$^3$s$^{-1}$; 3600 s) | | | | |
| IN $Q_{DIR}$ | 0 | 0 | 0 | 0 |
| IN STORAGE | 0 | 0 | 0 | 0 |
| OUT STORAGE | 0 | 0 | 0 | 0 |
| OUT FIXED HEAD | 0 | 0 | 0 | 0 |
| IN-OUT | 0.0000 | 0.0000 | 0.0000 | 0.0000 |
| ERROR % | 0.0000 | 0.0000 | 0.0000 | 0.0000 |
| **Period 2** ($C$ = 1000 mol m$^{-3}$ , $Q_{DIR}$ = 0.1 m$^3$s$^{-1}$, 7200 s) | | | | |
| IN $Q_{DIR}$ | 720 000 | 720 000 | 720 000 | 720 000 |
| IN STORAGE | 0 | 0 | 0 | 0 |
| OUT STORAGE | 98 175 | 96 858 | 98 175 | 98 174 |
| OUT FIXED HEAD | 621 825 | 605 339 | 621 907 | 620 624 |
| OUT ROCK DIFF | 0 | 17 899 | 6 | 1 300 |
| IN-OUT | 0.0000 | -96 | -87 | -98 |
| ERROR % | 0.0000 | -0.0133 | -0.0121 | -0.0136 |
| **Computer Run time** (T7500@2.2GHz, 3GB, WinXP) | | | | |
| | | ~ 22 sec ($\Delta x$ = 0.5 m) | ~ 28 sec ($\Delta x$ = 0.5 m) | ~ 22 sec ($\Delta x$ = 0.5 m) |

## Results – Advection, CBL, RMDIFF and Taylor dispersion

This scenario aims to demonstrate the overall significance of the different transport processes dispersion, solute exchange via the CBL and retarded rock matrix diffusion. The following parameters are used:

- $Q$ = 0.1 m$^3$s$^{-1}$ resulting in turbulent flow,
- $\Delta x$ = 0.25 m,
- Taylor dispersion according equation B1–9,

- CBL and RMDIFF as in the previous scenario ($\Delta r$ = 0.0002 m, $D_{Diff}$ = 2 x $10^{-10}$ $m^2s^{-1}$, $\rho_r$ = 2700 kg $m^{-3}$, $n_e$ = 0.03, $K_D$ = 6.1 l $kg^{-1}$).

Results are shown in Figure BT–20 for two model runs with and without sorption. Cumulative mass balances are very similar to those already presented in Table BT–8. As concluded yet, RMDIFF without sorption doesn't significantly affect results for the parameter sets used. In case RMDIFF acts in parallel with sorption, outflow concentrations are slightly damped and, therefore, might be able to reproduce tailing effects evident in field data (*Birk and Geyer*, 2006). However, under the conditions applied here dispersion respectively Taylor dispersion affects results much more than solute exchange via the concentration boundary layer, rock matrix diffusion, and sorption.

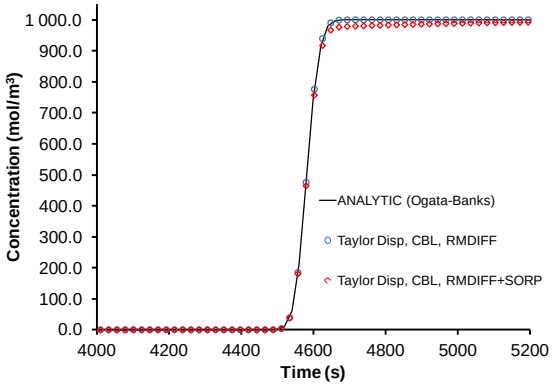


**Figure BT–20:** Model results for STM considering advection, Taylor dispersion, rock matrix diffusion and sorption

# Case 3 – Well boundary condition

This test case demonstrates the functioning of the implemented well boundary condition (see also case 10 in chapter AT) with the HTM and STM package. For this reason, solutes (STM) respectively heat (HTM) is introduced through a well instead of direct recharge (as in cases 1 and 2, compare also Figure BT–9). The well operates with an infiltration rate of $Q_{WELL}$ = 0.1 $m^3s^{-1}$. Beside this, the model setup is identical with cases 1 / 2.

Results are compared with those from cases 1 and 2 in terms of mass balances, shown in Tables BT–9 (solute transport) respectively BT–10 (heat transport), and in terms of spring signals whereas the accordance is rated in Tables BT–9 and BT–10. Mass balances as well as spring signals are identical to cases 1 / 2 demonstrating the correct implementation of the well transport boundary.

**Table BT–9:** Cumulative mass balance (in mol) for solute transport computed with STM considering advection and dispersion ($\alpha$ = 5 m); final model time step

| | **STM** *($\Delta x$ = 0.5 m)* | |
|---|---|---|
| Boundary condition | $Q_{DIR}$ = 0.1 $m^3s^{-1}$ | $Q_{WELL}$ = 0.1 $m^3s^{-1}$ |
| IN $Q_{DIR}$ | 720 000 | 0 |
| IN $Q_{Well}$ | 0 | 720 000 |
| IN STORAGE | 0 | 0 |
| OUT STORAGE | 98 175 | 98 175 |
| OUT FIXED HEAD | 621 830 | 621 830 |
| IN-OUT | -5 | -5 |
| ERROR % | -0.0006 | -0.0006 |
| Spring signal | see Fig. BT–14 left | identical to Fig. BT–14 left |

**Table BT–10:** Cumulative heat balance (in MJ) for heat transport computed with HTM considering convection, heat exchange via the TBL, and rock matrix conduction; final model time step

| | **HTM** *($\Delta x$ = 0.5 m)* | | | |
|---|---|---|---|---|
| Boundary condition | $Q_{DIR}$ = 0.1 $m^3s^{-1}$ | $Q_{DIR}$ = 0.1 $m^3s^{-1}$ | $Q_{WELL}$ = 0.1 $m^3s^{-1}$ | $Q_{WELL}$ = 0.1 $m^3s^{-1}$ |
| | $T_{DIR}$ = 12 °C | $T_{DIR}$ = 8 °C | $T_{WELL}$ = 12°C | $T_{WELL}$ = 8°C |
| IN $Q_{DIR}$ | 1 290 029 | 1 277 936 | 0 | 0 |
| IN $Q_{Well}$ | 0 | 0 | 1 290 029 | 1 277 936 |
| IN ROCK EXCHANGE | 0 | 319 | 0 | 319 |
| IN STORAGE | 0 | 811 | 0 | 811 |
| OUT STORAGE | 811 | 0 | 811 | 0 |
| OUT FIXED HEAD | 1 288 899 | 1 279 066 | 1 288 899 | 1 279 066 |
| OUT ROCK EXCHANGE | 319 | 0 | 319 | 0 |
| IN-OUT | -1 | 1 | -1 | 1 |
| ERROR % | -0.0001 | 0.0001 | -0.0001 | 0.0001 |
| Spring signal | *Fig. BT–12 right* | *Fig. BT–12 left* | *identical to Fig. BT–12 right* | *identical to Fig. BT–12 left* |

# Case 4 – Fixed head / FHLQ boundary condition

This test is to demonstrate the functioning of the implemented fixed head / FHLQ boundary condition with the HTM and STM packages. For this reason, solutes (STM) respectively heat (HTM) were introduced through a fixed head / FHLQ node instead of direct recharge as in cases 1 and 2. Two scenarios were considered, which are illustrated in Figure BT–21:

- Fixed head scenario: the model setup is comparable with cases 1 / 2 except the direct recharge node, which is replaced by a pumping well ($Q_{WELL}$ = -0.1 $m^3s^{-1}$); Figure BT–21 left.
- FHLQ scenario: the model setup is comparable with case 1 / 2 except the direct recharge node, which is replaced by a pumping well ($Q_{WELL}$ = -0.1 $m^3s^{-1}$), the fixed head boundary condition is limited to 0.05 $m^3s^{-1}$ inflow, and the water transfer coefficient of node 6 (FHLQ node) is set to 0.0006 $m^2/s$ to allow balancing out the water budget by matrix inflow; Figure BT–21 right.

For both scenarios, the concentration at the fixed head was set to $C_{FXH}$ = 1000 mol $m^{-3}$ (STM model runs). The temperature at the fixed head $T_{FXH}$ was set to 12 °C respectively 8 °C (HTM model runs).

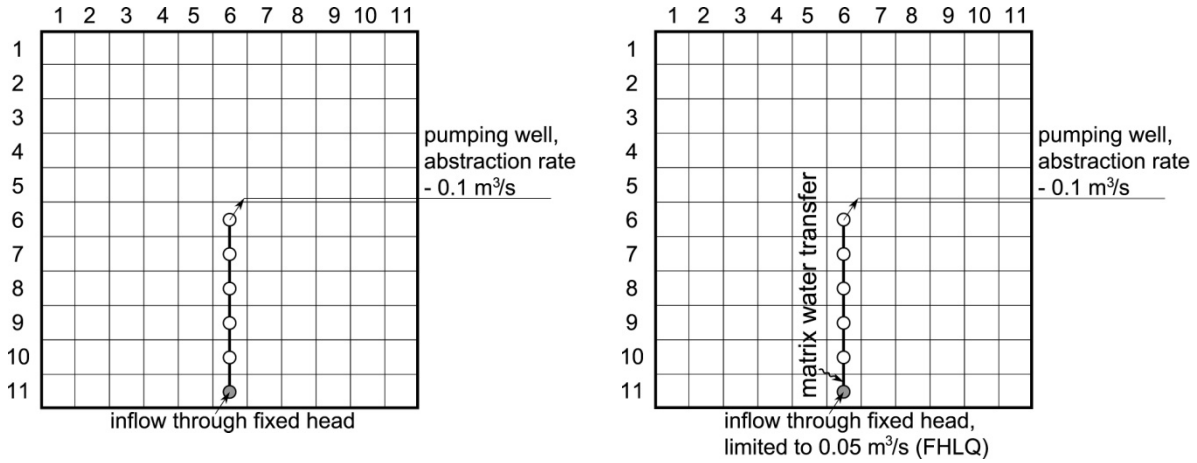


**Figure BT–21:** Schematic representation of both model setups; left: fixed head boundary; right: FHLQ boundary

Results for the fixed head scenario are compared with cases 1 / 2 in terms of mass balances, see Table BT–11 (solutes) respectively BT–12 (heat), and in terms of spring signals whereas the accordance is also rated in Tables BT–11 and BT–12. Mass balances as well as spring signals are comparable demonstrating the correct implementation of the fixed head boundary for transport.

**Table BT–11:** Cumulative mass balance (in mol) for solute flow computed with **STM** considering advection and dispersion ($\alpha$ = 5 m); final model time step, **fixed head scenario**

| | **STM** *(dx = 0.5 m)* | |
|---|---|---|
| Boundary condition | $Q_{DIR}$ = 0.1 $m^3s^{-1}$ | $Q_{WELL}$ = -0.1 $m^3s^{-1}$ |
| IN $Q_{DIR}$ | 720 000 | 0 |
| IN CONSTANT HEAD | 0 | 720 000 |
| OUT STORAGE | 98 175 | 98 175 |
| OUT FIXED HEAD | 621 830 | 0 |
| OUT WELLS | 0 | 621 830 |
| IN-OUT | -5 | -5 |
| ERROR % | -0.0006 | -0.0006 |
| concentration at the well (equal to the spring signal in case 1 to 3) | spring signal: see Fig. BT–14 left | identical to Fig. BT–14 left |

**Table BT–12:** Cumulative heat balance (in MJ) computed with **HTM** considering convection and rock matrix conduction; final model time step, **fixed head scenario**

| | **HTM** *(dx = 0.5 m)* | | | |
|---|---|---|---|---|
| Boundary condition | $Q_{DIR}$ = 0.1 $m^3s^{-1}$ | $Q_{DIR}$ = 0.1 $m^3s^{-1}$ | $Q_{WELL}$ = -0.1 $m^3s^{-1}$ | $Q_{WELL}$ = -0.1 $m^3s^{-1}$ |
| | $T_{DIR}$ = 12 °C | $T_{DIR}$ = 8 °C | $T_{FXH}$ = 12°C | $T_{FXH}$ = 8°C |
| IN $Q_{DIR}$ | 1 290 029 | 1 277 936 | 0 | 0 |
| IN CONSTANT HEAD | 0 | 0 | 1 290 029 | 1 277 936 |
| IN ROCK EXCHANGE | 0 | 319 | 0 | 319 |
| IN STORAGE | 0 | 811 | 0 | 811 |
| OUT STORAGE | 811 | 0 | 811 | 0 |
| OUT WELL | 1 288 899 | 1 279 066 | 1 288 899 | 1 279 066 |
| OUT ROCK EXCHANGE | 319 | 0 | 319 | 0 |
| IN-OUT | -1 | 1 | -1 | 1 |
| ERROR % | -0.0001 | 0.0001 | -0.0001 | 0.0001 |
| temperature at the well (equal to the spring signal in case 1 to 3) | *Fig. 10–12 right* | *Fig. 10–12 left* | *identical to Fig. 10–12 right* | *identical to Fig. 10–12 left* |

Results for the FHLQ scenario are compared with cases 1 / 2 in terms of mass balances; see Table BT–13 (solutes) respectively BT–14 (heat). Figure BT–22 compares the resulting temperature at the pumping well with the spring signal from case 1 (see also Figure BT–12).

**Table BT–13:** Cumulative mass balance (in mol) computed with **STM** considering advection and dispersion ($\alpha$ = 5 m); final model time step, **FHLQ scenario**

| | **STM** *(dx = 0.5 m)* | |
|---|---|---|
| Boundary condition | $Q_{DIR}$ = 0.1 $m^3s^{-1}$ | $Q_{WELL}$ = -0.1 $m^3s^{-1}$ |
| IN $Q_{DIR}$ | 720 000 | 0 |
| IN FHLQ (LQ CASE) | 0 | 360 000 |
| OUT STORAGE | 98 175 | 49 087 |
| OUT FIXED HEAD | 621 830 | 0 |
| OUT WELLS | 0 | 310 915 |
| IN-OUT | -5 | -2 |
| ERROR % | -0.0006 | -0.0006 |
| concentration at the well (equal to the spring signal in case 1 to 3) | spring signal: see Fig. BT–14 left | comparable to Fig. BT–14 left (half the concentrations) |

**Table BT–14:** Cumulative heat balance (in MJ) computed with **HTM** considering convection, conduction and rock matrix conduction; final model time step, **FHLQ scenario**

| | **HTM** *(dx = 0.5 m)* | | | |
|---|---|---|---|---|
| Boundary condition | $Q_{DIR}$ = 0.1 $m^3s^{-1}$ | $Q_{DIR}$ = 0.1 $m^3s^{-1}$ | $Q_{WELL}$ = -0.1 $m^3s^{-1}$ | $Q_{WELL}$ = -0.1 $m^3s^{-1}$ |
| | $T_{DIR}$ = 12 °C | $T_{DIR}$ = 8 °C | $T_{FXH}$ = 12°C | $T_{FXH}$ = 8°C |
| IN $Q_{DIR}$ | 1 290 029 | 1 277 936 | 0 | 0 |
| IN *FHLQ (LQ CASE)* | 0 | 0 | 645 014 | 638 968 |
| IN MATRIX EXCHANGE | 0 | 0 | 641 991 | 641 991 |
| IN ROCK EXCHANGE | 0 | 319 | 0 | 160 |
| IN STORAGE | 0 | 811 | 0 | 405 |
| OUT STORAGE | 811 | 0 | 405 | 0 |
| OUT FIXED HEAD | 1 288 899 | 1 279 066 | 0 | 0 |
| OUT WELLS | 0 | 0 | 1 286 441 | 1 281 524 |
| OUT ROCK EXCHANGE | 319 | 0 | 160 | 0 |
| IN-OUT | -1 | 1 | 0 | 0 |
| ERROR % | -0.0001 | 0.0001 | -0.0000 | 0.0000 |

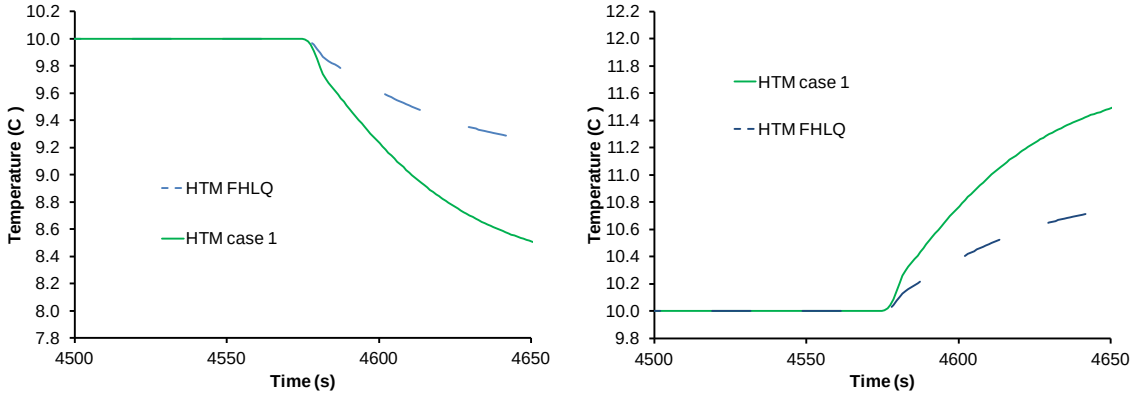


**Figure BT–22:** Results for heat transport with CFPM1-HTM (in comparison to results from case 1), whereas inflow through the fixed head is limited by the FHLQ boundary; left: heat removal scenario; right: heat injection scenario.

# Case 5 – Consideration of CADS for transport

CADS is considered for heat and solute transport. Specific influence on conduit temperatures respectively concentrations is assumed in case water transfer between conduits and CADS occurs. Subsequently, transport computations are performed for a simple catchment (similar to previously used ones) in order to demonstrate the proper functioning of CADS consideration. The catchment considered for this test is comparable to case 1. CADS width is set to 0.05 m. An additional well is placed at node 4. Node 6 (spring) acts as FHLQ boundary with limited inflow of 0.05 $m^3s^{-1}$, Figure BT–23.

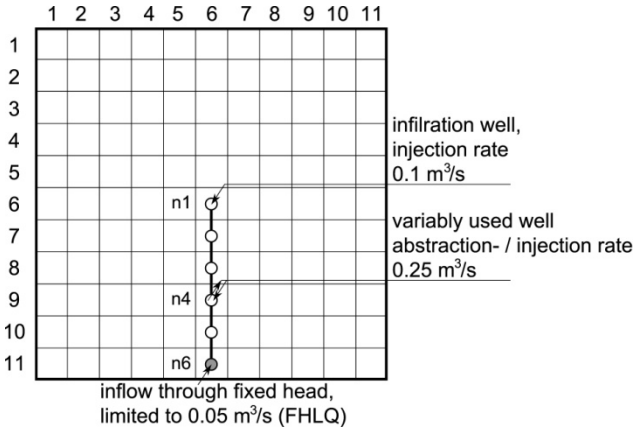


**Figure BT–23:** Schematic representation of the model setup

Scenario 1: Elution

Based on an initial state with $c_{ini} > 0$ respectively $T_{ini} = 10°C$ (in both conduits and CADS), pure water with $c = 0$ respectively $T = 8$ °C / 12 °C is infiltrated to the conduit at node 1 and occasionally by the infiltration through the FHLQ boundary. The model run consists of 5 periods with a length of 3 600 seconds each. The temporal sequence is:

- Period 1: initial situation, infiltration at node 1 with $c > 0$ respectively $T = 10°C$
- Periods 2 - 5: infiltration at node 1 with $c = 0$; $T = 8$ °C / 12 °C
- Period 3: additional water abstraction at node 4

*Results for solute transport:*

Model results are presented in Figure BT–24. The qualitative assessment of model results as subsequently provided is coherent.

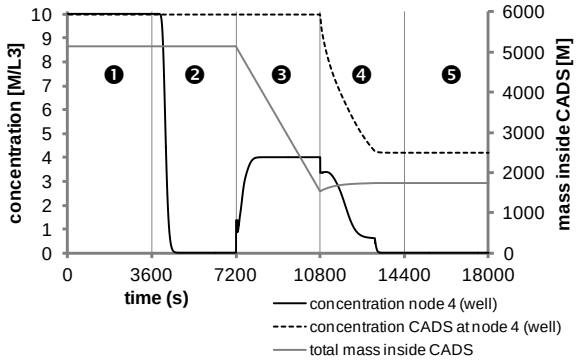


**Figure BT–24:** Scenario 1: model results for solute transport

- Period 1: initial concentration considered by both conduits and CADS; CADS with initial load.
- Period 2: elution in the conduit due to infiltration in node 1; CADS concentration remains constant.

- Period 3: CADS mass is reduced due to water abstraction; CADS concentration remains constant; conduit concentration increases due to mass inflow from CADS.
- Period 4: recovery after pumping results in water transfer from conduits into CADS; CADS concentration is depleted; concentration at the conduit node 4 is also depleted with an obvious stepwise drop close to the end of period 4. This is caused by the finalization of CADS refilling, i.e. pure infiltration water does not longer refill the CADS (e.g. at neighboring nodes).
- Period 5: pure water inside the conduit; remaining constant mass / concentration within the CADS.

Quantitative assessment is done by computing budget terms based on $V_{CADS}$ (eq. 3–3) and $c_{CADS}$ whereas mass inside CADS is $V_{CADS}$ times $c_{CADS}$. Results are provided by Table BT–15. Results for heat transport, shown in Figure BT–25, are comparable with solute transport. Both model runs with increasing and decreasing temperature produce reasonable results; see also Table BT–15.

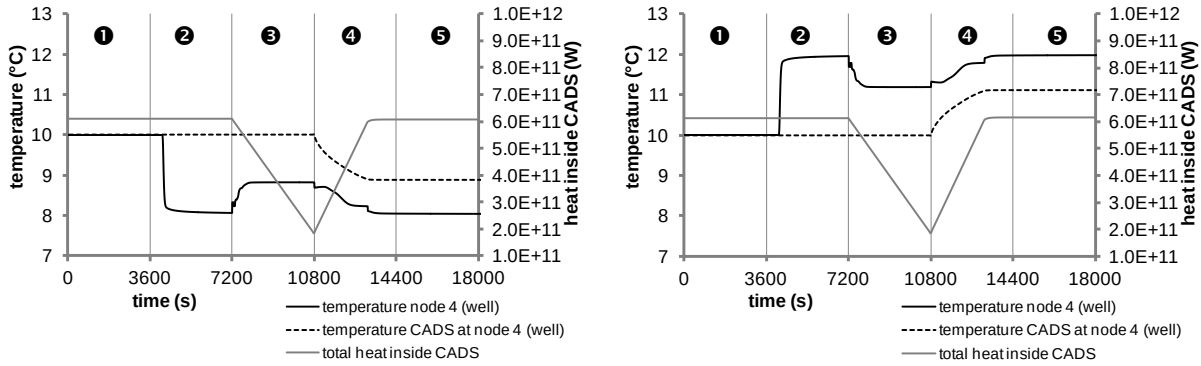


**Figure BT–25:** Scenario 1: model results for heat transport; left: $\Delta T$ = -2K, right: $\Delta T$ = +2K

Scenario 2: Infiltration

Based on an initial state with $c_{ini}$ = 0 respectively $T_{ini}$ = 10°C (in both conduits and CADS), loaded water with $c$ > 0 respectively $T$ = 8°C / 12°C is infiltrated into the system at node 1 and, additionally for a limited time, at node 4. The model run consists of 5 periods with a length of 3 600 seconds each. The temporal sequence is:

- Period 1: initial situation, infiltration well at node 1 with $c_{ini}$ = 0 respectively $T_{ini}$ = 10°C
- Periods 2–5: infiltration well at node 1 with $c$ > 0; $T$ = 8 °C / 12 °C
- Period 3: additional water infiltration at node 4

Model results are presented in Figure BT–26. The qualitative assessment of model results as subsequently provided is coherent.

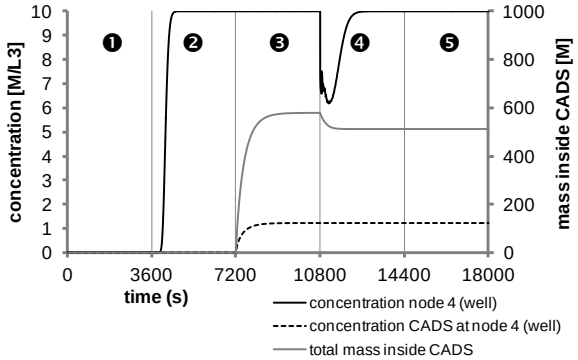


**Figure BT–26:** Scenario 2: model results for solute transport

- Period 1: initial state with $c$ = 0 in both conduits and CADS.
- Period 2: increased conduit concentration due to infiltration in node 1; $c_{CADS}$ remains zero.

- Period 3: additional water infiltration (c > 0) at node 4; water and mass transfer from conduits into CADS as shown by increased $c_{CADS}$ and total mass inside CADS.
- Period 4: recovery after infiltration results in water transfer from CADS into conduits; $c_{CADS}$ remains constant and mass inside CADS decreases; additional dilution at conduit node 4 due to water transfer from CADS with $c_{CADS} < c_{conduit}$.
- Period 5: remaining constant mass / concentration within CADS and conduit.

Quantitative assessment is done by computing budget terms based on $V_{CADS}$ (eq. A3–3) and $c_{CADS}$ whereas mass inside CADS is $V_{CADS}$ times $c_{CADS}$. Results are provided by Table BT–15. Results for heat transport, shown in Figure BT–27, are comparable with solute transport. Both model runs with increasing and decreasing temperature produce reasonable results; see also Table BT–15.

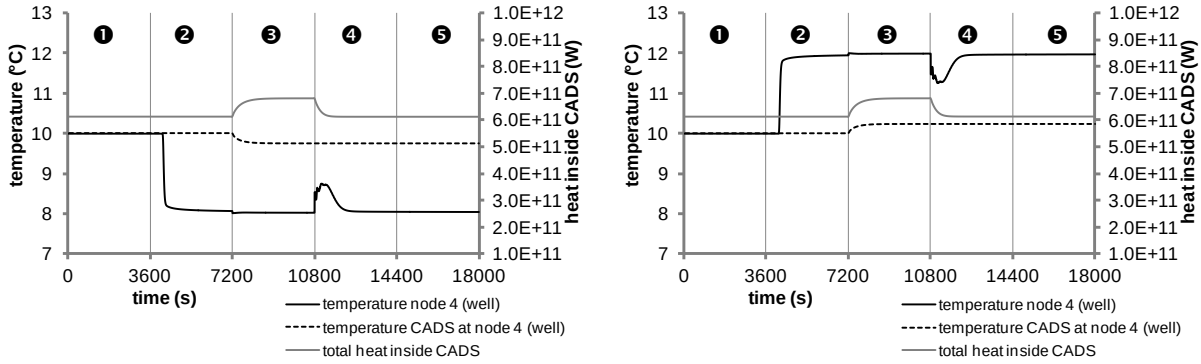


**Figure BT–27:** Scenario 2: model results for heat transport; left: $\Delta T$ = -2K, right: $\Delta T$ = +2K

Scenario 3: Infiltration and subsequent elution

Based on an initial state with $c_{ini}$ = 0 respectively $T_{ini}$ = 10°C (in both conduits and CADS), loaded water with $c$ > 0 respectively $T$ = 8°C / 12°C is infiltrated to the system by the infiltration well at node 1 and, additionally, at node 4. Subsequently, pure water is infiltrated in the system to represent elution. Additional pumping during the elution period is intended to facilitate the elution of the CADS. The model run consist of 8 periods with a length of 3 600 seconds each. The temporal sequence is:

- Period 1: initial situation, infiltration at node 1 with $c_{ini}$ = 0 respectively $T_{ini}$ = 10°C
- Periods 2–4: infiltration at node 1 with $c$ > 0; $T$ = 8 °C / 12 °C
- Period 3: additional water infiltration at node 4 with $c$ > 0; $T$ = 8 °C / 12 °C
- Periods 5–8: infiltration at node 1 with $c$ = 0 respectively $T$ = 10°C
- Period 6: additional water abstraction well at node 4

Model results are presented in Figure BT–28. The qualitative assessment of model results as subsequently provided is coherent.

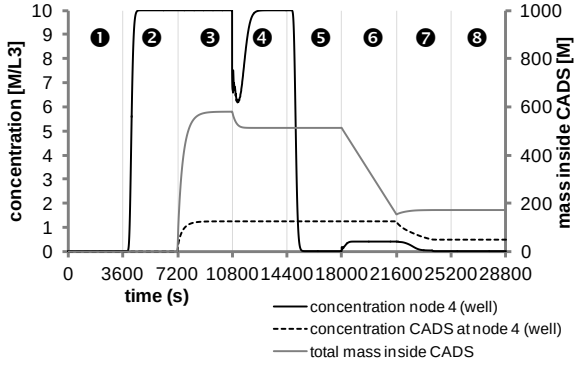


**Figure BT–28:** Scenario 3: model results for solute transport

- Period 1: initial state with $c$ = 0 in both conduits and CADS.
- Period 2: increased concentration in the conduit due to infiltration in node 1; CADS concentration remains zero.
- Period 3: additional water infiltration (c > 0) at node 4; water and mass transfer from conduits into CADS as indicated by increased $c_{CADS}$ and total mass inside CADS.
- Period 4: recovery subsequent to infiltration results in water transfer from CADS into conduits; $c_{CADS}$ remains constant and mass inside CADS decreases; additional dilution at node 4 due to water transfer from CADS with $c_{CADS} < c_{conduit}$.
- Period 5: elution in the conduit due to infiltration in node 1 with $c$ = 0; CADS mass / concentration remains constant.
- Period 6: CADS mass is reduced due to water abstraction; CADS concentration remains constant; conduit concentration increases due to mass inflow from CADS.
- Period 7: recovery after pumping results in water transfer from conduits into CADS; CADS concentration is depleted; concentration at node 4 is also depleted.
- Period 8: pure water inside the conduit; remaining constant mass / concentration within CADS.

Quantitative assessment is done by computing budget terms based on $V_{CADS}$ (eq. 3–3) and CADS concentrations whereas mass inside CADS is $V_{CADS}$ times $c_{CADS}$. Results are provided by Table BT–15. Results for heat transport, shown in Figure BT–29, are comparable with solute transport. Both model runs with increasing and decreasing temperature produce reasonable results; see also Table BT–15.

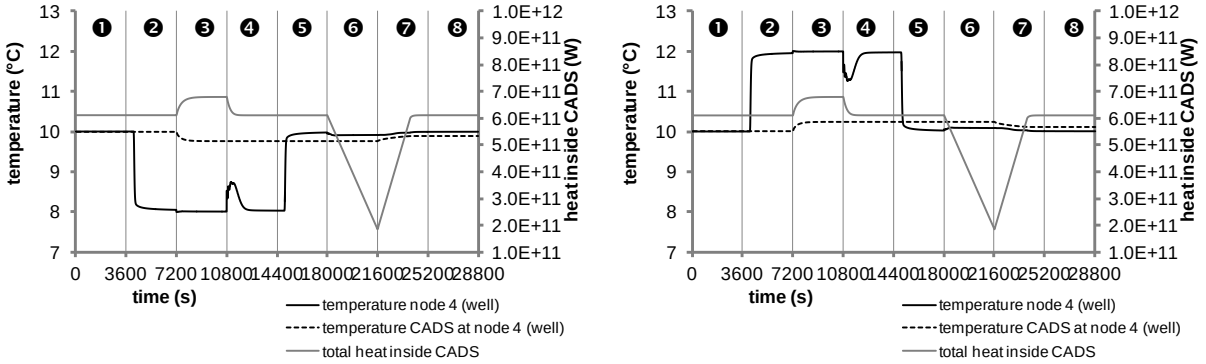


**Figure BT–29:** Scenario 3: model results for heat transport; left: $\Delta T$ = -2K, right: $\Delta T$ = +2K

**Table BT–15:** Calculated CADS related budget terms and budget terms computed by CFP

| | **FLOW** (in m³) | | | | | | **MASS** (in moles) / **HEAT** (in MJ) | | | | | |
|---|---|---|---|---|---|---|---|---|---|---|---|---|
| | calculated | | CFP budget | | % | | calculated | | CFP budget | | % | |
| Scenario | IN | OUT | IN | OUT | *IN* | *OUT* | IN | OUT | IN | OUT | *IN* | *OUT* |
| 1_STM | | | | | | | 3600 | 206 | 3600 | 206 | *100%* | *100%* |
| 1_HTM- | 360 | 360 | 360 | 360 | *100%* | *100%* | 428123 | 425319 | 428751 | 425942 | *100%* | *100%* |
| 1_HTM+ | | | | | | | 428123 | 430927 | 427994 | 430798 | *100%* | *100%* |
| 2_STM | | | | | | | 67 | 579 | 67 | 579 | *100%* | *100%* |
| 2_HTM- | 58 | 58 | 58 | 58 | *100%* | *100%* | 68774 | 68349 | 68754 | 68328 | *100%* | *100%* |
| 2_HTM+ | | | | | | | 68886 | 69311 | 68865 | 69291 | *100%* | *100%* |
| 3_STM | | | | | | | 425 | 597 | 425 | 597 | *100%* | *100%* |
| 3_HTM- | 418 | 418 | 418 | 418 | *100%* | *100%* | 496600 | 496444 | 496451 | 496295 | *100%* | *100%* |
| 3_HTM+ | | | | | | | 497306 | 497462 | 497157 | 497313 | *100%* | *100%* |

*CADS BUDGET TERMS (IN = INTO CONDUITS, OUT = INTO CADS)*

## Case 6 – Consideration of Cauchy boundaries for transport

Two situations are considered: unrestricted Cauchy flow and Cauchy inflow limited by a flow threshold (CYLQ). Unrestricted Cauchy flow is simulated with a scenario similar to case 1 (heat) respectively case 2 (solutes). The following parameter are used to result in an inflow of 0.1 $m^3s^{-1}$ at node 1

- CCY = 0.1 $ms^{-1}$
- HCY = 51.645220 m

Break through curves (Figure BT-30 to BT-32) and mass budgets (Table BT-16) proof the correct functioning of the Cauchy boundary condition.

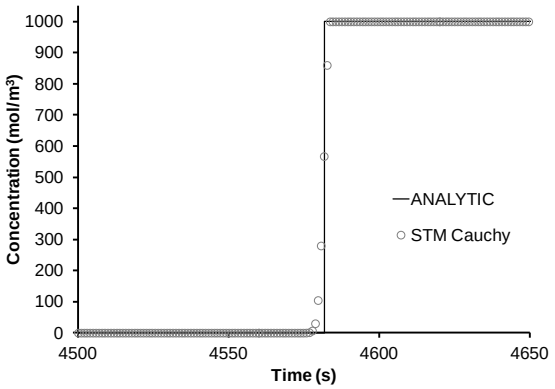


**Figure BT–30:** Case 6, solute transport equivalent to case 2

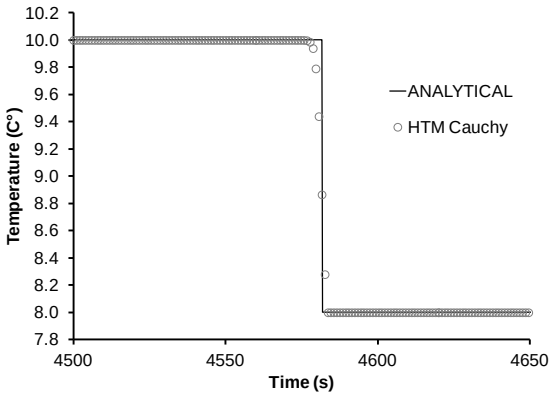


**Figure BT–31:** Case 6, heat transport (decreasing temperature) equivalent to case 1

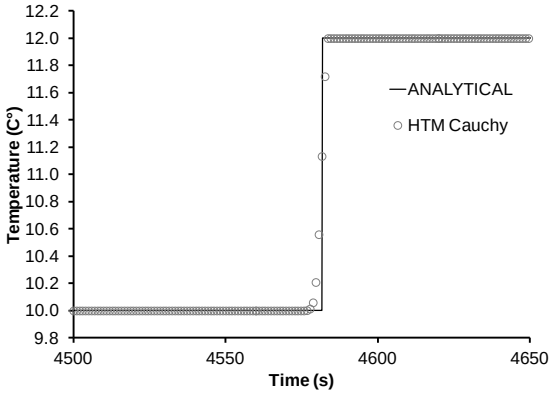


**Figure BT–32:** Case 6, heat transport (increasing temperature) equivalent to case 1

**Table BT–16:** Cumulative heat balance (in MJ) for transport case 6 equivalent to case 1 (heat transport, convection only)

| | **case 1** | **case 6** | **case 1** | **case 6** | **case 1** | **case 6** |
|---|---|---|---|---|---|---|
| | **Period 1** – both heat removal and heat injection scenario ($T$ = 10°C, $Q_{DIR/CY}$ = 0.1 $m^3s^{-1}$; 3600 s) | | **Period 2 – heat removal scenario** ($T$ = 8°C, $Q_{DIR/CY}$ = 0.1 $m^3s^{-1}$, 7200 s) | | **Period 2 – heat injection scenario** ($T$ = 12°C, $Q_{DIR/CY}$ = 0.1 $m^3s^{-1}$, 7200 s) | |
| IN $Q_{DIR}$ | 427 994 | 0 | 1 277 936 | 0 | 1 290 029 | 0 |
| IN $Q_{CY}$ | 0 | 427 995 | 0 | 1 277 940 | 0 | 1 290 032 |
| IN STORAGE | 0 | 0 | 824 | 824 | 0 | 0 |
| OUT STORAGE | 0 | 0 | 0 | 0 | 824 | 824 |
| OUT FIXED HEAD | 427 994 | 427 995 | 1 278 760 | 1 278 763 | 1 289 205 | 1 289 208 |
| IN-OUT | 0.0000 | 0.0000 | 0.8244 | 0.8244 | -0.8244 | -0.8244 |
| ERROR % | 0.0000 | 0.0000 | 0.0001 | 0.0001 | -0.0001 | -0.0001 |

**Table BT–17:** Cumulative mass balance (in mol) for solute flow for transport case 6 equivalent to case 2 (solute transport, advection only)

| | **case 2** | **case 6** | **case 2** | **case 6** |
|---|---|---|---|---|
| | **Period 1** ($C$ = 0, $Q_{DIR/CY}$ = 0.1 $m^3s^{-1}$; 3600 s) | | **Period 2** ($C$ = 1000 mol $m^{-3}$ , $Q_{DIR/CY}$ = 0.1 $m^3s^{-1}$, 7200 s) | |
| IN $Q_{DIR}$ | 0 | 0 | 720 000 | 0 |
| IN $Q_{CY}$ | 0 | 0 | 0 | 720 002 |
| IN STORAGE | 0 | 0 | 0 | 0 |
| OUT STORAGE | 0 | 0 | 98 175 | 98 175 |
| OUT FIXED HEAD | 0 | 0 | 621 923 | 621 925 |
| IN-OUT | 0.0000 | 0.0000 | -98 | -98 |
| ERROR % | 0.0000 | 0.0000 | -0.0136 | -0.0136 |

Restricted Cauchy flow is computed similar to transport case 4. The FHLQ boundary condition used there is replaced by a Cauchy boundary with the following parameters

- conductivity CCY = 1E10 $ms^{-1}$
- Cauchy head HCY = 50 m (similar to the fixed head in case 4)
- flow threshold CYLQ = 0.05 $m^3s^{-1}$ (similar to FHLQ LQ in case 4)

Results for the Cauchy LQ scenario are compared with case 4 in terms of mass balances; see Table BT–18 (solutes) respectively BT–19 (heat). There are no significant differences. Hence, the Cauchy LQ restriction is correctly implemented.

**Table BT–18:** Cumulative mass balance (in mol) computed with **STM** considering advection and dispersion ($\alpha$ = 5 m); final model time step, **Cauchy LQ scenario**

| | **FHLQ LQ** | **Cauchy LQ** |
|---|---|---|
| IN FHLQ (LQ CASE) | 360 000 | 0 |
| IN CAUCHY (LQ CASE) | 0 | 360 000 |
| OUT STORAGE | 49 087 | 49 087 |
| OUT WELLS | 310 915 | 310 915 |
| IN-OUT | -2 | -2 |
| ERROR % | -0.0006 | -0.0006 |
| concentration at the well (equal to the spring signal in case 1 to 3) | comparable to Fig. BT–14 left (half the concentrations) | comparable to Fig. BT–14 left (half the concentrations) |

**Table BT–19:** Cumulative heat balance (in MJ) computed with **HTM** considering convection, conduction and rock matrix conduction; final model time step, **Cauchy LQ scenario**

| | **FHLQ LQ** *(dx = 0.5 m)* | | **Cauchy LQ** | |
|---|---|---|---|---|
| | $T_{FXH}$ = 12°C | $T_{FXH}$ = 8°C | $T_{CY}$ = 12°C | $T_{CY}$ = 8°C |
| IN *FHLQ (LQ CASE)* | 645 014 | 638 968 | 0 | 0 |
| IN *CAUCHY (LQ CASE)* | 0 | 0 | 645 014 | 638 968 |
| IN MATRIX EXCHANGE | 641 991 | 641 991 | 641 991 | 641 991 |
| IN ROCK EXCHANGE | 0 | 160 | 0 | 160 |
| IN STORAGE | 0 | 405 | 0 | 405 |
| OUT STORAGE | 405 | 0 | 405 | 0 |
| OUT FIXED HEAD | 0 | 0 | 0 | 0 |
| OUT WELLS | 1 286 441 | 1 281 524 | 1 286 441 | 1 281 524 |
| OUT ROCK EXCHANGE | 160 | 0 | 160 | 0 |
| IN-OUT | 0 | 0 | 0 | 0 |
| ERROR % | -0.0000 | 0.0000 | -0.0000 | 0.0000 |

# Case 7 – Consideration of time dependent input for transport

The ability to process time dependent boundary data is validated for each applicable transport boundary condition (direct recharge, fixed concentration, fixed head, Cauchy, matrix inflow, and well). A first scenario replicates case 1 (heat transport, convection only) respectively case 2 (solute transport, advection). The model setup was modified to result in the same flow and heat / solute input as case 1 / case 2. For a second scenario, time dependent data were slightly varied as subsequently described. An overview about both scenarios is given below:

- period 1 from $t$ = 0 to $t$ = 3 600 s with temperature = 10°C / concentration = 0,
- period 2 from $t$ = 3 600 s to 10 800 s:
  - scenario 1: constant temperature 12°C respectively constant concentration 1000 mol/m$^3$
  - scenario 2 (heat): temperature decrease from 12°C to 11°C from $t$ = 3 600 s to 7 200 s and increase from 11°C to 12°C from $t$ = 7 200 s to 10 800 s.
  - scenario 2 (solutes): concentration decreases from 1000 to 500 mol/m$^3$ from $t$ = 3 600 s to 7 200 s and increases from 500 to 1000 mol/m$^3$ from $t$ = 7 200 s to 10 800 s,

Additionally, data input was considered as "bulk" (one value for all nodes) and "array" (one specific value for each node, please refer to the HTM / STM input file description in previous sections). Specific data for both scenarios are subsequently provided:

direct recharge:

- this is the basic model similar to case 1 (heat) respectively case 2 (solutes)
- TD data for the fixed head temperature / concentration in node 1

fixed concentration:

- similar to the direct recharge model except the transport boundary in node 1, which is a fixed temperature / concentration boundary
- TD data for the fixed temperature / concentration in node 1

fixed head boundary:

- fixed head in node 1 with $h$ = 50.64521423 m and in node 6 with $h$ = 50.0 m
- TD data for the fixed head temperature / concentration in node 1

Cauchy:

- Cauchy boundary in node 1 with HCY = 50.64525 m and CCY = 1E10 ms$^{-1}$
- TD data for the Cauchy flow temperature / concentration in node 1

matrix inflow:

- water transfer coefficient in node 1 is $\alpha$ = 0.1 m$^2$s$^{-1}$; matrix heads are modified by the fixed head boundary in the lower left corner ($h$ = 113.0 m)
- TD data for the matrix inflow temperature / concentration in node 1

well:

- well boundary in node 1 with $Q_{well}$ = 0.1 m$^3$s$^{-1}$
- TD data for the well temperature / concentration in node 1

Results for scenario 1 (constant temperature / concentration in period 2) are presented in Table BT-20 and BT-21. The same results are computed in case node-specific "array" input is used (instead of uniform "bulk" values). Exceptions are scenarios with fixed temperature / concentration. Here, results for "bulk" input (i.e. the value is valid for all nodes) differ from "array" input, where the fixed value is applied to node 1 only.

**Table BT–20:** Cumulative heat balance (in MJ) for case 7

| | case 1 | dir rech | fixed temp* | fixed head | Cauchy | matrix inflow | well |
|---|---|---|---|---|---|---|---|
| IN $Q_{DIR}$ | 1 290 029 | 1 290 029 | 1 283 983 | 0 | 0 | 0 | 0 |
| IN FIXED CONC | 0 | 0 | 6 046 | 0 | 0 | 0 | 0 |
| IN FIXED HEAD | 0 | 0 | 0 | 1 290 029 | 0 | 0 | 0 |
| IN CAUCHY | 0 | 0 | 0 | 0 | 1 289 685 | 0 | 0 |
| IN MATRIX | 0 | 0 | 0 | 0 | 0 | 1 290 027 | 0 |
| IN WELLS | 0 | 0 | 0 | 0 | 0 | 0 | 1 290 029 |
| OUT STORAGE | 824 | 824 | 824 | 824 | 824 | 824 | 824 |
| OUT FIXED HEAD | 1 289 205 | 1 289 205 | 1 289 205 | 1 289 205 | 1 289 241 | 1 289 203 | 1 289 205 |
| IN-OUT | -1 | -1 | -1 | -1 | -380 | -1 | -1 |
| ERROR % | -0.0001 | -0.0001 | -0.0001 | -0.0001 | -0.0295 | -0.0001 | -0.0001 |
| | spring signal: see Fig. BT–10 right | | | | | | |

** results for node specific "array" input*

**Table BT–21:** Cumulative solute balance (in mol) for case 7

| | case 2 | dir rech | fixed conc* | fixed head | Cauchy | matrix inflow | well |
|---|---|---|---|---|---|---|---|
| IN $Q_{DIR}$ | 720 000 | 720 000 | 0 | 0 | 0 | 0 | 0 |
| IN FIXED CONC | 0 | 0 | 720 000 | 0 | 0 | 0 | 0 |
| IN FIXED HEAD | 0 | 0 | 0 | 720 000 | 0 | 0 | 0 |
| IN CAUCHY | 0 | 0 | 0 | 0 | 719 808 | 0 | 0 |
| IN MATRIX | 0 | 0 | 0 | 0 | 0 | 719 998 | 0 |
| IN WELLS | 0 | 0 | 0 | 0 | 0 | 0 | 720 000 |
| OUT STORAGE | 98 175 | 98 175 | 98 175 | 98 175 | 98 175 | 98 175 | 98 174 |
| OUT FIXED HEAD | 621 923 | 621 923 | 621 923 | 621 923 | 621 943 | 621 922 | 621 923 |
| IN-OUT | -98 | -98 | -98 | -98 | -310 | -98 | -98 |
| ERROR % | -0.0136 | -0.0136 | -0.0136 | -0.0136 | -0.0431 | -0.0136 | -0.0136 |
| | spring signal: see Fig. BT–13 left | | | | | | |

** results for node specific "array" input*

Input temperatures / concentrations for scenario 2 are presented in Figure BT-33. Input temperatures / concentrations are similar for all used types boundary conditions (direct recharge, fixed concentration, fixed head, Cauchy, matrix inflow, and well).

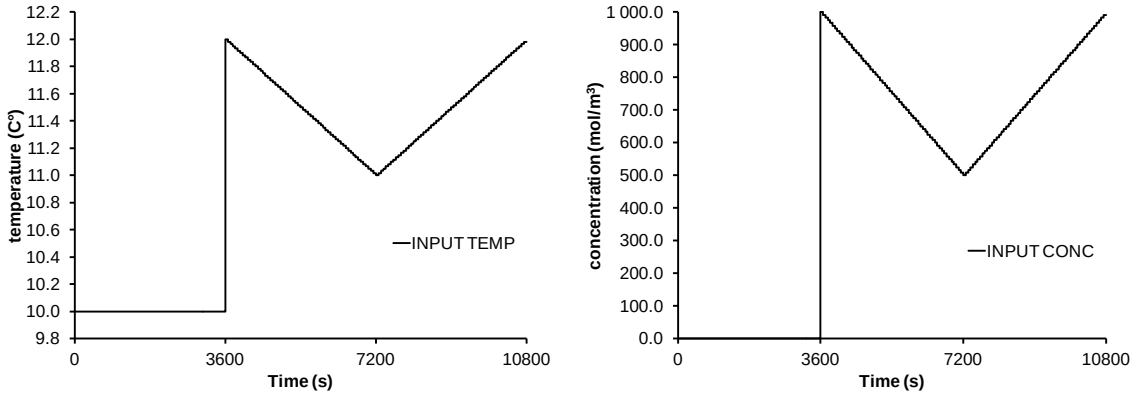


**Figure BT–33:** Time dependent input values for scenario 2, left: heat (HTM) right solutes (HTM)